Etude de la mise à l'échelle des piles à combustible microbiennes : collecteurs de courant et hydrodynamique

Agathe Paitier

N°d'ordre NNT : 2017LYSEI107

THESE de DOCTORAT DE L'UNIVERSITE DE LYON
opérée au sein de
INSA de Lyon

Ecole Doctorale A160
ELECTRONIQUE, ELECTROTECHNIQUE, AUTOMATIQUE

Spécialité / discipline de doctorat : Ingénierie pour le vivant

Soutenue publiquement le 17/11/2017, par :
Agathe Paitier

Etude de la mise à l'échelle des Piles à Combustible Microbiennes: collecteurs de courant et hydrodynamique

---

Devant le jury composé de :

Pascal Simonet	Directeur de recherche – Ecole Centrale de Lyon	**Président**
Giuliano Premier	Professeur - University of South Wales	**Rapporteur**
Théodore Bouchez	Chargé de recherche – IRSTEA	**Rapporteur**
Wafa Achouak	Directeur de recherche - CEA Cadarache	**Examinatrice**
Hervé Morel	Directeur de recherche - INSA de Lyon	**Directeur de thèse**
Timothy M. Vogel	Professeur Université Claude Bernard Lyon 1	**Co-directeur de thèse**

DOCTORAL THESIS OF THE UNIVERSITE DE LYON
at
INSA de Lyon

Doctoral school A160
ELECTRONIQUE, ELECTROTECHNIQUE, AUTOMATIQUE

Speciality : Bioengineering

defended on the 11th November 2017, by :
Agathe Paitier

Microbial Fuel Cells scale-up: current collectors and hydrodynamics

---

In front of the jury composed of :

Pascal Simonet	Directeur de recherche – Ecole Centrale de Lyon	**President**
Giuliano Premier	Professor - University of South Wales	**Reviewer**
Théodore Bouchez	Chargé de recherche – IRSTEA	**Reviewer**
Wafa Achouak	Directeur de recherche - CEA Cadarache	**Examiner**
Hervé Morel	Directeur de recherche - INSA de Lyon	**Thesis adviser**
Timothy M. Vogel	Professeur Université Claude Bernard Lyon 1	**Co-adviser**

Microbial Fuel Cells Scale-up: Current Collectors and Hydrodynamics

Agathe Paitier

Thesis adviser :

Hervé Morel

Co-advisers :

Timothy M. Vogel
Naoufel Haddour
Olivier Ondel

Résumé

Répondre aux besoins énergétiques croissants de nos sociétés et limiter leur impact sur l'environnement est un enjeu actuel majeur. Le développement d'énergies renouvelables est nécessaire et de nouvelles technologies alternatives comptent tirer profit de sources d'énergie négligées. Les stations d'épuration représentent un contexte de choix pour le développement et l'optimisation de procédés innovants de production d'énergie. En effet, le potentiel énergétique des eaux usées peut être judicieusement exploité par de nouvelles technologies telles que les piles à combustible microbiennes (PACM). Ces piles, pouvant produire de l'énergie électrique à partir d'eaux usées, montrent un rendement énergétique intéressant à petite échelle. Toutefois, leur efficacité diminue de manière drastique lorsque leur taille augmente, ce qui ne permet pas encore leur application industrielle. Ces travaux de thèse visent à identifier certains verrous de ce changement d'échelle et à proposer de nouvelles directions pour leur optimisation.

Une première partie de l'étude s'est intéressée à l'influence des collecteurs de courant anodiques sur les performances électriques et sur le développement du biofilm électro-actif. En effet, les collecteurs de courant, reliant l'anode au circuit externe, sont très peu étudiés dans les PACM. Nous avons émis l'hypothèse qu'à grande échelle, les collecteurs de courant peuvent être un élément limitant à la production d'électricité. Pour vérifier cette hypothèse, quatre PACM avec une anode de 490 cm² connectée de différentes manières ont été étudiées. L'augmentation du nombre de collecteurs a permis une hausse de la puissance produite par les PACM. La disposition des collecteurs affecte la répartition du potentiel sur la surface d'anode et peut engendrer dans certains cas, des gradients de potentiel qui influencent la structure microbiologique du biofilm. Cette dépendance au potentiel concerne en particulier *Geobacter*, dont le clade *G. metallireducens* est favorisé aux potentiels plus négatifs. Par ailleurs, des mesures d'impédance ont montré que multiplier les collecteurs augmente la capacité de double couche de l'anode et engendre un courant capacitif dont l'importance pour les performances de fonctionnement en cycles de charge/décharge est non négligeable.

La suite du travail s'est attachée à considérer les PACM comme des bioréacteurs et à prendre en compte différents aspects physiques, notamment l'aspect hydrodynamique, afin de modéliser leur fonctionnement. Pour cela, trois PACM de volumes différents ont été mises en œuvre et testées à différents débits. Les données de configuration, d'opération et de performances de ces piles ont permis de construire deux modèles statistiques de régression linéaire multiple prédisant la valeur de puissance maximale : le premier par sélection de variables (LASSO) et le second basé sur des nombres adimensionnels construits grâce au théorème de Vaschy-Buckingham. Ces deux modèles ont montré que la puissance

maximale produite était principalement corrélée à la vitesse de l'électrolyte circulant dans la pile et à la contrainte de cisaillement appliquée à l'anode par le mouvement du fluide.

Ces deux parties ont également montré que l'abondance dans le biofilm de *Geobacter*, une bactérie électro-active très répandue dans les PACM, n'était pas corrélée avec la puissance maximale. Tout en étant très abondante, son seul nombre n'explique donc pas entièrement les performances électriques d'une PACM.

De ce travail, il a été mis en évidence que la connexion électrique des anodes était d'une grande importance et que la conception d'une PACM conditionnait en partie le choix du débit de fonctionnement. Ces travaux ont également contribué à montrer pour le développement à grande échelle des PACM l'intérêt d'associer recherche fondamentale sur les biofilms électro-actifs, génie des procédés et modélisation, afin de généraliser des résultats empiriques et les expliquer.

Mots-clés : Pile à combustible microbienne ; Mise à l'échelle ; Collecteurs de courant ; Hydrodynamique

Abstract

Facing increasing energy needs and limiting their impact on the environment are current and major issues for society. Renewable energy development is needed and new alternative technologies could benefit from exploiting neglected energy sources. Wastewater treatment plants concentrate all these concerns and are useful platforms for developing and optimizing innovative processes, such as microbial fuel cells (MFC), for energy production. MFCs can be operated with wastewater and produce a reasonable quantity of energy at the small laboratory-scale. Unfortunately, when their size is increased, their efficiency dramatically decreases, which prevents their industrial use. This thesis aims at identifying some obstacles to scale-up of MFC and proposing new directions for its optimization.

The first part of the study was focused on the influence of anodic current collectors on electrical performance and on electroactive biofilm development. Current collectors, linking the anode to the external circuit, are poorly studied and our hypothesis was that they could be a limiting factor for electricity production at large scales. To test this hypothesis, four MFCs were operated with a 490 cm^2 anode connected to the external circuit in a different ways. Increasing the number of collectors improved the power. Collector's layout influenced electrical potential on the anode surface and created an electrical potential gradient on the anode and this gradient shaped the microbiological structure of the biofilm. This effect especially concerns *Geobacter*, whose clade *G. metallireducens* is favored at strongly negative potentials. In addition, impedance measurements showed that multiplying collectors increased the double layer capacitance and, thus, generated a capacitive current that was important for MFC functioning in cycles of charge/discharge and that would improve its performance.

Then, MFCs were considered as bioreactors and their different aspects, notably hydrodynamics, were taken into account to model their power output. Three MFCs of different volumes were operated under continuous-flow conditions and tested at four different flow rates. Configuration, operation and performance data were used to build two multiple linear regression statistical models: the first with variables selection through LASSO, the second with dimensionless numbers created with the Vaschy-Buckingham theorem. These two data-driven models showed that the maximal power was mostly correlated to electrolyte transfer rates inside MFC chamber and to shear stress at the anode generated by fluid movement.

These two major experimental projects also showed that the abundance of *Geobacter*, an electroactive bacteria, inside the biofilm was widespread in MFCs, but it was not correlated to maximal power. Despite its large abundance, its quantity alone does not entirely explain the

performance of a MFC. This work showed that electrical connection of the anodes and that MFC operational parameters, such as the choice of the flow rate, were critical to power production. In order to succeed at MFC scale-up, fundamental research on electroactive biofilms, process engineering and modeling need to be associated and generalized as empirical results and their explanation.

Keywords : Microbial fuel cell ; Scale-up ; Current collectors ; Hydrodynamics

Table of content

List of abbreviations

AC	Alternating Current
BES	Bioelectrochemical System
CBL	Concentration Boundary Layer
COD	Chemical Oxygen Demand
CPE or Q_x	Constant Phase Element
CT	Charge Transfer
CV	Cyclic Voltammetry
DBO	Demande Biologique En Oxygène
DCO	Demande Chimique En Oxygène
DL	Double Layer
EEC	Equivalent Electrical Circuit
EH	Equivalent Habitant
EIS	Electrochemical Impedance Spectroscopy
FISH	Fluorescence In Situ Hybridization
HRT	Hydraulic Retention Time
MEC	Microbial Electrosynthesis Cell
MFC	Microbial Fuel Cell
OCV	Open Circuit Voltage
OECD	Organisation For Economic Co-Operation And Development
PACM	Pile A Combustible Microbienne
PE	Population Equivalent
PBS	Phosphate Buffer Saline
PCR	Polymerase Chain Reaction
PVC	Polyvinyl Chloride
qPCR	quantitative PCR
RDE	Rotating Disc Electrode
RTD	Residence Time Distribution
SHE	Standard Hydrogen Electrode
SIP	Stable Isotope Probing
SSU	Small Subunit
WWTP	Wastewater Treatment Plant

List of figures and tables

Figures

Tables

Synthèse en français

1. Les stations d'épuration : protection des ressources, énergie et économie

L'environnement et les questions économiques associées sont un enjeu actuel majeur. La raréfaction des énergies fossiles, l'augmentation de leur coût, la protection des ressources naturelles comme l'eau favorisent l'émergence de solutions alternatives permettant à la fois des économies d'énergie et le développement d'énergies renouvelables [1]. Les institutions gouvernementales sont conscientes de l'effort à fournir et fixent des objectifs à atteindre, comme l'Union Européenne, qui prévoit d'augmenter la part des énergies renouvelables dans la consommation totale d'énergie à 20 % d'ici 2020 [2]. Les stations d'épuration sont l'exemple parfait d'installations où ces idées définissent actuellement de nouveaux standards d'exploitation et où sont testées de nouvelles technologies. L'enjeu est important car les services d'eau et d'assainissement sont souvent les infrastructures publiques nécessitant les plus lourdes dépenses énergétiques, entre 5 et 20 % de la facture d'électricité d'une ville française [3,4]. La France compte environ 20 000 [5] stations d'épuration parmi lesquelles 60 % fonctionnent grâce à un procédé de boues activées [6]. Cette technique élimine la matière organique, principale charge polluante et la plus facilement éliminable des eaux usées, grâce à des bactéries contenues dans ces eaux. Une fois concentrées et sous aération, ces bactéries forment des flocs et dégradent efficacement les composés carbonés, c'est-à-dire la matière organique [6]. Ces flocs finissent par sédimenter et former des boues qui sont ensuite séparées de l'eau épurée. Celle-ci est ensuite relarguée dans le milieu naturel ou subit d'autres traitements (élimination de phosphore, métal, micropolluants…).

Les aspects énergétiques et économiques du traitement de l'eau sont étroitement suivis. En France, on estime que le traitement des eaux usées a exigé, en 2011, 60 kWh par habitant [7]. Habituellement, la consommation électrique des stations d'épuration est exprimée en kWh nécessaires pour éliminer un kilogramme de DBO_5. La DBO_5 (demande biochimique en oxygène) est la quantité d'oxygène nécessaire aux micro-organismes pour dégrader la matière organique par son oxydation en CO_2, mesurée au bout de 5 jours. Elle correspond ainsi à la dégradation d'environ 68 % de cette charge organique et permet une estimation de la quantité totale de matière organique biodégradable présente dans l'échantillon. Les grandes stations d'épuration, c'est-à-dire d'une capacité de traitement de plus de 10 000 EH (équivalent-habitant), utilisant un procédé de boues activées, consomment en moyenne 3,4 kWh d'électricité par kilogramme de DBO_5, ce qui représente une consommation

électrique de 7,2 GWh par an pour une station d'épuration de 100 000 EH. Les boues activées sont très performantes pour l'épuration de l'eau. En revanche, ce procédé consomme énormément d'énergie, principalement pour l'aération des bassins nécessaire à l'activité des bactéries. En effet, le fonctionnement des systèmes d'aération représente entre 40 et 80 % de la facture électrique des lignes de traitement de l'eau [8]. Plusieurs autres postes des stations d'épuration sont également très consommateurs, comme le pompage des effluents, le traitement thermique des boues pour leur élimination ou la désodorisation.

Pour limiter ces coûts énergétiques, des stratégies d'optimisation se sont mises en place : équipements plus efficaces, capteurs permettant une meilleure gestion de la consommation d'énergie, dimensionnement de la station adapté à la charge polluante des eaux à traiter, production de biogaz à partir de la digestion des boues, micro-turbine ou récupération de la chaleur des eaux usées [9]. Même si ces solutions permettent d'alléger l'empreinte environnementale, leur coût de maintenance est souvent lourd, ce qui limite leur intérêt économique. Par conséquent, d'autres technologies innovantes tirant profit du potentiel énergétique des eaux usées et des boues pourraient aider à limiter les coûts d'exploitation des stations d'épuration et même conduire à des stations au bilan énergétique positif.

En effet, il a été estimé que les eaux usées contiendraient plus d'énergie sous forme chimique que nécessaire à leur propre traitement. Cette énergie est contenue par les électrons des liaisons C-C des molécules. Une analyse calorimétrique d'eaux usées domestiques brutes arrivant dans une station d'épuration de Toronto a montré qu'elles contenaient 1,8 kWh/m^3, soit 4,1 Wh par gramme de DCO (demande chimique en oxygène, c'est-à-dire la quantité d'oxygène moléculaire nécessaire pour oxyder chimiquement la totalité de la matière organique présente) [10]. Les 35 000 m^3 d'eaux que traite cette station contiendraient donc 9,3 fois plus d'énergie que ce qui est requis pour son traitement. Une autre étude a estimé que les eaux usées domestiques contenant 500 mg de DCO par litre renfermeraient une énergie de 2 kWh/m^3 [11]. En comparaison avec l'énergie nécessaire pour l'aération des bassins de boues activées, qui varie de 0,2 à 0,4 kWh/m^3 [12], on comprend l'intérêt à développer des moyens pour récupérer ce potentiel énergétique des eaux usées domestiques.

2. Les PACM : une technologie pour les stations d'épuration

2.1. Principe de fonctionnement

De l'énergie est donc présente dans les eaux usées sous forme de matière organique qui peut être consommée par les bactéries, très nombreuses et diversifiées, contenues dans ces eaux. Depuis 1911, grâce aux travaux de Potter, on sait que certaines bactéries, qualifiées d'électro-actives, sont capables de produire du courant électrique [13]. Les piles à combustible microbiennes (PACM ou MFC en anglais) utilisent ces bactéries pour extraire l'énergie qu'elles ont puisée dans la matière organique des eaux usées sous la forme d'un transfert d'électrons entre la bactérie et la pile, produisant un courant électrique.

Les PACM sont en général constituées d'un compartiment anaérobie comprenant une première électrode : l'anode (Figure 1). Ce compartiment est rempli d'une solution nutritive, l'électrolyte, et inoculée avec des bactéries. Certaines bactéries peuvent se développer sur l'anode et former un biofilm, une structure bactérienne complexe et robuste. Elles tirent l'énergie nécessaire à leur croissance de l'oxydation de la matière organique présente dans l'électrolyte. Parmi elles, les bactéries électro-actives sont capables d'utiliser l'anode, faite à partir d'un matériau conducteur d'électricité, comme accepteur final des électrons de leur chaîne respiratoire anaérobie, le processus cellulaire permettant de produire leur énergie métabolique. Les électrons ainsi transmis à l'anode par les bactéries empruntent un circuit électrique externe reliant l'anode à la seconde électrode. Cette seconde électrode, la cathode, peut se trouver dans un autre compartiment rempli avec un électrolyte adapté et relié au compartiment anodique par une membrane ou un pont salin. Dans le cas de cathode à air, celle-ci est directement en contact avec l'électrolyte de l'anode d'un côté et l'air extérieur de l'autre. En parallèle du transport des électrons, des protons sont relargués à l'anode par l'oxydation bactérienne et diffusent vers la cathode où ils permettent, avec les électrons provenant de l'anode, la réaction de réduction de l'oxygène. Le flot d'électrons ainsi produit entre les deux électrodes génère un courant électrique qui peut être récupéré.

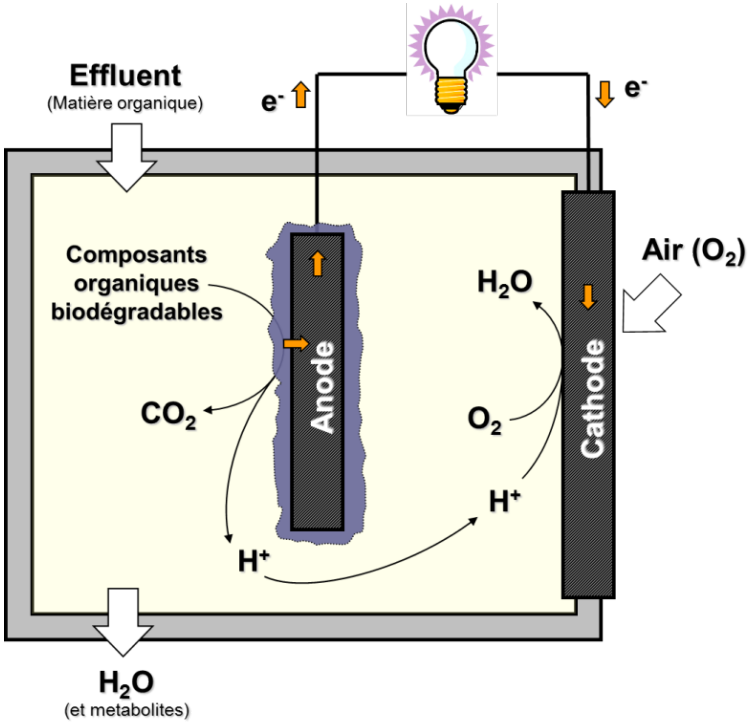

Figure 1. Principe de fonctionnement d'une PACM à cathode à air.

2.2. Intérêt pour les stations d'épuration

Plusieurs aspects des PACM en font une solution adaptée et intéressante aux problématiques économiques des stations d'épuration. Tout d'abord, les eaux usées contiennent à la fois les bactéries utiles et la matière organique dont elles se nourrissent. Les PACM peuvent ainsi fonctionner sans inoculation ni apport de substrat extérieurs [14]. De plus, les PACM produisent directement de l'électricité, une forme d'énergie très répandue et facile à utiliser. Son utilisation ne nécessite donc pas de transformations intermédiaires, comme c'est par exemple le cas pour le méthane issu de la fermentation des boues d'épuration qui doit être brûlé afin de récupérer une énergie utilisable (chaleur et électricité), entraînant des pertes énergétiques [15] et la libération de polluants atmosphériques lors de la combustion [16]. Tout en produisant de l'électricité, les PACM réduisent également la quantité de matière organique des eaux grâce aux bactéries qui la consomment. Cela contribue à l'épuration des eaux en éliminant une part de la charge polluante, principalement organique dans le cas des eaux usées domestiques, et habituellement traitée par les micro-organismes aérobies à l'œuvre dans les bassins d'aération. Les PACM limiteraient par là même les coûts en réduisant les besoins en aération, l'étape la plus consommatrice du traitement de l'eau. De même, l'utilisation de ces piles entraînerait des économies sur le traitement des boues. On

estime en effet que le traitement par PACM produit en moyenne 20 % de boues de moins que le procédé aérobie [17]. Ce faible taux de production de boues représente d'importantes économies sur deux points : la réduction de la taille du bassin d'aération et du décanteur secondaire (où a lieu la séparation des boues et de l'eau épurée après aération) ce qui diminue les coûts d'opération et d'infrastructures, ainsi que la réduction des coûts qu'engendre le lourd retraitement de ces boues [14].

A part ces économies de fonctionnement au sein de la station, les PACM pourraient également permettre des économies et même des revenus grâce à l'électricité produite. Prenons l'exemple d'une station d'épuration française moyenne traitant 100 000 EH qui consomme environ 6×10^6 kWh d'électricité [7] et traite $65,7\times10^6$ m^3 d'eaux usées par an [18]. En parallèle, d'après Lefebvre *et al.*, une PACM de laboratoire typique réalise un abattement de DCO de 80 % avec une efficacité coulombique de 80 % (efficacité de la transformation de la charge organique en électricité) pour un rendement de 0,65 kWh/m^3 [11]. A partir de ces performances, cette station pourrait produire annuellement $42,7\times10^6$ kWh, ce qui représente plus de sept fois sa consommation d'électricité annuelle. A l'échelle nationale cette technologie pourrait aussi devenir une source d'énergie substantielle. Le volume total d'eaux usées en France est de 7×10^9 m^3/an (chiffre de 2008) [19] et la consommation totale d'électricité du pays est de $475,4\times10^9$ kWh (chiffre de 2015) [20]. Il apparaît que $4,55\times10^9$ kWh par an sont potentiellement disponibles grâce à cette technique, ce qui constitue 0,96 % de la consommation d'électricité française. Outre un intérêt écologique, les PACM ont aussi un potentiel avantage économique.

2.3. Technologies concurrentes

D'autres technologies alternatives auxquelles doivent se comparer les PACM sont actuellement opérationnelles ou dans un développement avancé pour produire et valoriser des énergies renouvelables dans les stations d'épuration. La principale concurrente est la production de biogaz par digestion anaérobie de boues activées. Le biogaz contient entre 50 et 75 % de méthane et entre 20 à 30 % de CO_2. Le nombre de ces installations est en augmentation en France et on prévoit 130 stations d'épuration équipées d'ici 2020 [4]. Son succès s'explique par plusieurs avantages : la réduction des volumes de boues à traiter à la fin de la filière ainsi que leur stabilisation chimique et leur désodorisation, la production d'une énergie renouvelable que l'on peut stocker et la réduction des émissions de CO_2 [9]. Il y a néanmoins toujours plusieurs contraintes à la production de biogaz. Premièrement, l'installation requiert un investissement financier important, pour sa construction et sa

maintenance. Cette installation sert principalement à la combustion du biogaz, l'étape intermédiaire pour transformer le gaz en énergie utilisable, et elle comporte des risques d'explosion [9]. La cogénération est la principale façon d'utiliser le biogaz et son rendement n'est en moyenne que de 35 % sous forme d'électricité, 55 % sous forme de chaleur et 10 % de pertes [21]. Par ailleurs la production de certains gaz indésirables, tels les siloxanes, les gaz chlorés ou fluorés, endommagent les conduites et augmentent les coûts de maintenance. Enfin on estime que le biogaz, même si sa production est optimisée, ne peut couvrir que 50 à 80 % des besoins énergétiques d'une station d'épuration [9].

Hormis la production de biogaz, d'autres technologies, moins répandues, contribuent à collecter un maximum d'énergie des eaux usées. On peut citer les pompes à chaleur qui récupèrent les calories des effluents dont la température en entrée de station se situe entre 12 et 25 °C, ou les turbines hydrauliques qui produisent de l'énergie mécanique [9]. La production d'hydrogène par la fermentation de biomasse en est autre exemple, mais seuls 15 % de l'énergie contenue dans la matière organique dissoute dans les eaux usées peuvent être convertis en hydrogène [22]. En revanche, les métabolites primaires de la fermentation produits lors de la formation du biohydrogène, les acides acétique et butyrique, sont des substrats utilisables par les bactéries électro-actives [23]. Les PACM pourraient donc extraire le reste de cette énergie non récupérée par fermentation. Cela montre par ailleurs la potentielle synergie de différents systèmes de production d'énergie alternative au sein d'une même installation pour limiter les pertes énergétiques.

3. Du laboratoire à l'application industrielle

3.1. Développement des PACM en laboratoire

Des recherches s'intéressent aux PACM depuis plus de vingt ans afin de développer cette technologie jusqu'à la rendre économiquement viable pour une application industrielle. Aujourd'hui, seule l'entreprise Emefcy commercialise une unité de traitement des eaux usées (« Electrogenic BioReactor ») utilisant le principe de la PACM pour la rendre autonome en énergie. En parallèle, de nombreuses équipes de recherche continuent de mener des études sur plusieurs aspects des PACM pour comprendre leur fonctionnement et améliorer leur efficacité.

Une partie de cette recherche est dédiée à l'ingénierie de ces systèmes et s'attache à tester différentes configurations [24,25], des caractéristiques d'anode et de cathode [26–28] et des paramètres opérationnels comme les substrats [29,30], les conditions de circulation d'électrolyte [31,32] et les résistances des circuits externes [33,34]. Ces travaux ont mené à des améliorations notables de densité de puissance électrique produite par une PACM. Malheureusement, ces progrès, réalisés chacun sur des modèles de PACM précis, sont peu généralisables dès que la configuration ou les matériaux changent.

Un autre champ de recherche sur les PACM, plus fondamental, est l'étude des populations microbiennes de l'anode, qui contiennent les bactéries électro-actives responsables de la production d'électricité. La biologie moléculaire et la microscopie ont grandement affiné nos connaissances sur la composition et la structure du biofilm anodique, les mécanismes de transfert d'électrons ou les interactions entre bactéries [35–37]. Néanmoins, beaucoup reste à découvrir concernant l'initiation et le développement du biofilm, les dynamiques des populations anodiques ou la complexité des interactions entre micro-organismes.

L'électrochimie est également un sujet clé dans l'étude des PACM. Une abondante bibliographie répertorie les processus électrochimiques en jeu lors du fonctionnement des PACM tout comme les techniques utilisées pour leur étude [38–40]. Elles permettent par exemple de mettre en évidence les différents types de résistances internes limitant la production d'électricité ou d'évaluer les performances de différents matériaux d'électrode.

Malgré ces progrès et une explosion du nombre de recherches dans les années 2000, aucune avancée assez importante pour lancer cette technologie sur le marché n'a eu lieu, et une partie de la communauté de scientifiques impliqués dans ce domaine de recherche se tourne vers des applications dérivées des PACM et des systèmes bioélectrochimiques en général plutôt que vers le développement des PACM comme sources d'électricité. On peut citer les PACM benthiques, fonctionnant avec des électrodes enfouies dans les sédiments [41] ou les PACM associées à des plantes [42], toutes deux potentiellement utilisées comme capteurs isolés *in situ*, car ne nécessitant qu'une faible puissance. De façon plus générale, de petites PACM peuvent être utilisées comme capteurs de polluants et de substances toxiques, de DBO ou d'activité microbienne [43]. Les systèmes d'électrosynthèse microbienne attirent également de plus en plus l'attention. Ces systèmes, construits comme des PACM, sont capables de produire des molécules d'intérêt ou des biofuels comme l'hydrogène [44] ou les acides organiques [45] lorsqu'un courant électrique est fourni. D'autres technologies combinant bactéries et électrochimie permettent la production de méthane [46], la désalinisation [47] ou encore la production de carboxylates et d'alcools [48]. Mais la plupart de ces nouveaux systèmes bioélectrochimiques en sont encore à un stade de développement.

3.2. Vers une mise à l'échelle des PACM

Comme décrit précédemment, de nombreuses études sont menées pour améliorer les performances des PACM. De multiples aspects ayant été étudiés et quantifiés indépendamment, il est difficile de comparer la très grande quantité d'études menées à partir de PACM complètement différentes pour en extraire quelques paramètres qui semblent être prépondérant dans la production d'électricité. Ici ont été compilés un grand nombre d'articles scientifiques, afin de rassembler des données, de les analyser dans leur totalité et d'essayer d'identifier des paramètres qui semblent être corrélés avec la puissance électrique produite dans la perspective de focaliser nos recherches sur ces aspects prometteurs.

3.2.1. Pilotes de PACM

Très peu d'articles décrivent des études de pilotes de PACM installés en stations d'épuration (*in situ*). Seuls sept études publiées entre 2011 et 2016 rapportent ce genre de résultats [49–55]. Ce sont dans chaque cas des PACM à cathode à air, suggérant que les piles comprenant un deuxième compartiment à cathode et nécessitant donc la mise en place d'un électrolyte propre, souvent avec un système de recirculation, ne semblent pas adaptées à une installation à grande échelle en station d'épuration. Ces pilotes sont disposés dans les bassins d'aération ou installés en parallèle et alimentés en continu avec des effluents. Des PACM tubulaires ou planes sont les seules configurations retenues pour ces essais. En comparant ces résultats, on note une diminution de la puissance électrique avec l'augmentation du volume de la pile : respectivement 9, 0,6 et 0,464 W/m^3 pour des piles de volumes de 4, 200 et 250 L. 9 W/m^3 est la meilleure valeur de puissance relevée parmi ces tests *in situ*. Elle a été obtenue avec un réacteur d'un volume total de 4 L formé de deux PACM tubulaires en série de 2 L chacune. Les PACM dont le volume du compartiment anodique est beaucoup plus grand ne semblent pas pouvoir fournir de puissance comparable. Cette combinaison de deux PACM de 2 L, qui affiche les meilleures performances, suggère que le développement des PACM à grande échelle pourrait passer par l'association de plusieurs modules de volume relativement faible (de l'ordre du litre) plutôt que par l'agrandissement des compartiments anodiques. Néanmoins, nous sommes encore loin d'un consensus en ce qui concerne l'avenir des PACM et de leur application en stations d'épuration, en partie à cause du faible nombre d'essai en situation réelle et du nombre encore plus faible de ces essais réalisés avec des pilotes de grands volumes. Ces études ont tout de même permis de mettre en évidence plusieurs difficultés inhérentes à

l'installation en station. La plus grosse est le colmatage et l'encrassement des compartiments, conduites, membranes et électrodes. De plus, avec les moyens actuels, le coût de certaines pièces, comme les membranes et cathodes à air, est un frein au développement des PACM à grande échelle [55].

Cette étude comparative n'a pas pris en compte les aspects microbiologiques (développement et composition du biofilm, diversité et dénombrement des populations bactériennes…). En effet, presqu'aucune étude sur les pilotes de PACM, *in situ* ou en laboratoire, ne prend ces aspects en considération. Cette partie du fonctionnement des PACM est souvent éludée alors que la caractérisation du biofilm anodique est probablement un point d'intérêt dans la comparaison de systèmes et l'identification de paramètres nécessaires pour construire une stratégie de mise à l'échelle.

3.2.2. Identifier les paramètres limitants

Comme la comparaison des seuls pilotes à grande échelle est limitée par le nombre d'études et n'a pas apporté d'indices majeurs pour l'amélioration de la production d'électricité, l'étude comparative s'est élargie aux PACM à toutes les échelles, de quelques millilitres à plusieurs litres, en compilant plus de 200 cas. Le but étant toujours d'identifier ce qui contraint la production d'électricité lors de l'agrandissement de la pile, les premières caractéristiques à être examinées sont celles directement liées aux dimensions des réacteurs : volume du compartiment anodique, surface d'anode, surface de cathode. Mais aucune ne semble être corrélée à la puissance. Ces paramètres, pris indépendamment, ne permettent pas de prédire la puissance électrique d'une PACM.

La source d'inoculum bactérien ainsi que le ou les substrats utilisés influencent directement le développement du biofilm anodique et la sélection bactérienne qui s'y opère. Ces paramètres pourraient donc expliquer également les performances électriques des PACM. La comparaison fait ressortir que les meilleurs résultats de production d'électricité sont obtenus lorsque le système est inoculé avec des échantillons de biofilm électro-actif d'une ancienne PACM, des boues activées ou des eaux usées brutes et lorsque la pile est alimentée avec de l'acétate ou bien simplement en apportant des eaux usées fraîches. De très bons résultats adviennent également quand la pile est alimentée avec de l'acétate, la molécule de substrat qui convient particulièrement bien à *Geobacter*, une bactérie électro-active modèle très répandue et associée à de bonnes performances électriques, faisant l'objet de nombreuses études dans les PACM. Cependant, on remarque bien plus de travaux utilisant les inoculums et substrats listés ci-dessous que d'autres. Un problème statistique

apparaît donc pour valider cette observation, sans parler du fait que beaucoup de travaux utilisant une de ces combinaisons d'inoculum-substrats montrent eux des résultats très faibles.

Enfin, pour les cas de réacteur alimentés en continu, les paramètres opérationnels liés à l'alimentation de la PACM ont été testés, à savoir le débit de circulation de l'électrolyte, son temps de rétention et sa concentration en DCO. Aucun n'a montré non plus de corrélation avec la puissance. La même conclusion apparaît lorsqu'on s'intéresse à la valeur de la résistance externe.

Au final, il ne semble pas qu'il y ait de paramètre qui montre individuellement une corrélation avec les performances électriques, même lorsqu'on recoupe plus de 200 études de PACM. La production d'électricité doit donc être conditionnée par des caractéristiques plus subtiles du système et probablement par la combinaison de plusieurs paramètres.

4. Objectifs de la thèse et résultats

Ces travaux visent à mettre en lumière de nouveaux aspects et différentes approches du problème de développement de l'échelle des PACM. Comme décrit précédemment, l'agrandissement des PACM a jusqu'à présent plutôt été traité par des méthodes d'ingénierie, en testant différentes configurations, matériaux et conditions opérationnelles. Cela a néanmoins peu mené à des principes de fonctionnement généraux. Cela a également rarement inclut des considérations microbiologiques avec la caractérisation approfondie du biofilm anodique. La stratégie employée consiste plutôt à observer uniquement l'effet de différentes conditions (configuration, débit, concentration en substrat etc.) sur les performances électriques, alors qu'elles sont directement influencées par les réponses biologiques et électrochimiques aux changements appliqués. La compréhension de ces mécanismes intermédiaires pourrait aider à généraliser plus facilement une amélioration particulière. Ces travaux sont aussi fondés sur l'hypothèse que les transformations apportées à une PACM par le changement d'échelle modifient certains paramètres qui deviennent non négligeables à partir d'une certaine dimension. Cela se répercute sur le biofilm anodique et son efficacité de transfert des électrons, ce qui devient une cause majeure des variations de production d'électricité observées.

4.1. Influence des collecteurs de courant anodique

Parmi ces paramètres Figurent les collecteurs de courant des électrodes, dont l'importance croît avec la taille de la PACM. Ces collecteurs ne focalisent pour l'instant pas vraiment l'attention des recherches sur l'agrandissement des PACM et ne sont en général pas étudiés ou même décrits dans la littérature. Une anode de grande dimension permettra certes le développement d'une plus grande quantité de bactéries électro-actives, mais si le système de collection du courant est mal adapté, les électrons ne pourront pas efficacement être canalisés de leur site de transfert jusqu'à la cathode et toute autre amélioration de matériau ou de configuration sera inutile. L'hypothèse testée ici est que les collecteurs de l'anode limitent la puissance de la pile, en particulier en restreignant et en modelant le développement spatial des bactéries. En effet, plus les bactéries se développent près des collecteurs, plus la résistance ohmique de la portion d'anode entre le site de transfert d'électrons par la bactérie et les collecteurs est faible. Cela pourrait favoriser le développement des bactéries électro-actives à proximité des collecteurs. La disposition des collecteurs affecte la répartition du potentiel sur la surface d'anode et engendre des gradients de potentiel. Comme il a été suggéré que le potentiel de l'anode influence le développement du biofilm anodique [56], cette distribution de potentiel à la surface de l'anode peut aussi influencer la structure microbiologique du biofilm. Pour vérifier cette hypothèse, quatre PACM planes à cathode à air de 1 L (Figure 2) avec une anode en tissu de carbone de 490 cm^2 connectée de différentes manières par des bandes de titane (Figure 3) et fonctionnant en batch ont été étudiées. La puissance produite et le comportement électrochimique de l'anode, puis la quantité totale de bactéries, la quantité de *Geobacter*, la bactérie électro-active modèle, et la composition taxonomique du biofilm ont été suivis en fonction du nombre de collecteurs et de leur disposition. L'augmentation du nombre de collecteurs a permis une hausse de la puissance produite par les PACM. Un seul point de connexion sur toute l'anode, comme c'est communément réalisé dans la littérature, de seulement 1 cm^2, entraîne une résistance d'étranglement et une augmentation de la densité de courant aux abords du collecteur, [57] ce qui a empêché une canalisation suffisante des électrons transférés à l'anode par les bactéries. De plus, on y a observé une abondance moindre des bactéries électro-actives principales (*Geobacter* et *Desulfuromonas*), peut-être à cause d'une sensibilité aux fortes densités de courant. Par comparaison entre les différents systèmes, il a été montré que l'abondance de *Geobacter* n'était pas corrélée avec la puissance. En revanche, ce genre bactérien était associé avec une présence plus importante de micro-organismes capables de produire, par fermentation, des molécules de substrat pour *Geobacter*, comme l'acétate, et avec les zones d'anode où le potentiel local était plus faible. Dans ces zones, il est apparu que les espèces de *Geobacter* favorisées appartenaient

au clade *G. metallireducens*. Il a aussi été mis en évidence par spectroscopie d'impédance que la résistance du biofilm augmentait avec l'abondance de bactéries électro-actives. Ces mesures d'impédance ont également fait apparaître que la capacité de double couche de l'anode augmente avec le nombre de collecteurs et que celle-ci crée un courant capacitif non négligeable qui améliore la puissance générée lors des décharges de la pile. Cette observation suggère l'intérêt qu'il y aurait à faire fonctionner des PACM de grande dimension en cycles de charges et décharges, pour tirer parti de ce courant capacitif. Les collecteurs de courant anodiques ont donc bien un impact significatif sur le fonctionnement et la production d'électricité des PACM à grande échelle.

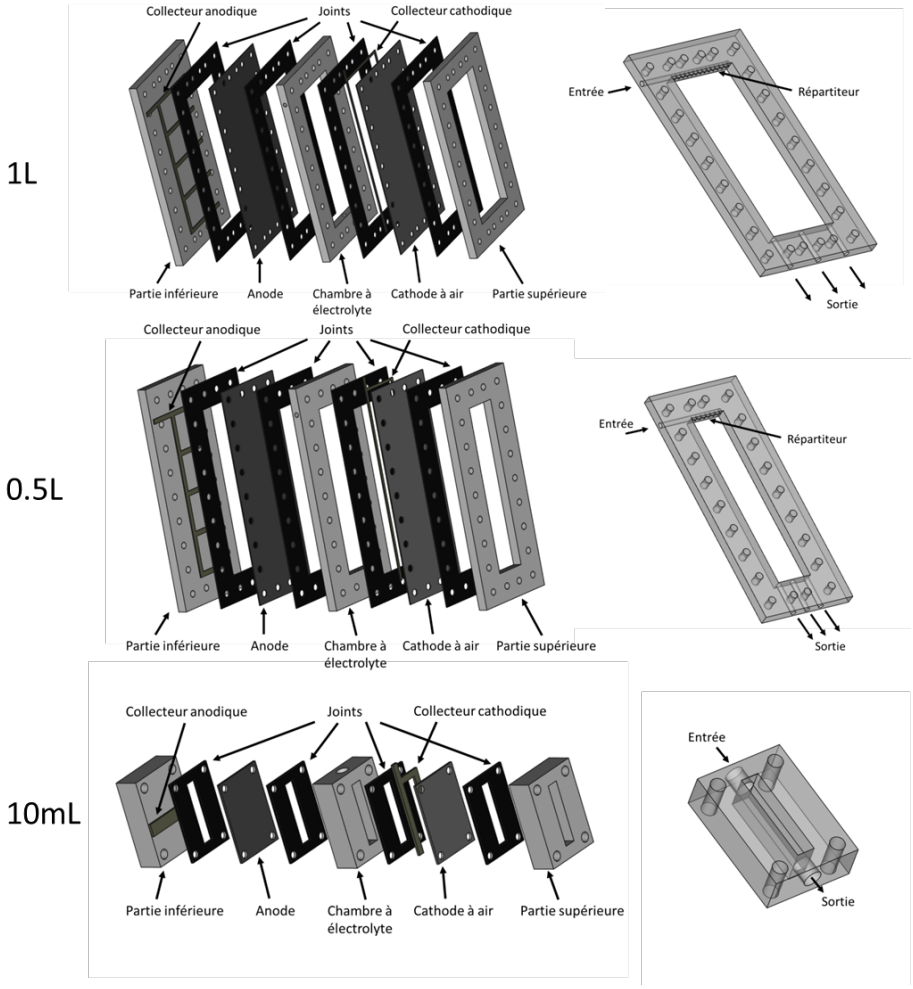

Figure 2. Réacteurs utilisés.

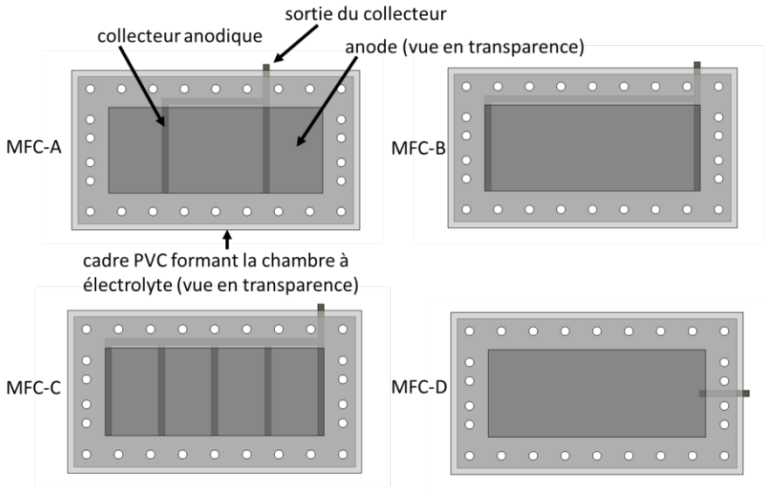

Figure 3. Disposition des collecteurs de courant anodiques dans les 4 PACM utilisées. Les collecteurs sont situés sous l'anode, elle-même au fond de la chambre à électrolyte. Ici, seuls les collecteurs, l'anode et le cadre de la chambre sont représentés.

4.2. Importance de l'hydrodynamique dans les PACM et modélisation statistique

De la même manière, la dynamique des fluides des PACM en flux continu n'est pas souvent prise en compte lors du changement d'échelle. Peu d'études ont décrit ces aspects, et celles qui l'ont fait se concentrent sur une caractéristique, le plus souvent le temps de rétention ou la contrainte de cisaillement à l'anode. Or, en station d'épuration, il paraîtrait assez évident d'installer les PACM directement sur les lignes de traitement des eaux, pour limiter les aménagements additionnels. La PACM en question devrait donc supporter et tirer profit des forces hydrodynamiques inhérentes à la circulation des effluents. Le but de cette partie a été de caractériser l'influence de ces forces sur le système, et plus généralement l'influence des divers paramètres décrivant les PACM, et de tenter de modéliser leurs performances électriques. Pour cela, trois PACM plates de tailles différentes (1 L, 0,5 L et 10 mL) (Figure 2) ont été mises en œuvre en flux continu et testées chacune à quatre débits. Du point de vue des performances électriques, un point de rupture apparaît entre les très faibles débits (ici 5 L/h) et les plus importants, suggérant un comportement des PACM différent suivant les gammes de régimes hydrodynamiques. Les données de configuration, d'opération et de performances de ces piles ont permis de construire deux modèles statistiques de régression linéaire multiple prédisant la valeur de puissance maximale : le premier par sélection de variables (LASSO) et le second fondé sur des nombres adimensionnels construits grâce au théorème de Vaschy-Buckingham. Ces deux modèles ont montré que la puissance maximale produite était principalement positivement corrélée à

la vitesse de l'électrolyte circulant dans la pile et négativement corrélée à la contrainte de cisaillement appliquée à l'anode par le mouvement du fluide, confirmant l'impact significatif des aspects hydrodynamiques sur le fonctionnement d'une PACM. De plus, il est ici aussi apparu que l'abondance de *Geobacter* n'était pas une bonne variable explicative pour la puissance électrique, malgré sa très forte présence (jusqu'à 70 % d'abondance relative). Cela semble confirmer que la puissance produite et les capacités électro-actives du biofilm ne dépendent pas entièrement de *Geobacter*.

5. Conclusion et perspectives

Après une décennie de recherches sur les piles à combustible microbiennes, le sentiment général qui émane de cette communauté scientifique est que l'utilisation à l'échelle industrielle de cette technologie n'a pas d'avenir. Ainsi, beaucoup d'entre eux se tournent vers le développement de technologies alternatives issues de ce concept malgré le fait que certains aspects des PACM, comme les collecteurs de courant ou les régimes d'écoulements de l'électrolyte, n'aient pas été suffisamment étudiés, ou du moins, publiés. Ce sont pourtant des points d'importance particulière pour le développement d'une application industrielle. A titre de comparaison, de nombreuses études sur les piles à combustible électrochimiques se focalisent sur leurs collecteurs de courant anodiques [57–60] et une grande partie de la conception et du développement des réacteurs électrochimiques ou des bioréacteurs est consacrée à l'étude de l'influence de l'hydrodynamique sur les performances, grâce à des méthodes d'ingénierie des procédés [61–64]. Les PACM ne sont pas si éloignées : ce sont des réacteurs électrochimiques utilisant un catalyseur biologique (le biofilm électro-actif). Le développement à échelle industrielle des PACM devrait donc également tirer profit de ce genre d'études et de techniques, à la fois pour améliorer leurs performances et pour comprendre et déterminer leurs limites de fonctionnement.

Ce travail a aussi tâché d'associer microbiologie et ingénierie pour répondre à ces problématiques. Les recherches sur les bactéries électro-actives et le développement des biofilms sont souvent complètement dissociées des travaux de changement d'échelle, qu'on taxe souvent d'ingénierie. Or ces deux approches sont essentielles et des études combinant ces deux aspects permettraient d'améliorer notre connaissance globale du système. Cela serait par exemple particulièrement judicieux pour comprendre comment un paramètre opérationnel influence la communauté anodique et comment cette modification joue sur les performances de la pile, ou pour évaluer les causes et conséquences de l'homogénéité du biofilm sur une anode de grande échelle. Les PACM fonctionnent grâce aux bactéries, et

même dans les systèmes de grande taille souvent complexes, c'est-à-dire inoculés avec des communautés mixtes et alimentés avec des substrats complexes, comme c'est le cas avec les boues activées et les eaux usées, l'étude des communautés du biofilm a un intérêt et doit être menée. Aujourd'hui, les outils de biologie moléculaire, la microscopie ou les analyses chimiques sont courants dans nos laboratoires et peuvent être assez facilement inclus dans les études sur les PACM. En parallèle, les outils du génie des procédés et la modélisation peuvent améliorer et formaliser le développement à grande échelle des PACM, qui reste pour l'instant très empirique. La science des procédés apporte des méthodes et des outils pour concevoir, optimiser et faire fonctionner des réacteurs biologiques, chimiques ou électrochimiques, ce qui est aussi nécessaire à la mise à l'échelle des PACM. La modélisation statistique à partir de données réelles fournit quant à elle des modèles empiriques capables de prédire les performances d'une PACM et peut aider à l'identification de paramètres critiques pour optimiser la conception du système et définir les paramètres opérationnels. Les modèles numériques de la structure des biofilms ou des performances des piles publiés jusqu'ici sont fondés sur des jeux d'équations physiques et biochimiques qui décrivent le système suivant les aspects que les auteurs considèrent. Ces modèles sont de plus en plus complexes et prennent en compte à la fois le développement des bactéries, leurs interactions, le transport de masse ou les champs électriques. Mais actuellement, aucune PACM, encore moins celles fonctionnant à partir d'inoculums et de substrats complexes, ne peut être complètement décrite par de tels modèles. Il est donc très difficile de construire un modèle numérique de ce type prédisant le comportement d'une pile. En revanche, les modèles statistiques basées sur les données réelles peuvent construire une relation mathématique entre des variables d'entrée (configuration du réacteur, paramètre d'alimentation etc.) et de sortie d'un système (puissance électrique, caractéristiques du biofilm, consommation du substrat, etc.), qu'importent la nature et l'importance de ces variables. Ces modèles présentent donc toujours la PACM comme une « boîte noire » où la pertinence physique de l'équation générée n'est pas garantie, surtout à partir d'un jeu de données limité. On ne peut donc pas s'appuyer uniquement sur ces modèles, mais les deux approches semblent utiles. Malgré d'évidentes limites à leur application à certaines études (peu de conditions différentes, peu de paramètres suivis, peu de répliques, etc.), ces modèles statistiques peuvent par contre être utiles pour extraire des informations de l'amas de données considérables produites par les nombreux travaux issus de cette communauté scientifique. On peut ensuite imaginer l'utilisation de méthodes plus complexes issues de la théorie des systèmes ou de l'apprentissage automatique pour identifier des paramètres décisifs parmi ces données.

Nous avons mis en évidence dans ces travaux deux aspects importants pour l'optimisation de la production d'électricité d'une PACM : le mode de connexion de l'anode au circuit

externe et le régime hydrodynamique à l'intérieur du réacteur. Outre le constat des différences de puissance produite en fonction des conditions, nous avons tenté de généraliser ces résultats en les couplant aux observations microbiologiques pour comprendre et expliquer les performances des PACM. Ainsi, ce travail a montré que les collecteurs de courant anodiques ne sont pas uniquement des pièces de métal reliant l'anode au circuit externe, mais qu'ils influencent la structure du biofilm en modelant les lignes de courant et le champ électrique. Il a ensuite été montré que l'augmentation de puissance n'est pas proportionnelle au débit sur une large gamme et que le comportement d'une PACM dépend peut-être du régime hydrodynamique appliqué (laminaire, intermédiaire, turbulent). En parallèle, des résultats intéressants à propos de *Geobacter* sont apparus. Il a en particulier été mis en évidence que son abondance n'est pas linéairement corrélée avec la puissance, que la PACM fonctionne en batch ou en flux continu. Mais on peut tout de même noter une grande augmentation de la densité de *Geobacter* lorsqu'une circulation en continu de l'électrolyte est mise en place, ce qui montre que le développement de *Geobacter* est influencé par les conditions opérationnelles de la pile. On en retient que la relation entre les paramètres de configurations et d'opération d'une PACM et leur impact sur les communautés mixtes anodiques en général et sur *Geobacter* en particulier ne sont pas simples. Cela semble créer différents effets sur la sélection bactérienne, l'électro-activité de *Geobacter* ou les interactions entre membres du biofilms. Ces effets sont difficiles à démêler, en partie à cause de la complexité de l'inoculum utilisé et du fait que ces inoculums, même s'ils proviennent de la même source, ne sont probablement pas parfaitement reproductibles. En effet, la composition des boues séchées dont ils proviennent varie au quotidien avec le fonctionnement de la station d'épuration qui les génère. *Geobacter* n'en reste pas moins un membre important du biofilm anodique, mais la façon dont les conditions de fonctionnement de la PACM déterminent son abondance et son électro-activité n'est pas très claire. Pour éclaircir ce point, davantage d'information sont nécessaires sur les caractéristiques de chaque clade, la manière dont ils sont sélectionnés au sein du biofilm et leurs interactions avec les autres membres du biofilm.

La puissance maximale produite a été modélisée à partir des paramètres des PACM. Ces résultats doivent être interprétés avec beaucoup de prudence au vu du faible nombre d'observations utilisées dans ce modèle. Le but de cette modélisation est principalement de montrer qu'il est possible et intéressant d'utiliser ces techniques dans le développement à grande échelle des PACM. Une rapide simulation avec le modèle généré par LASSO montre que le débit est le paramètre qui a un effet maximal sur la puissance produite. La longueur et la largeur du réacteur améliore la puissance en s'allongeant, mais dans une mesure bien moindre que le débit, même si l'on peut décrire une amélioration de la puissance notable avec une augmentation de la largeur du réacteur jusqu'à 15 cm. Voici par exemple le point

de départ d'une série d'optimisation : conserver une longueur de 35 cm, élargir le réacteur à 15 cm et augmenter le débit dans les limites de résistances de la PACM en s'attachant à avoir un flux le plus régulier et homogène possible dans le réacteur et vérifier la validité du modèle par de nouvelles observations. En l'occurrence, cela suggère qu'une PACM de grande dimension avec la configuration actuelle n'est pas un réacteur optimisé, et qu'il serait plus judicieux de multiplier celui-ci et d'associer ces modules afin d'additionner leurs puissances. Cela aurait d'ailleurs l'avantage de limiter les problèmes techniques inhérents à la fabrication de PACM à cathode à air (étanchéité du réacteur, limitation des tailles de cathodes etc.), ce qui n'est pas négligeable au vu de notre expérience de construction en laboratoire…

Chapter I - Literature Review: MFC as a Technology for Wastewater Treatment Plant

1. Wastewater treatment plants: energy, economic considerations and resource protection

Environmental and associated economic issues are always an important challenge for society. Depletion of fossil energies and their price increase, protection of natural resources, like water, and the need of their recycling foster the emergence of alternative solutions to save energy and develop renewable energies [1]. Governing bodies, like the European Union, are well aware of the effort that has to be made and have set objectives to increase the share of renewable energies in energy consumption to 20 % [2].

Wastewater treatment plants are good examples of facilities where these ideas are currently defining new standards and spurring new technologies. What is at stake is important because water and sanitation services are the field requiring the highest energy expenditure, between 5 and 20 % of electricity consumption of a French city [3,4]. France has around 20,000 WWTP [5] of which 60 % use activated sludge [6]. This technique eliminates the organic load contained in wastewater due to bacteria metabolism. When concentrated and under aeration, those bacteria form flocs and can efficiently degrade carbon compounds, i.e. organic matter, the most easily removable part of the water pollution load [6]. These flakes finally settle and form sludge that is then separated from clean water. The water is released afterwards or undergoes other treatments (phosphorus, metal, micropollutant removal, etc.).

Energetic and economic aspects of wastewater treatment are closely monitored. In France in 2011, it was estimated that 60 kWh per inhabitant per year was used for wastewater treatment [7]. Usually electricity consumption in WWTPs is expressed as kWh needed to eliminate one kilogram of BOD_5. BOD_5 is the amount of oxygen needed for microorganisms to oxidize organic matter to CO_2 over 5 days and, hence, represents a fraction (usually about 68 %) of the biodegradable organic content. Large WWTPs (*i.e.* with a treatment capacity for communities with more than 10,000 population equivalents or PE) using activated sludge consume in average 3.4 kWh/kg BOD_5, meaning that a 100,000 PE WWTP has an electric consumption of 7.191 GWh per year. This treatment is very efficient but energy-greedy mostly because of aeration needed for those aerobic bacteria. Indeed aeration system

account for 40 up to 80 % of consumed energy of wastewater treatment lines [8]. Several processes in wastewater treatment plants are also requiring a lot of energy, like effluents pumping, thermic treatment of sludge or deodorization.

Strategies for energetic optimization are put in place, including more efficient equipment and sensors for a better management of energy consumption, correct organic load of the wastewater, biogas production from sludge digestion, micro turbine or wastewater heat recovery [9]. But even if these solutions allow a lower environmental footprint, they often need a high maintenance cost which limit their economic interest. So additional innovative technologies taking advantage of energetic potential of wastewater and sludge could help lowering the costs of WWTP exploitation, and even lead to plants with a positive energy balance.

Estimate of wastewater energetic content exceeds chemical energy than is needed for its own treatment. This energy lies in the electrons of the C-C bonds of molecules. Calorimetry analysis of raw domestic wastewater from a WWTP in Toronto showed that it contained 14.7 kJ/g COD (Carbon Oxygen Demand, *i.e*. the molecular oxygen needed by chemical oxidants to completely oxidize the total matter, organic and inorganic), namely 6.46×10^3 kJ/m^3 [10]. The 35,000 m^3/day of wastewater treated by this WWTP has been calculated to contain 9.3 times more energy that what is needed for its treatment. Another study based on the previously measured value of energy per COD mass calculated that a domestic wastewater with a COD content of 500 mg/L would actually contain a volumetric energy of 7350 kJ/m^3 or 2 kWh/m^3 [11]. In comparison with the energy demand for aeration with activated sludge, which ranges from 0.2 to 0.4 kWh/m^3 [12], the energetic potential of domestic wastewater and the interest of its recovery drives much of the interest in applied MFCs.

2. Microbial fuel cells and wastewater

2.1. Principle

Microbial fuel cells (MFCs) are one approach to recover energy from wastewater. This energy in the form of organic matter can be consumed by microorganisms that are present as a rich and diverse population in wastewater. Since 1911 with Potter's work [13], we know that some bacteria, called electroactive bacteria, can produce electrical currents. MFCs use those bacteria as a means to extract energy from wastewater. Usually MFCs are formed in

an anaerobic compartment (*i.e*. a medium that does not contain dioxygen) containing an anode (Figure 4). This compartment is fed with a nutritive solution and inoculated with anaerobic bacteria (which cannot grow in presence of dioxygen) that could be derived from wastewater microflora. Some bacteria can develop on the anode and form a biofilm, a complex and robust bacterial community attached to the anode. These bacteria oxidize organic matter diffusing from the bulk solution. While electron acceptors are relatively limited, a range of anaerobic metabolism can be expressed and among them, the electroactive bacteria are able to use the anode, which is made out of an electrically conductive material, as the final electron acceptor of their anaerobic respiratory chain. Electrons are thus released to the anode and then travel to the second electrode through an external electrical circuit. This second electrode, the cathode, can be in another compartment filled with a catholyte (*i.e*. the electrolyte in the cathodic compartment) and linked to the anode compartment by a membrane or a salt bridge, or, if it is an air-cathode, it can be directly in contact with the anolyte (*i.e*. the electrolyte in the anodic compartment) on one side and the air on the other. Protons released in the anolyte by bacterial oxidation diffuse to the cathode, where it allows a reduction reaction with electrons from the anode. In the meantime, the flow of electrons between the two electrodes generates an electrical current that can be harnessed.

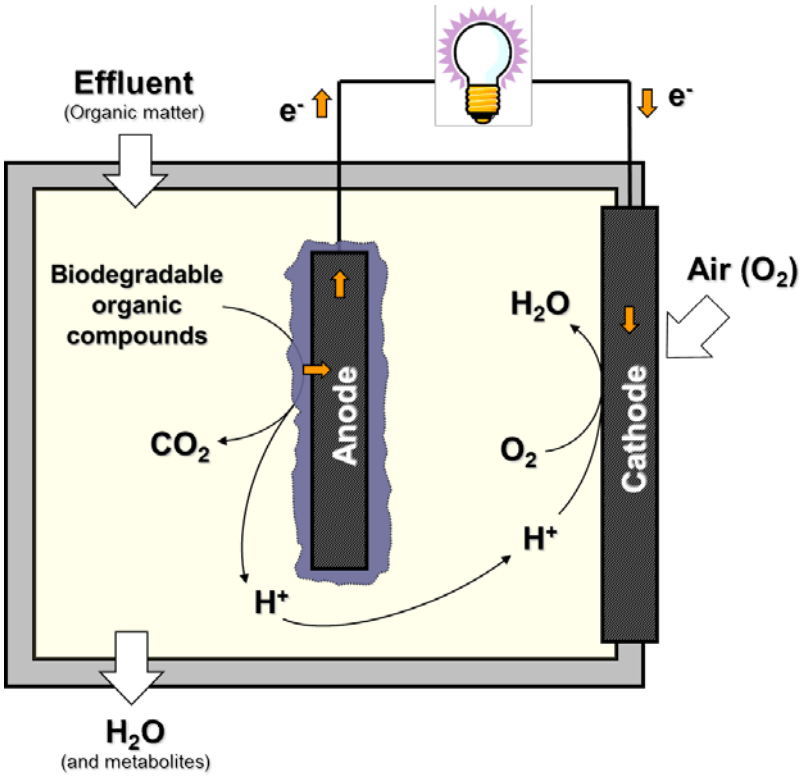

Figure 4. Principle of an air-cathode MFC.

2.2. Interest for WWTP

Several aspects of MFC's technology make it a suitable and interesting alternative solution for WWTPs. First, wastewater contains both microorganisms and the organic matter on which they will feed. Thereby, MFC can operate without any external supply of inoculation or substrate [14]. Secondly, MFCs are producing electricity directly, a widely and easily used form of energy. Despite low voltage and low power, efficient energy scavenging is possible through the development of electronic circuits that track maximal power point and allow energy recovery from MFCs association showing deleterious hydraulic and electrical couplings [65,66]. No intermediate processing to recover energy is needed as it is the case for methane produced from fermentation and that has to be combusted to be turned into usable energy (heat, and then electricity with a lower yield) which imply energetic losses [15] and the release of air pollutants [16]. In addition, while producing electricity, MFCs reduce wastewater organic load as anodic bacteria degrade (metabolize) the organic matter. This contributes to wastewater treatment by removing a part of the pollution load, mainly organic compounds in municipal wastewater. This organic load reduction is classically done by energy intensive aerobic microorganisms. Therefore, MFCs could reduce operational cost by reducing aeration required, the most expensive step in water treatment. Another reduction of costs would arise from sludge production decrease. MFC, as an anaerobic process, produce on average only 20 % of the sludge of an aerobic process [17,67]. This low sludge yield represents economical savings because of two main advantages: reducing the size of aeration tank and of the secondary clarifier (which allows separation of sludge and clear water after the aeration step) and thus the cost of operation and infrastructure, and by limiting sludge treatment, which requires effort and energy [14].

Besides savings on WWTP operation, MFCs could provide substantial savings and/or income through electricity production. A typical large French WWTP that treats 100,000 PE consumes around $6x10^6$ kWh of electricity [7] and treats $65.7x10^6$ m^3 of wastewater per year as 1 PE is equivalent to 180 L per day [18]. In the meantime, a MFC yield is 0.65 kWh/m^3 [11], based on a 80 % COD removal and 40 % coulombic efficiency. As a result, this typical WWTP could produce $42.7x10^6$ kWh/year such that its current electricity bill represents only 14 % of the total potential electricity production by the MFC. At the national level in France, this technology would not be a negligible source of energy. The total volume of treated wastewater in France is about $7x10^9$ m^3/year (in 2008) [19] while the total electrical consumption of the country was $475.4x10^9$ kWh (in 2015) [20]. So, $4.55x10^9$ kWh/year are potentially available from MFCs, which represents almost 1 % of the total French electrical

consumption. Thereby, aside from ecological interest, MFCs have the potential to be economically profitable.

2.3. Comparison to other side technologies

Other technologies are currently operational or in advanced development to produce and valorize renewable energies in WWTP and have thus to be compared with MFC. The main alternative is the production of biogas from anaerobic digestion of activated sludge obtained after the aeration step. This biogas contains between 50 to 75 % of methane and between 20 to 30 % of carbon dioxide. The number of these installations is increasing in France with a forecast of 130 equipped WWTPs in 2020 [4]. Indeed it provides several advantages such as the reduction of sludge volumes to treat, their stabilization and deodorization, the production of a renewable and storable energy, and the reduction of CO_2 emissions [9]. At the same time, there are still constraints about methane production. First of all, methane production from wastewater requires a large financial investment for infrastructure and maintenance (and explosion risk management) mostly because of biogas combustion, which is the intermediate step between gas production and available electrical energy [9]. Co-generation is the main way of transforming this biogas and this yields, on average, 35 % energy as electricity, 55 % as heat, and 10 % losses [21]. In addition, the presence of some undesirable gases cannot be avoided, such as siloxanes, chlorinated and fluorinated gases and H_2S, which can damage pipes and, hence, increase maintenance costs. Even if biogas production is maximized and its use optimized, it could only cover 50 % to 80 % energetic needs of wastewater treatment plants [9].

Besides methane production, other less widespread technologies are helping WWTPs to recover a maximum of wastewater energy. This is the case for heat pumps that recover heat from effluents that usually enter the WWTP at between 12 and 25°C or from hydraulic turbines producing mechanical energy [9]. Another example is hydrogen production from biomass fermentation. However, only 15 % of the energy from the dissolved organic matter in wastewater can be recovered as hydrogen [22]. The primary fermentation end products during biohydrogen formation are acetic and butyric acids, which have been shown to be suitable substrates for MFCs [23]. MFCs could extract energy from the 85 % energy left. This also shows that association of different systems, in particular developing technologies such as MFC, could increase energy production from wastewater and limit losses.

3. MFC scale-up toward application

3.1. Development in MFC research area

Interest in MFCs has grown especially during the last 20 years for developing the technology to a level of efficiency good enough to be economic for concrete applications. Today, Emefcy is the only company using MFC technology for electricity production via the Electrogenic BioReactor, a wastewater treatment unit, whose produced electrical current is able to power the treatment unit. Otherwise, laboratory research is still working to improve the technology. Several potential process-limiting factors of MFCs have been investigated. The difficulty is determining which parameters are critical to increasing power production in laboratory studies and which are critical to scaling up the MFC process for real world applications.

3.1.1. Lab-scale engineering

The initial research dealt with some lab-scale engineering with tests of different configurations of the reactor [24,25], anode and cathode characteristics [26–28], operational parameters like substrate [29,30], flow condition [31,32] and external resistance [33,34]. Among interesting advances, anode chemical modification succeeded in increasing the power density by 24.5 % by modifying the anode with MnO2 electrodeposition [68] and increased the power density by 38.1 % after modification of the anode with formic acid [69]. Some work with different flow regimes showed improved power as the power density increased from 19.4 to 37.4 mW/m² by increasing the flow rate from 0.8 to 4 mL/min [31]. Interesting improvements in power density were achieved in these studies, but they were not easily generalizable as configuration or material changed. Process engineering could be used to better characterize and understand how hydrodynamics affect MFC performance. MFC are bioreactors and refined industrial approach for scale-up of other bioreactors could be of interest for MFC development. More structured and fundamental knowledge is also needed to predict and improve electricity production from every MFC.

3.1.2. Anodic microbial population study

One important fundamental aspect of MFC is the anodic microbial population. Many bacteria are capable of electricity production and because MFC configuration diversity leads also to microbial community diversity, the insight into the role of the bacterial community on power production is difficult. A lot about structure, composition and functioning of anodic biofilm is still to be discovered despite recent advances concerning two major genus *Geobacter* and *Shewanella's* metabolism and strategies for electron transfer [35,36]. Molecular and microscopy technology development has improved studies about anodic biofilms. Sequencing is now widespread and useful for determining potential functions encoded by bacterial genes and identifying members of the biofilm. Identification is done by targeting the 16S ribosomal RNA (16S rRNA) gene, which is the gene coding for a component of the small subunit of prokaryotic ribosome. This gene is highly conserved among bacteria and archaea and thus widely used for phylogenetic studies. Sequencing of MFCs identified known electroactive bacteria as belonging to the phyla *Proteobacteria*, *Acidobacteria*, *Bacteroidetes* and *Firmicutes* [37]. Sequencing data requires considerable bioinformatics, so quantitative polymerase chain reaction (qPCR) is used to identify specific members or functions in an anodic community by targeting specific genes. For example, the cell density of key phylotypes were monitored by qPCR as a function of time and anode potential [70]. *Geobacter* spp. numbers were correlated with particulate organic carbon and ammonium concentration. In addition of the analysis of genes present in MFCs, (extracted DNA), transcriptomic studies have focused on messenger RNA, (*i.e*. on which genes are actively being transcribed). For example, a transcriptomic microarray analysis showed that when the anode was available as final electron acceptor (closed circuit MFC), *Geobacter sulfurreducens* biofilms had higher transcript levels of *pilA* genes (used for coding a pili structural peptide) and *OmcB* and *OmcZ* genes (both coding for outer c-type cytochromes) than when this bacterium could only use dissolved fumarate as an electron acceptor (open circuit MFC) [71]. This suggested that *Geobacter sulfurreducens* was able to develop a specific strategy to transfer electrons to an electrode. To obtain physical and spatial information about an anodic biofilm, one could use microscopy with fluorescence *in situ* hybridization (FISH). This would visualize specific bacteria due to a fluorescent DNA probe targeting the specific 16S rRNA gene coding region. This technique was used to confirm and visualize a synergistic effect for growth on an anode of *Geobacter sulfurreducens* and *Shewanella oneidensis* in co-culture compared to each separately [72]. Few studies have used stable isotope probing (SIP) to identify special metabolic processes to-date. Substrate enriched with heavier isotope (*e.g*., C-13) is fed to the microorganisms. Then a biomarker, usually DNA, is used to differentiate between microbes that used the enriched substrate from those that did not. *Hydrogenophaga* sp.

appeared to be a hydrogenotrophic electroactive based on this SIP approach [73]. *Hydrogenophaga* sp. might be in a syntrophic cooperation in acetate-fed MFCs with *Geobacter sulfurreducens*. Through these initial studies, molecular biology and microscopy greatly improved our fundamental knowledge of anodic biofilm composition, electron transfer mechanisms or interaction between bacteria. Nevertheless, the initiation and development of the biofilm, population dynamics and complex interactions between microorganisms in relation to a complex bioreactor environment needs to be further explored.

3.1.3. Electrochemistry tools

While microbiology is a key issue in MFC operations, electrochemistry also plays a role either directly or indirectly. There are several reviews dealing with electrochemical processes in MFCs and the electrochemical techniques used to study them [38–40]. Basic techniques are widely used as common and basic methods for characterizing MFCs. For example, polarization curves are used to monitor current while the whole MFC voltage is swept from open circuit voltage (quasi infinite resistance) to zero resistance. This can be performed by either changing the external resistance [34] or by linear sweep voltammetry with a potentiostat [74]. This measurement evaluates the three different kinds of resistance that arise in MFC systems and that are part of the total internal resistance and limit the power output of MFCs. These three types of resistance are activation overpotential (at low currents, because of charge transfer losses), ohmic overpotential (at intermediate currents) and concentration overpotential (at high currents, due to mass transport losses) [11] (Figure 5a). From this measurement, it is possible to obtain a power curve by multiplying voltage by the corresponding current (Figure 5b) and, thus, determine the maximum power available from the system.

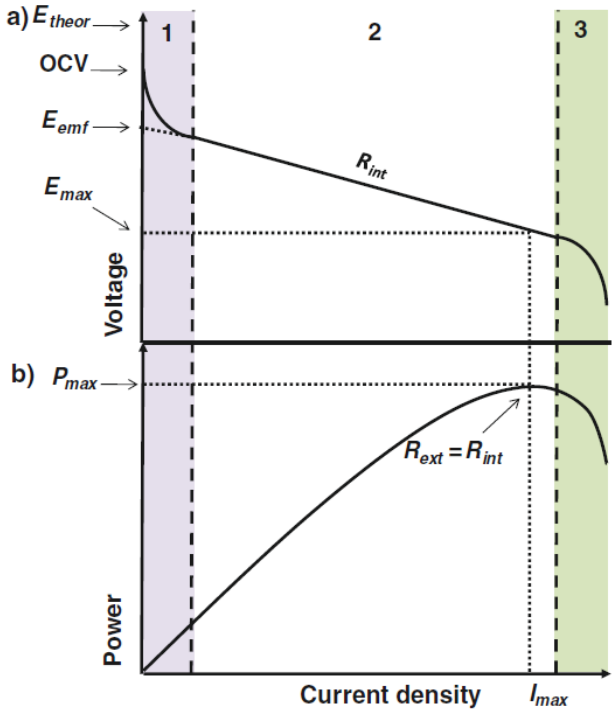

Figure 5. Panel a: Typical polarization curve for an MFC showing the three overpotential zones that affect the cell voltage at increasing current density: 1 activation polarization, 2 ohmic losses, 3 concentration polarization. Also displayed are the variations between the different voltages that can be used to characterize an MFC: E_{theor} > OCV > E_{max} = $E_{emf}/2$; Panel b: typical power curve for an MFC where P_{max} = $E_{max} \times I_{max}$ and is achieved when $R_{ext}=R_{int}$ (from Lefebvre *et al.* [11]).

Another common electrochemical measurement is produced by voltammetry, either linear (one voltage sweep) or cyclic (multiple cycles of forward and backward voltage sweeps), which is easily done with a potentiostat by connecting the anode to the work electrode, the cathode to the auxiliary electrode and placing a reference electrode in between them. By sweeping the voltage at the anode, the current peak when an oxidation/reduction potential of a redox molecule at the interface is reached can be observed. Depending on the scan rate, the peak intensity, their number and potential, electron transfer mechanisms can be investigated and electrode material performance evaluated [38]. For example, cyclic voltammetry (CV) was performed on a wild type *Geobacter* biofilm and on a mutant *Geobacter* biofilm, which lacked different targeted proteins involved in electron transfer [75]. The two outer membrane c-type cytochrome, OmcB and OmcZ, were shown to have different roles in extracellular transfer of electrons: OmcZ is involved in electron transfer in the bulk biofilm through a network of bound mediators, whereas OmcB participates in electron transfer between biofilm and anode [75].

In addition to tools for characterizing MFCs, electrochemical techniques can also be used to set a particular voltage or current condition on the anode biofilm. One such technique is called chronoamperometry and, with the use of a potentiostat, the potential of an electrode

can be set. At the anode, different potentials might affect biofilm activity and microbial cell growth and the use of chronoamperometry could help explore this phenomenon [38]. When an anode was poised (set) at 0, -200 and -400 mV vs an Ag/AgCl reference electrode in an MFC, no influence of the anode potential on the start-up time was observed, but the -200 mV poised anode had the highest power production [56]. An anode potential might exist that optimizes microbial activity and growth in the electroactive biofilm. Rotating disc electrode (RDE) is a common electrochemistry tool that has been applied to MFCs. Mass transfer is controlled by the applied rotational force to the electrode to study kinetic parameters of electron transfer in the biofilm present at the surface of the electrode [38]. Power output and anode resistance were apparently highly influenced by concentration losses, diffusion layer thickness and mixing velocity in MFCs based on the use of the RDE and complementary electrochemical measurements [76]. Unfortunately, the mechanical force of the rotation can destroy the biofilm and therefore a specific MFC set-up is needed and the RDE cannot be implemented in a commonly build MFC.

3.1.4. Electrochemical impedance spectroscopy: focus on an electrochemistry tool

On the other hand, electrochemical impedance spectroscopy (EIS) is a non-destructive technique used to study the electrochemical behavior of the anode in any kind of MFC as long as a reference electrode can be inserted into anaerobic chamber near the anode. With a frequency response analyzer coupled to a potentiostat, a small amplitude alternating signal (between 5 and 10 mV), which does not disturb the biofilm, can be applied to an electrode within a frequency range usually of 100 kHz to 1 mHz and the current response is monitored [77]. Two modes can be used: 2- or 3-electrodes. The 3-electrodes mode can be used to study one specific electrode, the anode or the cathode. For example, to study the anode, which is used as the working electrode, the cathode is used as the auxiliary electrode and a reference electrode is added near the anode. The 2-electrodes mode can be used to study the full cell impedance: one electrode is the working electrode and the other is both the auxiliary and the reference electrode. As detailed above, the internal resistance of MFCs includes different components (charge transfer losses, ohmic losses, mass transport losses). EIS can characterize each of them independently (in a deeper way than cyclic voltammetry) and is thus useful for evaluating strategies to reduce the overall internal resistance. Impedance is usually represented as a complex number and Nyquist and Bode plots are the most common way to graphically represented the impedance data [77]. One way to interpret

them is to fit them to an equivalent electrical circuit (EEC). These circuits are mostly composed of simple electrical elements like resistors, capacitors and inductors that are connected in series and/or parallel. The simple Randles circuit is widely used in electrochemistry to model the interface between a flat electrode and an electrolyte (Figure 6). This consists of a solution resistance in series with a parallel combination of a charge transfer resistance and a double-layer capacitance. This double-layer capacitance accounts for the capacitor behavior due to the electrical charge separation (electrical double-layer) that occurs at any interface between an electrode and the electrolyte. This model circuit depends on several elements : biofilm presence, electrode roughness, temperature, ions concentration, electrode polarization, etc. [77].

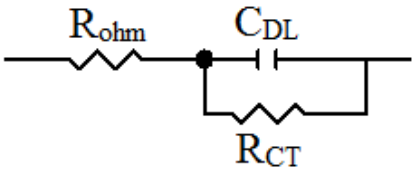

Figure 6. Randles circuit. R_{ohm}: solution resistance; C_{DL}: double-layer capacitance; R_{CT}: charge transfer resistance.

MFC anodes can exhibit more complex electrochemical behavior than this simple circuit and in that case, a more complex equivalent electrical circuit would be needed. Some examples are shown in Figure 7 [78]. New elements could be modeled like constant phase elements (CPE or Q) instead of capacitors for a pseudo-capacitor behavior that takes into account the heterogeneity of the interface or Warburg impedance to account for diffusion limitations [78]. Structures that are more complex can also be used for a more detailed combination of charge transfer processes. Nevertheless, the use of such equivalent electrical circuits must be done cautiously [38,78]. Each electrical element must have a physical meaning in the real system for the EEC to have a relevant data fitting. The impedance data could potentially be fitted with an infinite number of equivalent electrical circuits, so multiplying the number of elements should be avoided, as they would not represent any physical phenomenon. EIS use in MFC studies is more recent than the previously cited electrochemical techniques, but it has already participated in the development of new approaches for MFCs by emphasizing the importance of anode capacitance in power output. While CV and chronoamperometry have shown that electroactive *Shewanella* [79] and *Geobacter* biofilms [80] were able to store electrical charge, EIS showed that the capacitance of the anode increased after MFC inoculation with bacteria [81]. These EIS results were used to suggest that the phospholipid

bilayer of electroactive bacteria cell membrane acts as a capacitor and that it exists a biological capacitance of the biofilm. In addition, a negative correlation between capacitance and resistance of the biofilm that highlights the impact of anode capacitance on power density was observed. EIS was also used to measure capacitance of a MFC anode and to model an EEC that distinguished between capacitance from the anode material double-layer and from the biofilm [82]. The anode material had a high capacitance that was useful in cycles of closed and open circuit in order to accumulate electrical charges at the interface during open circuit and release it when the circuit was closed. The subsequent improved power density was consistent with MFC being used as capacitors and improving power production.

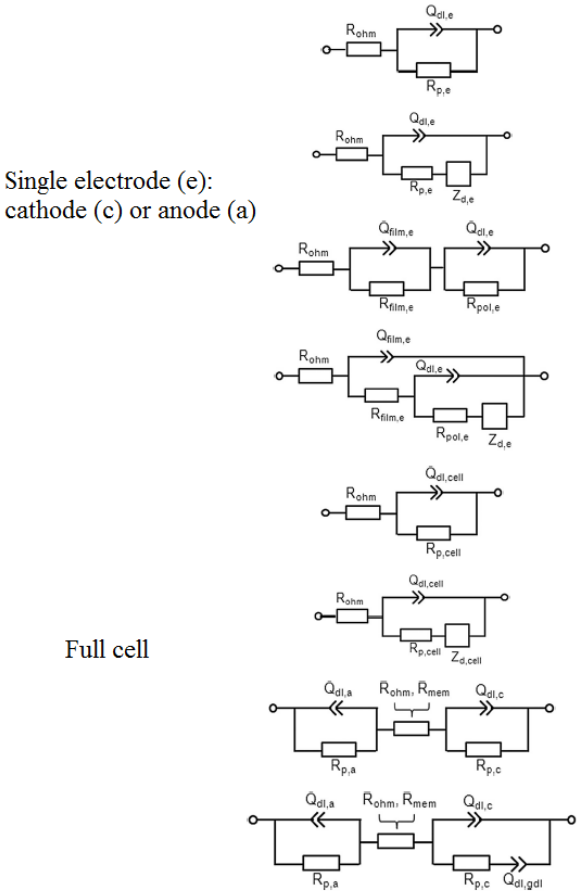

Figure 7. Equivalent electrical circuits used to model anodes, cathodes or full cells. R_{ohm}: ohmic resistance; $Q_{dl,e}$, constant phase element associated to the double layer at the electrode; $R_{p,e}$, polarization resistance at the respective electrode; Z_d, Warburg impedance associated to diffusional limitations; $Q_{film,e}$, constant phase element associated to a film developed at the electrode; $R_{film,e}$, resistance at the respective film developed at the electrode; R_{mem}, membrane resistance (from Dominguez-Benetton *et al.* [78]).

3.1.5. Today's applications of MFC and other BES

Despite these advances and a boom in MFCs research in the 2000s, the absence of a major breakthrough in power output led the MFC community to consider other applications for MFCs and bioelectrochemical systems (BES) than producing substantial electricity even in association with wastewater treatment. Sediment-MFCs [41] or plants-MFCs [42] have been developed for applications that need remote and low power like LED power or biosensors. More broadly, biosensor MFCs have also been developed to monitor pollutants, biochemical oxygen demand, microbial activity or toxicants [43]. Lately, microbial electrosynthesis cells (MECs) have received considerable interest. These systems, constructed as MFCs, are able to produce chemicals and biofuels like hydrogen [44] and organic acids [45] when electricity is provided. Other microbial electrochemical technologies are capable of methane production [46], desalination [47] and electrochemically influenced fermentation for carboxylate and alcohol production [48]. Most of these new BES applications are in their early stages but "classical" MFCs still have potential for large-scale applications.

3.2. Laboratory-based scale-up research

As discussed previously, considerable research concerning MFCs and their performance is ongoing. Unfortunately, a range of different MFC systems are investigated and different parameters are measured so these studies are difficult to compare and it is difficult to extract critical parameters related to power output. This following section is a compilation of MFC research in an attempt to identify these critical parameters. When possible, results were extrapolated based on MFC characteristics to express performance as power, power per unit of anode surface or power per unit of anodic compartment volume.

3.2.1. *In situ* attempts

Since the goal here is to determine scale-up strategies for MFC application in WWTPs, the first step was to examine and evaluate research describing MFC pilots *in situ*, although few such pilot-scale studies have been described. Only four research groups have reported

evaluating *in situ* MFCs between 2011 and 2016 [49–55] (Table 1). All were air-cathode MFCs, which implies that dual-chamber MFCs, which need a proper catholyte with its own recirculation system, do not seem to be adapted to WWTPs. MFCs were directly operated in a WWTP aeration tank, thus, they did not require any supplementary energy for feeding. One MFC with a tubular configuration produced 0.74 mW total or 0.37 W/m^3 of anode compartment volume. This low power output, together with a low COD removal and cathode biofouling might explain the low electricity production as well as the MFC wastewater quality variation over time. The addition of spacers to the brush anode of the MFC increased the power output to 1.2 W/m^3 (Table 1). These results are encouraging for using the aeration tank for MFCs in WWTPs. Other studies have opted for continuously pumping wastewater into the reactor, thus, they avoid managing aeration, flow rate and retention time in the aeration basin. Two tubular and one planar MFCs have been described. Volumetric power densities decreased with increasing anodic compartment volume: 9, 0.6 and 0.464 W/m^3 for respectively 4, 200 and 250 L MFC volumes. The highest reported power density (9 W/m^3) was obtained with a combination of two identical 2 L tubular MFCs in the aeration tank. This power density was obtained despite tubing clogging, membrane biofouling and wastewater quality variations, and therefore, demonstrated the potential of such simple configurations in WWTPs. Nevertheless, this MFC configuration seemed to be more suitable to treat low-strength wastewater as electricity production with high-strength wastewater could not compete with anaerobic digestion. In addition, very large MFCs did not succeed in sustaining the same volumetric power density. The 200 L MFC was made with 96 of the same 2 L tubular MFCs and yet produced less than 10X less power per volume. Hydraulic and electrical connections and association of all these modules could be the cause of power losses. Yet, since the 2 x 2 L MFCs produced significant electricity, an improvement in these multiple modules could be worth considering for future MFC assemblies. The 250 L MFC was made out of a single anodic compartment that contained several brush anodes organized in two layers at the bottom and at the top of the MFC. Identifying the reason for this weak performance is not obvious since the configurations and operation conditions were different in all these cases. However, the flow rate, as this reactor was fed too slowly (42 L/day versus 238 and 400 L/day in the previous studies), or the distance between the brush anode layers (around 16 cm), might prevent the anodes from extracting energy from the majority of the wastewater. Lastly, two studies have been included here because they were using wastewater at a WWTP site, but they were not directly inserted into the wastewater treatment system. The first was continuously fed with fresh wastewater stored in a tank, but it used acetate for its acclimation, had a volume of 4 L filled with activated carbon granules, and used multiple anode/cathode pairs. This resulted in a power output of 3 mW or 0.75 W/m^3, which is similar to other MFC performances. The second was operated under

batch conditions and composed of four modules containing brush anodes with a total volume of 45 L. This resulted in a power output of 0.875 W/m^3, which is also similar to other MFC performances.

Table 1. WWTP *in situ* MFCs installation.

Reference	Volume (L)	Duration (days)	MFC configuration	Anode material	Feeding	Flow rate (L/day)	Power in running operation (W)	Volumetric power density in running operation (W/m^3)
Jiang *et al.* [83]	4	105	Cylindrical anodic chamber with an air-cathode box on top	Activated carbon granules + graphite rods	Continuously fed, from a tank filled with fresh wastewater; used acetate for acclimation	11520	0.003	0.75
Zhang *et al.* [50]	2	400	Tubular air-cathode MFC	Graphite fiber brush	Openly immersed in aeration tank	288	0.00074	0.37
Zhang *et al.* [51]	2	60	Tubular air-cathode MFC	Graphite fiber brush	Openly immersed in aeration tank	288	0.0024	1.2
Zhang *et al.* [52]	4	400	2 tubular air-cathode MFCs	Graphite fiber brush	Continuously fed with effluent pumped from primary settling tank	238	0.036	9
Hiegemann *et al.* [53]	45	275	Stack of 4 air-cathode single chambers	Graphite fiber brush	Fed-batch with primary clarifier effluent	50	0.039	0.875
Ge *et al.* [54]	200	300	96 tubular air-cathode MFCs	Graphite fiber brush	Continuously fed with effluent pumped from primary settling tank	400	0.12	0.6
Feng *et al.* [55]	250	30	Planar air-cathode MFC	Graphite fiber brush	Continuously fed with domestic wastewater pumped from pipeline	42	0.09	0.464

These *in situ* studies show that the application of MFCs in WWTP still requires further progress. So, while few *in situ* studies have been conducted and even fewer have been tested as scale-up pilots, the variations in wastewater quality appear to influence electricity production even at the WWTP scale as confirmed by several laboratory studies [74,84]. In these studies, current generation correlated with organic concentration, conductivity and temperature of the treated effluent [52,53], although this was not generalized over all *in situ* studies (Figure 8). Therefore, while one specific and important feature for scaled up MFCs was not elucidated for improving power output, some common problems occurred during their tests. First problem was clogging and biofouling of cathodes, membranes, and tubing that arose from using municipal wastewater and long-term (greater than a month) operation. Thus, MFCs would probably need to be monitored and maintained to keep the system

operating despite the general robustness of the anodic biofilm. A second major limitation for MFC applications is the cost of the cathode and the membrane (if used) [54,55]. Despite some common limitations, which are linked to power generation or cost, a larger comparison of scaled-up and pilot MFCs is needed to determine the key parameters in electricity production.

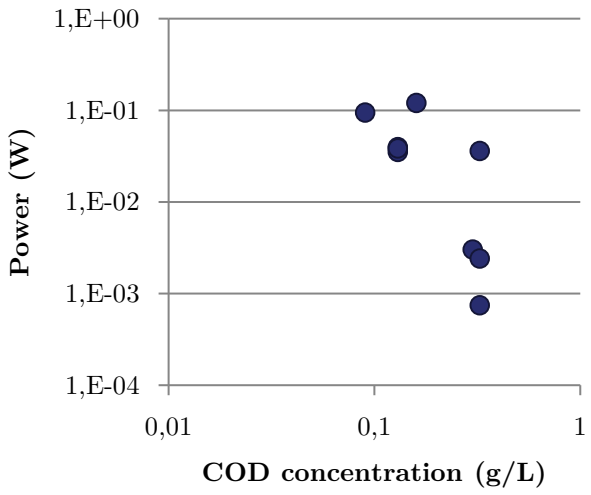

Figure 8. Power output versus influent carbon oxygen demand (COD) for *in situ* MFCs.

3.2.2. Large laboratory MCFs (>10L)

The convenience of working in a lab in order to control different operating parameters and to make measurements that might require heavy or expensive equipment explains why most MFC studies have been performed under laboratory conditions, despite the difficulty (even the impossibility) of continuous feeding MFCs with real wastewater. The lack of real wastewater in these studies limits the simulation of real applications. MFCs with large volumes (volume > 10 L) and operated under 19 different conditions have been reported [85–94]. Several of these MFCs produced more power than the best of *in situ* attempts, however, the best power density (200 and 144 W/m^3) were always with the lowest volumes (around 10 L) [92,93]. Their total power output (*i.e.*, 40 and 1.44 W) was much higher than that of the largest laboratory MFCs: 120 mW in a 100 L MFC, 6 mW and 3.4 mW with 90 L MFCs. Similar to the *in situ* studies, no common parameter shows a clear correlation with power output, other than reactor volume (Figure 9). In the figure 9, operating power (red points) was plotted separately from maximum power based on polarization curves (blue points). The correlation coefficient for all the red points is quite low (R^2=0.107); and without the eccentric

point, the correlation is much improved (R^2=0.608), but only 6 points are included in this analysis. On the same figure, the correlation for maximum power is reasonably good (R^2= 0.750), but the trend is the opposite from that for the operating power. The lack of a consistent trend for both power measurements hinders any conclusions about reactor volume effects. This difficulty might be due to the wide variation of reactor characteristics. For example, a very wide range of anode material, such as graphite fiber brush, graphite felt, activated carbon granules and titanium-coated mesh, was used in these studies. Substrates varied among acetate, glucose, and wastewater and mixtures of these. The different range of operational parameters (electrode number from 1 to 48, influent COD concentration from 0.156 to 10 g/L and hydraulic retention time from 0.125 to 154 h) when compared to power output provides no clear trend. Therefore, conclusions concerning the relevant configuration and operating conditions with so few cases is difficult.

Microbial aspects (anode biofilm development, composition and diversity, detection and numeration of electroactive bacteria and components involved in electrons transfer …) were not reported in these studies (and therefore not compared in figure 9) with one exception [87]. Two pilot-scale MFCs had total DNA sequenced to determine microbial community structures [87]. Both systems showed a similar core biofilm microbial community composition, with *Proteobacteria*, *Firmicutes* and *Bacteroidetes* as major phyla. They detected methanogens and the presence bacteria capable of extracellular electron transfer. However, some differences between the two pilots were observed. The first MFC (60 L, operated at 27°C) had sequences linked to genes coding for outer membrane and periplasmic c-type cytochromes involved in electron transfer to solid electron acceptor. These cytochromes are required for the conductive pili referred to as nanowires [95,96]. These sequences were not detected in the second MFC biofilm (64 L, operated at 10°C) nor were those related to *Geobacter*, which is the well-known and nanowires producer in anodic biofilm [95,96]. Sequences associated with genes involved in electron shuttle synthesis pathways were found in both MFC biofilms. Both direct (nanowires) and mediated (electron shuttles) electron transfer are probably significant (hence detected genes) in the first MFC whereas only mediated electron transfer was probably occurring in the second MFC, which could explain the better power output in the first (10.36 W/m^3) compared to the second (2.56 W/m^3). These two MFCs were operated in different countries and important differences were observed between the microbial community compositions of their inocula. This one study [87] showed that the microbial component of MFCs is a critical parameter that can help to understand and possible predict how the MFC system works. Unfortunately, microbiological analyses are generally lacking in MFC scale-up research although anodic microbial characterization could be used to compare studies and identify trends in order to develop a strategy for scaling-up.

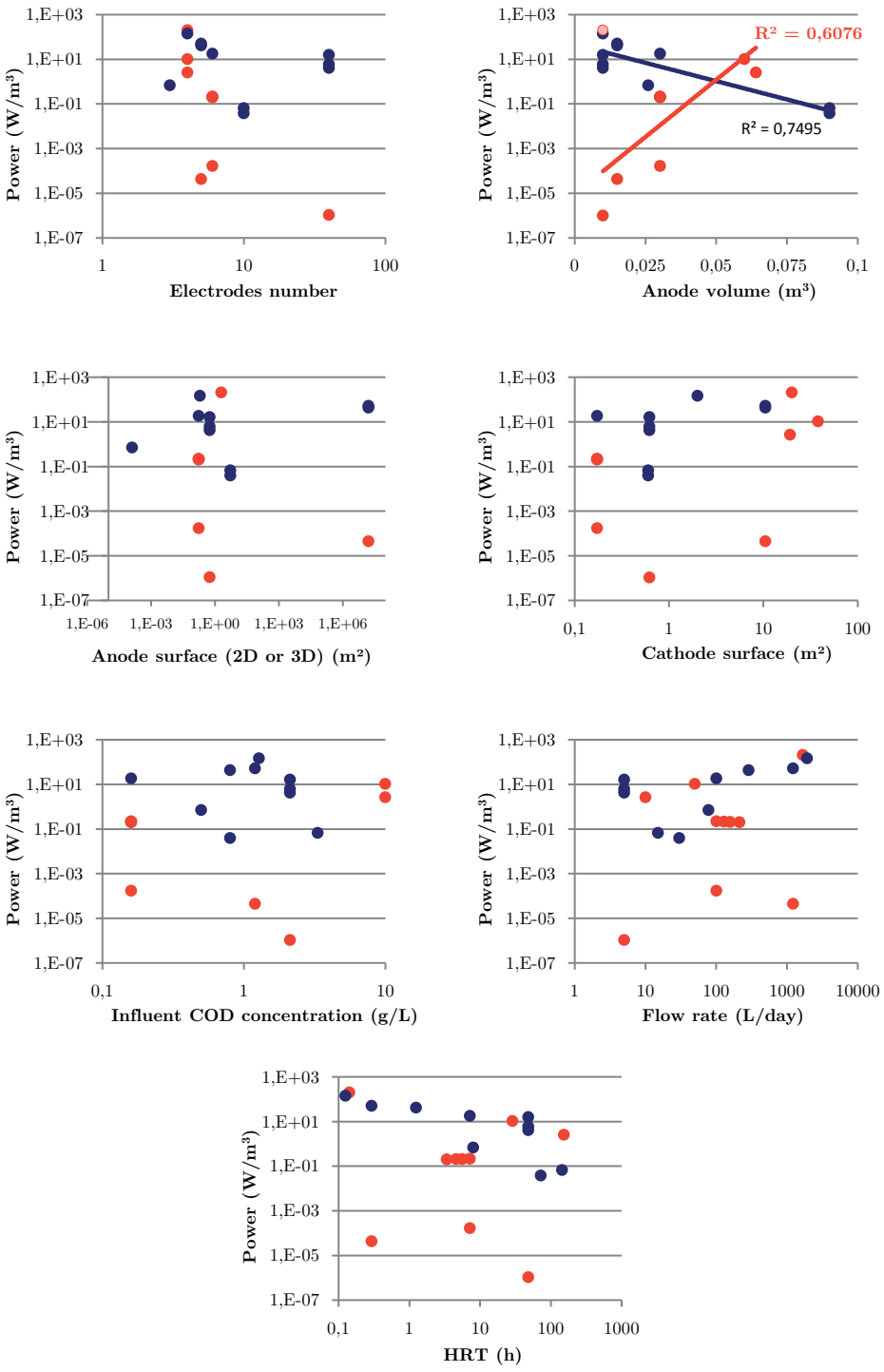

Figure 9. Anode volumetric power density vs different parameters for MFCs larger than 10L (red dots: power while MFC is operating; blue dots: maximal power in polarization curve). The second panel (power vs anode volume) shows the linear regression lines for the data while MFC is operating (red dots) without the eccentric point (light red dot) and from polarization curves (blue dots).

3.2.3. Identified limiting factors

No clear correlation between power output and selected MFC parameters emerged from the comparison of *in situ* or large-scale studies. As the number of such studies was low, statistically relevant correlations were unlikely, therefore, 230 case studies from 2003 to 2016, which related to electrical performance improvement at any scale, including the above works related to scale-up and *in situ* attempts were used to evaluate possible trends in MFC power prediction.

As a start to identify what is driving electricity production in a scale-up strategy, characteristics directly linked to size were compared. The anodic compartment volume and the anode geometric surface (in case of planar electrodes like carbon cloth and paper or graphite plates) are not clearly drivers of power output (Figure 10). In figure 10, the correlation for the relationship of the anodic compartment volume with the operating power was extremely low (R^2=0.029, regression line not shown) as was that (R^2=0.342) for maximum power (blue points – polarization curve). Specific surface of planar anodes was deliberately not taken into account here, as it and its electrical resistivity are characteristic of the material. On the other hand, concerning "3D" materials, such as graphite granules, activated carbon granules and graphite fiber brushes, predicted total surface areas were estimated from references ([97] for graphite granules, [98] for activated carbon granules and [99] for graphite fiber brushes). Despite being more prone to clogging and thus reducing treated effluent volume, the "3D" materials greatly increase anode surface apparent availability. Their potential as scaled-up anodes is often suggested [49,99,100]. Nevertheless, the comparison of electrical performance from MFCs using 2D or 3D anodes does not show an improvement in power output (Figure 11). Cathode surface for air-cathode MFCs is also a characteristic directly linked to size. Increasing this surface has been described to have a positive impact on power production [101,102], but literature data here with cathode surfaces ranging from 4.9 cm^2 to 37.9 m^2 do not illustrate a clear increase in power output when the cathode surface is increased (Figure 12). In summary, the different MFC physical dimensions cannot be used alone to predict electrical performance.

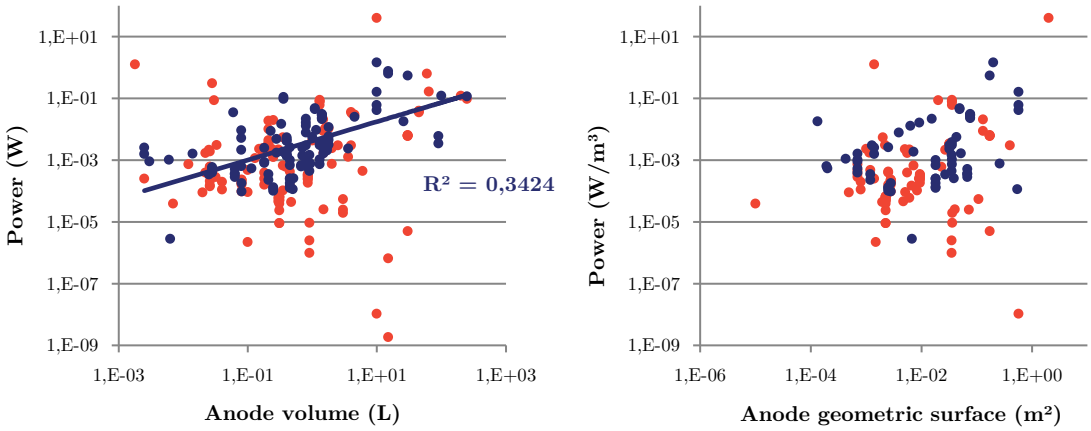

Figure 10. Power vs anode compartment volume and anode geometric surface (red dots: power while MFC is operating; blue dots: maximal power in polarization curve). The first panel (power vs anode volume) shows the linear regression line for the data from polarization curves (blue dots).

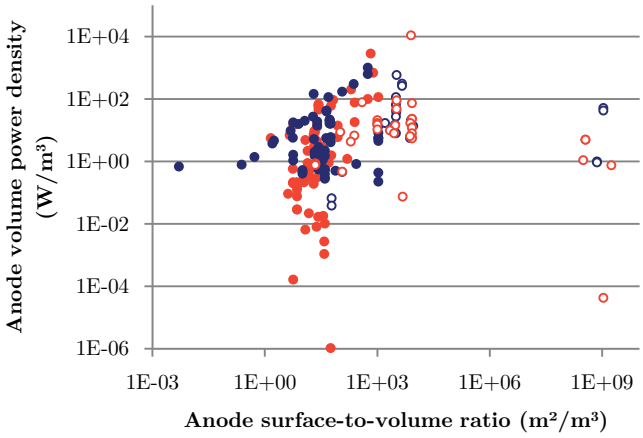

Figure 11. Volume power density vs anode surface-to-volume ratio for 2D (closed dots) or 3D anodes (open dots) (red dots: power while MFC is operating; blue dots: maximal power in polarization curve).

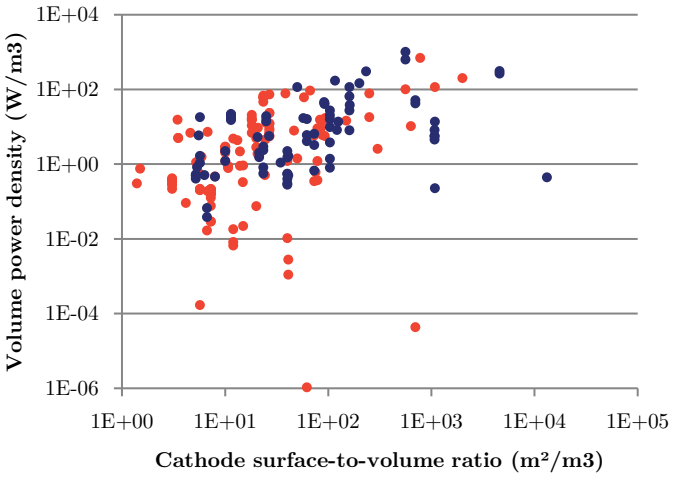

Figure 12. Volumetric power density vs cathode surface-to-volume ratio in air-cathode MFCs (red dots: power while MFC is operating; blue dots: maximal power in polarization curve).

Inoculum sources and carbon substrate can be mechanistically linked to anodic biofilm development and selection and could thus be reliable parameters for predicting power output. Most of the reported studies used biological material from already operating MFC (effluent or anodic biofilm), sludge or wastewater. Inoculum from previous MFCs are associated with relatively good power outputs up to 2.87 k W/m^3 (Figure 13A). This inoculum has already undergone selection for anode utilizing bacteria, anodic biofilm, and anaerobic conditions. This enriched inoculum could provide a more efficient start to electroactive biofilm development. Nevertheless, MFCs using fresh sludge and wastewater can also exhibit comparable power with values up to 779 W/m^3 for sludge and 11 kW/m^3 for wastewater. Therefore, pre-selected inoculum is not necessary for good electroactive biofilm and power output. Inoculum from pure cultures of known electroactive bacteria, such as *Geobacter sulfurreducens* or *Shewanella oneidensis*, are often use in fundamental studies, essentially for investigation of outer surface component involved in electrons transfer [36,71,103,104]. In applied MFCs, only three studies used pure cultures [105–107]. Due to the difficulty in inoculation and sterility during operation, anodic compartment volumes were low, ranging from 7 to 800 mL. Even in such small MFCs, the power output did not exceed 27 W/m^3, thus, a mixed fresh inoculum is better for electricity production and one electroactive bacteria strain on its own is not sufficient for electrical performance in applied MFCs. Some other inocula have been tested such as landfill leachate [108], manure [32], sediment [109] although the corresponding MFC power output never reached values previously shown with sludge or wastewater. Similarly with substrate variations, the best power results, which are above 100 W/m^3, were all obtained with the most commonly used substrates, acetate and wastewater (Figure 13B), while MFCs fed with all the other substrates show much lower power output. As a result, the

best power outputs were obtained with material from a previous MFC, sludge or wastewater as inoculum, and acetate or wastewater as substrates. However, as there are much more studies using these conditions, this observation is tenuous and in addition, most of the cases using the hypothetically better inoculum-substrate combinations showed power output in the same range as those rarely used substrate/inoculum combinations.

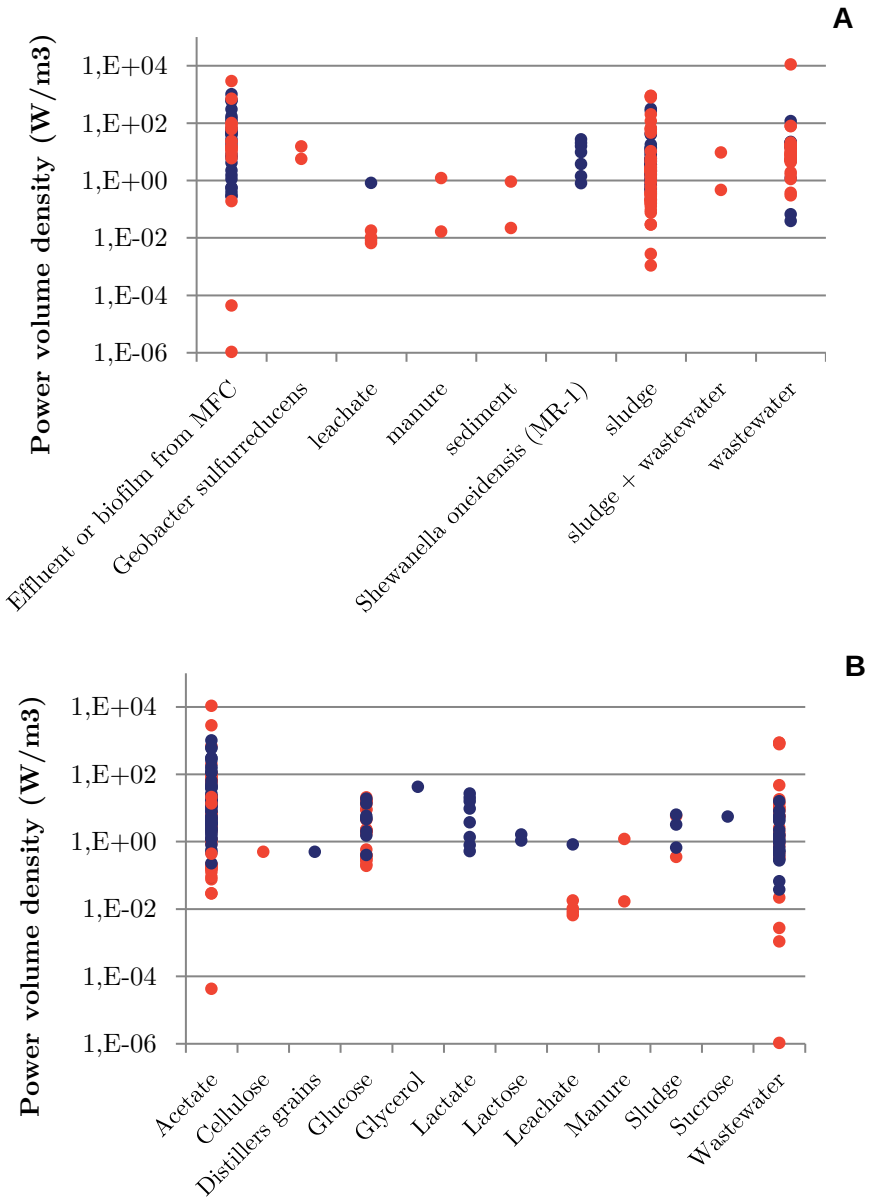

Figure 13. Power volume density depending on inoculum source (A) and substrate (B) (red dots: data from operating MFC; blue dots: data from polarization curve).

Another set of parameters concerns the physical operation of the MFC. Many of these parameters are linked to hydrodynamics and mass transfer. Different studies used a variety of influent flow rates, hydraulic retention times and organic carbon ("COD") concentrations. None of them seems to be correlated to power output (Figure 14A, B, C). The same conclusion could be made for the comparison of external resistance and output power

(Figure 14D). Defining the most important parameters for power production in MFC even by compiling more than 200 MFCs results is not straightforward. The factors driving electricity generation must reside in more subtle aspects not linearly nor singularly explicit. Possible nonlinear and combined parameters were not assessed with the bibliographic data, although as described later, the results from this work were modeled more sophistically.

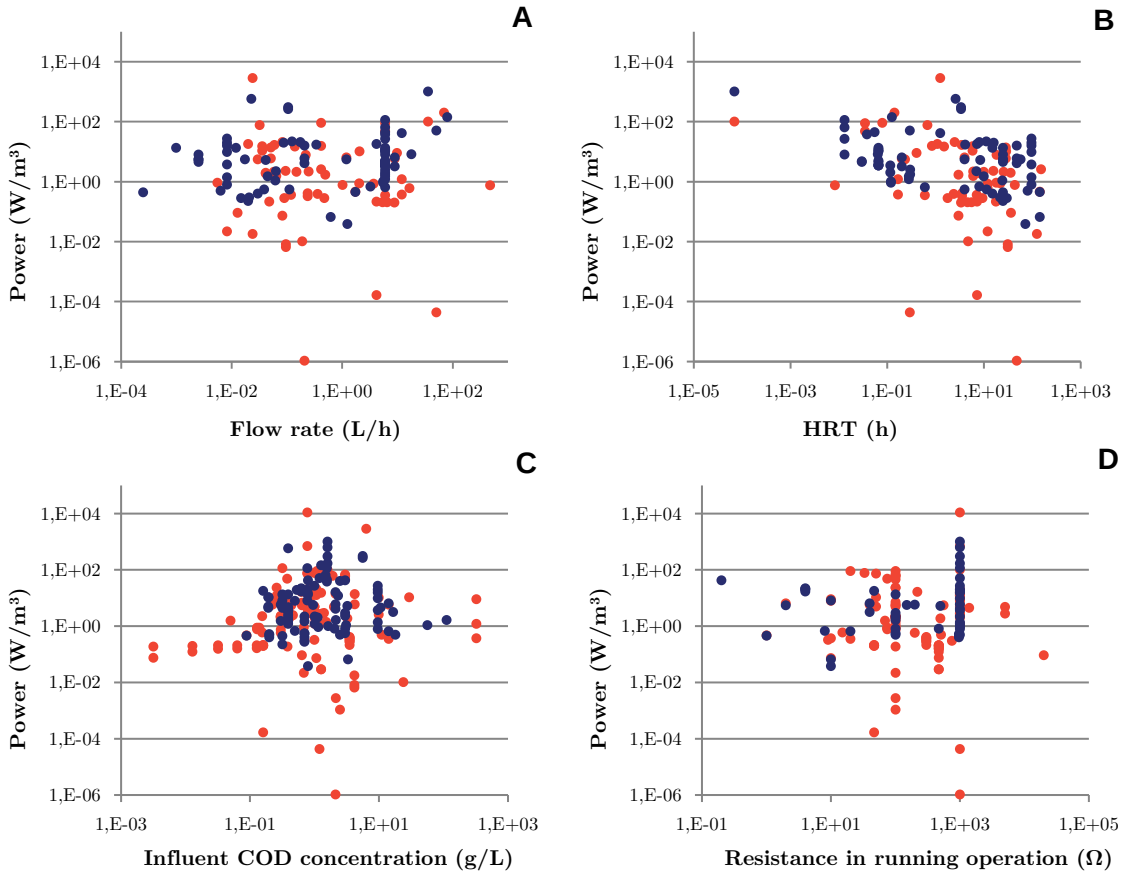

Figure 14. Anodic volume power density vs different MFCs operational parameters: Flow rate (A), Hydraulic retention time (B), Influent COD concentration (C), external resistance (D) (red dots: data from operating MFC; blue dots: data from polarization curve).

4. Objectives of the study

This work aimed at determining new aspects and different approaches to the scale-up problem in MFCs. We have seen above that until now, scale-up dealt more with an engineering method, by testing different configurations, materials or operating conditions. Nevertheless, this approach rarely led to general knowledge (especially concerning microbial

ecology) that could be applied in all MFC systems. The characterization of the anodic biofilm was also rarely addressed and instead studies went from the application under one condition (new design, particular flow rate of substrate concentration, use of a specific anode material, etc.) to the resulting electrical performance, even though this effect is necessarily due to modified biological and electrochemical responses. The understanding of these intermediate mechanisms could help generalize MFC improvements. This work here also took into consideration the hypothesis that typical scale-up efforts modify specific parameters that become significant at large scales. They would in turn affect the anodic biofilm and its efficiency of electron transfer to the anode and that could explain electric yield variations.

Among these parameters, current collectors have a growing importance as the anode size increases while scaling-up MFCs. More electroactive bacteria would develop on a larger anode surface, but if electrons could not flow efficiently from their transfer site to the cathode because of poor connections, any configuration or material improvement will be unsuccessful. That is why one part of this work was dedicated to this aspect. Hydrodynamics would also have greater importance in scaled-up MFCs than in small lab-scale MFCs for which it is often not considered when operated under continuous-flow in the lab. Given that the easiest and most direct way for MFC installation in already existing WWTPs would be in treatment flow, the system should be able of using continuous flow. Therefore, hydrodynamics need to be considered for scaling-up. This was done with a process engineering approach, which is not common in MFC studies even though MFCs are bioreactors. This approach considers multiple physical and chemical parameters globally rather than only one parameter. Dimensionless numbers are often used in such studies and can highlight correlations between outputs (power production, voltage, biomass, etc.) and one or a combination of reactor parameters. This approach was used in this work to characterize reactors of increasing size that are operating under continuous-flow conditions. Relationships between parameters and energy production were described with dimensionless numbers that could help understand and predict MFC performance.

4.1. Current collectors

Current collectors have not received any significant attention as a limiting parameter in MFC scale-up. More surprisingly, most MFC reviews dedicated to describing the challenge of scale-up and applications did not even discuss issues that could arise from current collector limitations. While some reviews mentioned this issue, they were concerned with either obviously bad electrical contacts with 3D granules anodes [28] or with cathodes when they

were involved in degradation and cost problems [110]. When reviews dealt with anodic current collectors, their importance for increasing anode conductivity and power production were cited [111] and categorized as « ohmic voltage loss sources » along with membranes and electrolyte. In addition, studies concerning new MFC configurations for large-scale applications did not often describe their collector system and rarely discussed the importance of them for power output. This was particularly true for current collectors of flat anode, made from carbon cloth or graphite felt, for example. Some only described the material, like titanium [94] or copper [112], used for electrical wires. As it was usually considered that current collector's unique problem is anode conductivity, additional information was rare. Dewan *et al.* used copper wires and checked that the resistance of the electrical connections was lower than 1 Ω [107]. Ewing *et al*. used titanium woven into a graphite felt anode and connected to copper wires that ensure a low resistance from every anode point (< 1 Ω) [41]. But Liu *et al*. recognized that their current collector, a strip of carbon cloth anode left to extend outside, could be a source of potential loss in their system and proposed a collector plate to reduce electron travel distance and contact resistance [113]. Similarly, Feng *et al*. described the MFC internal resistance as the sum of a resistance proportional to the cross-sectional area of the reactor and a resistance that cannot be normalized and is mainly due to contact resistance between the electrodes and the external circuit [55]. This second resistances is often neglected in lab-scale reactors but should not be ignored in pilot-scale MFCs. As a result, they suggested a predictive equation for similar MFCs to calculate maximal power from a smaller reactor performance but this was not tested on several different MFC sizes. Moreover, this resistance was not directly measured and no detailed hypothesis for its causes and effects were suggested. To our knowledge, only Cheng *et al*. investigated flat anode current collector's impact on power loss [114]. With modeling approach and experimental verification with carbon mesh anodes, they showed power losses and potential drop distribution on the surface arising from resistivity of anode material and current collector configurations. Power loss sharply increased when the anode size was over 0.16 m² with one electrical connection point. Nevertheless, their model was based on the assumption that microbes grow evenly on the anode, which implies that the effect of anode ohmic resistance and potential drop on biofilm development was not considered when evaluating power loss.

Here, we investigated the hypothesis that anode external electrical connections could also limit power production by shaping and restricting the spatial development of microbes. The closer the electroactive bacteria are to external connections, the lower the ohmic resistance for electrons flowing from these bacteria to external connection would be. Since anodic biofilm development was favored under a specific anodic potential [56], potential drop distribution could also shape the bacterial community on the anode. This idea was tested first here in a 1 LMFC with 4 different external connection configurations with carbon cloth

anodes. Power output and anode electrochemical behavior were evaluated in relation to collector number and configuration. Total bacteria and *Geobacter* quantities were assessed in relation to distance to collectors.

4.2. Hydrodynamic parameters

Until now, few studies have explored flow related questions and have mainly focused on residence time or shear stress. For example, Moon *et al*. [115] used a residence time distribution test to assess the flow characteristics of their reactor. This test consisted of injecting a tracer solution in a step input and recording its concentration in the effluent to evaluate the mixing inside and compare the observed behavior to ideal-flow models. In their study, they showed that the MFC with flow characteristic closer to ideal plug-flow had improved electricity generation. Unfortunately, most studies about flow dynamics in MFCs consist of modifying influent flow rate or retention time without examining what really happens to a fluid particle inside the reactor. This can lead to a wrong interpretation if there are fluidic dead zones or short circuits as the actual flow rate or retention time would be different from the theoretical value. On the other hand, Pham *et al*. [116] examined the effect of shear rate of anodic biofilm. High shear rate (about 120 s^{-1}) seemed to result in a denser, thicker, and more electrically productive biofilm with a bacterial community different from that of the control at low shear rate (about 0.3 s^{-1}).

Non-MFC studies investigating effect of fluid flow on biofilm can improve our understanding of the underlying processes at stake when dealing with hydrodynamics. Stewart stated that this effect acted on biofilm development and activity by two important means: transport of compounds into and out of the biofilm and shear forces on the biofilm that cause it to move and detach [117]. Various flow conditions led to different biofilm morphologies [118]. They attempted to optimize flow condition that would enhanced biofilm growth because of a balance between shear force and substrate transport [118]. Fluid velocity improves mass transport by convection, and thus, facilitates substrate supply to biofilm, but led to a denser biofilm where substrate diffusivity was limited. Shear forces have in particular been shown to increase adhesive strength of bacteria on the substratum [119], to decrease the thickness of biofilm and make it more stable [64], whereas biofilm tends to be porous and heterogeneous when these forces are weak [120]. Liu and Tay also suggested that hydrodynamic shear forces were involved in metabolic regulation of energy metabolism in biofilms [121].

To explain and in the end control the influence of hydrodynamic forces on biofilms, researchers introduced fluid mechanic tools and concepts. For example, hydrodynamic boundary layers are linked to fluid velocity profiles at the surface. They are also related to concentration boundary layers that partly determine the efficiency of mass transfer occurring at the reactor walls: convection in the bulk fluid versus diffusion in the layer toward the biofilm. To link these elements to reactor size, electrolyte properties and flow conditions, dimensionless numbers could be used. Picioreanu *et al*. suggested that several of those numbers, like Reynolds, Schmidt or Péclet numbers, currently used in process and biochemical engineering could significantly affect and be correlated to biofilm development [122]. Thus, this approach could be usefully applied to MFC with the addition of electrical aspect to account for electroactivity of biofilms. As hydrodynamic forces and mass transport are influencing biofilm development, they should also affect electron transfer and biofilm electrical resistance. Finally, these dimensionless numbers that describe the MFC configuration and flow could be used to explain and predict electrical performance of MFC and develop scale-up strategies.

This part of the thesis aimed at correlating reactor parameters and power output by running three MFCs with different volumes operated at different flow rates. Several parameters from different science domains: fluid mechanics, electrochemistry and microbiology were monitored and modeled. Dimensionless numbers of the systems, characteristic electrochemical values and quantitative bacterial description of biofilms were used to establish correlations with electrical performance and highlight parameters that appear to drive power output and orient future MFC scale-up.

Chapter II - Materials and Methods

1. MFC construction, operation and monitoring

1.1. Construction of MFCs of different volumes

The choice of the MFC design for these studies was based on several criteria. The design of the MFC was simplified in order to keep the same distance between anode and cathode and the same surface ratio regardless of the size of the constructed reactor. The anode material was chosen so that it could be easily sampled and maintain constant regular flow inside the reactor. As a result, filter-press type reactors were built (Figure 15) [123], which are rectangular channels with two plane parallel electrodes on opposite sides and a flow distributor system at the inlet and outlet to control the flow inside. The anode material was carbon cloth, which was chosen for its conductivity, biocompatibility and ease of installation and sampling. The distance between electrodes was set at 2 cm as suggested to be the balance between a short distance to decrease solution resistance and a long distance to prevent oxygen diffusion to the anode [124]. Cathode reactions are often described as limiting factors in MFCs [27] and increasing cathode surface area improves power output [125,126]. Thus, an air-cathode as large as the anode was chosen to reduce cathode limitations and to keep the same electrode surface area ratio for all reactors to maintain the same influence of cathode performance on MFC operation.

For the study of the influence of current collectors, four approx. 1.0 L planar MFCs were constructed from PVC frames and plates with internal dimensions of 35×14×2 cm^3 (≈1 L) (Figure 16, top). The anodes consisted of 35×14 cm^2 pieces of CCP-2M plain carbon cloth (Fuel Cell Earth, USA) heated to 450°C for 30 min and placed in an ultrasonic bath for 20 min. The resistivity of the anodes was 1.7 Ω.cm. Untreated titanium strips (1 cm wide) were used as current collectors by pressed contact with the anode. Four anodic contacts patterns were tested (Figure 17). An air-cathode with the same surface area as the anode was made out of the same carbon cloth prepared as previously described [127] by applying platinum (0.25 mg/cm^2 of electrode) and four diffusion layers and connected to the external circuit using two titanium strips along each long edge. Based on the internal resistance measured in a similar MFC previously operated, the external resistance was set at 8.2 Ω.

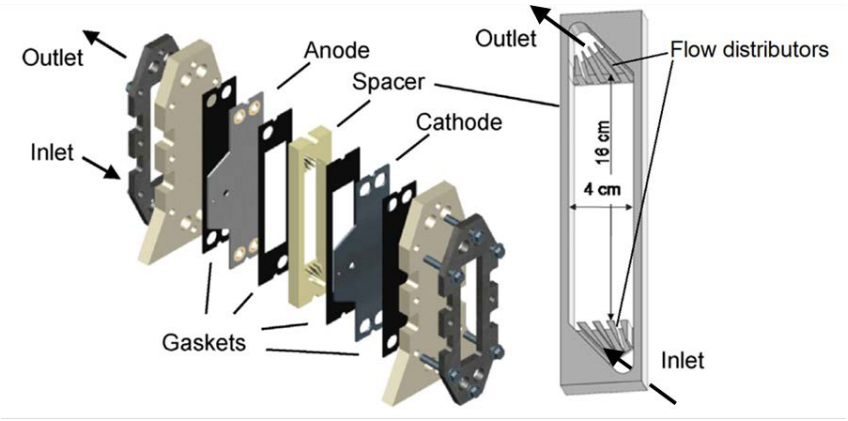

Figure 15. Filter-press reactor (modified from Rivero *et al.* [128]).

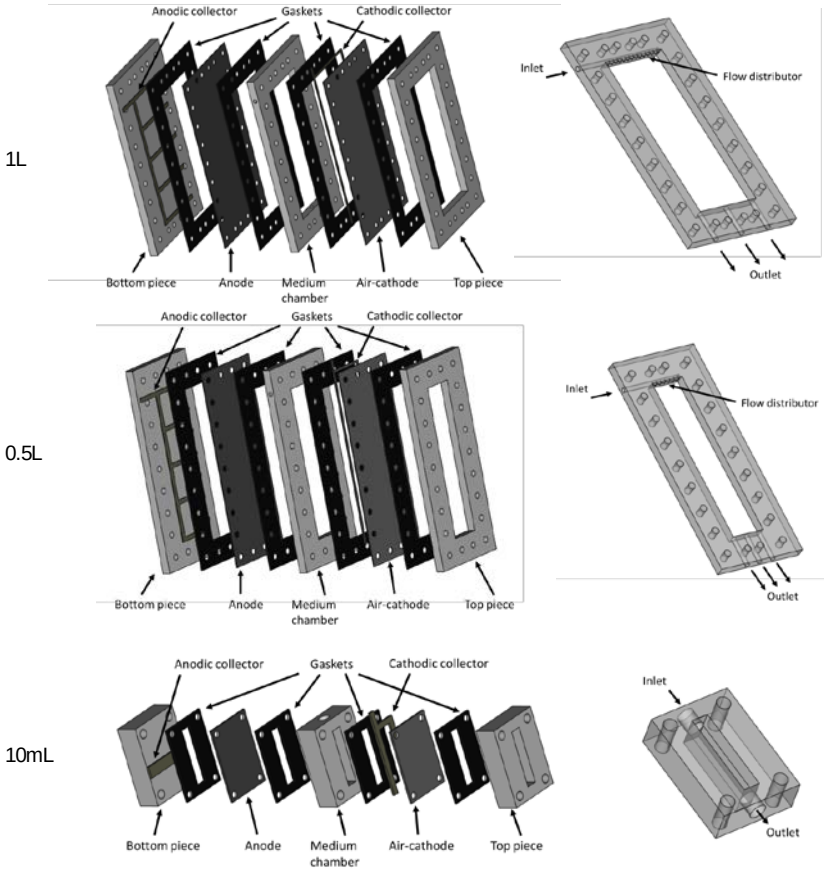

Figure 16. Reactors used in this work.

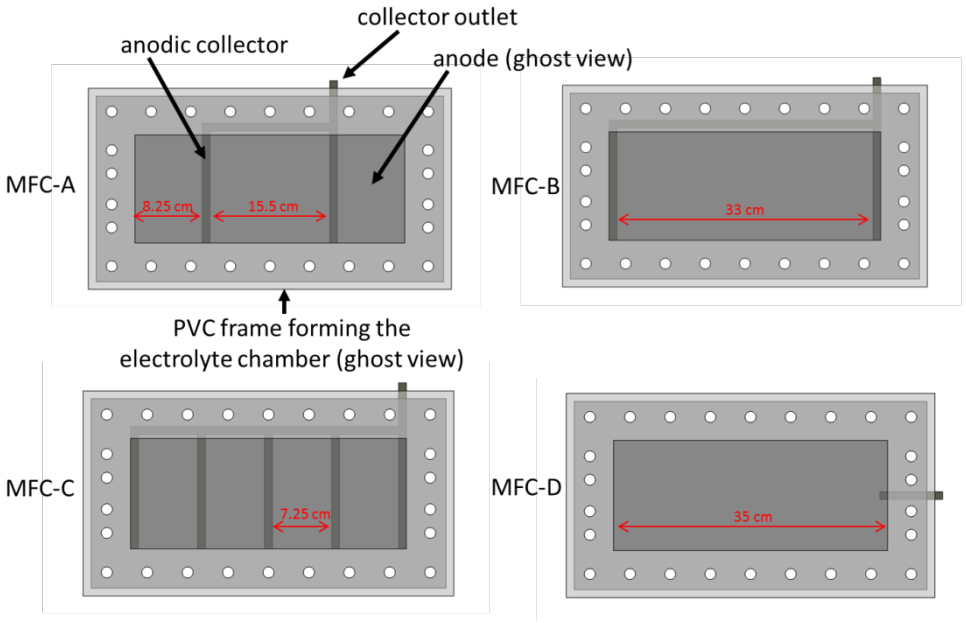

Figure 17. The four anodic contact patterns. Dark grey strips represent titanium electrical contacts.

The same MFC was used under continuous-flow conditions for the assessment of the effect of hydrodynamics (1L-MFC). Two smaller MFCs: the second of 0.5 L (dimensions 35×7×2 cm^3, 0.5L-MFC) and the third of 10 mL (dimensions 5×1×2 cm^3, 0.01L-MFC) were also used (Figure 16). They were constructed with the same inter-electrodes spacing of 2 cm, and the same anodes and cathodes. To ensure good electron recovery, 5 titanium collectors across the width of the anode were installed at equal distance from each other in the 1L-MFC and 0.5L-MFC. Due the small anode surface in the 0.01L-MFC, only one collector was placed across the width of the anode. The external resistance was set at 50 Ω.

To be able to describe the hydrodynamics by simple equations, it is needed for the flow to be regular inside the reactors, by avoiding dead zones and eddies. To do so, flow distributors were constructed for the 1L-MFC and 0.5L-MFC, which consisted in leading the flow from the inlet pipe through holes in the inlet side wall. These holes allowed to approximately distribute the flow evenly in a cross-sectional plane and along the reactor length. Due to its volume, the 0.01L-MFC did not need flow distributor, as the inlet diameter was equivalent to the height and thus flow was assumed to be regular.

1.2. Synthetic wastewater composition and operational conditions

The MFCs were filled with synthetic wastewater (adapted from « OECD guideline for the testing of chemicals »[129]) to a final concentration of 500 mg COD/L as used by Lefebvre *et al.* [11] and with equivalent carbon and nutrients (See Table 2 for composition). The MFCs were inoculated with 5 g of dried sewage sludge (75 % water mass/mass) from a Grand Lyon domestic wastewater treatment plant (Lyon, France). They were operated at room temperature. 1 L-MFCs used for current collectors study were operated with a recirculation loop at 15 mL/min with a peristaltic pump. This recirculation was used to improve homogeneity in the medium and avoid inoculum particles settling.

Table 2. Composition of synthetic wastewater for 500 mg COD/L.

Compounds dissolved in tap water	Mass for 1 L of solution (mg)
tryptone	800
yeast extract	550
urea (CH_4N_2O)	150
anhydrous dipotassium hydrogen phosphate (K_2HPO_4)	140
sodium chloride (NaCl)	35
calcium chloride dihydrate ($CaCl_2.2H_2O$)	20
magnesium sulphate heptahydrate ($MgSO_4.7H_2O$)	10

For the assessment of the effect of hydrodynamics, different flow rates, from 5 L/h to 280 L/h, were applied to the other MFCs (1 L, 0.5 L and 0.01 L) (Table 3). For each MFC a complete loop consisted of a 20 L tank containing synthetic wastewater, a pump, a flowmeter and the MFC. Due to flow restriction in the small bore tubes used for the 0.01L-MFC, the pump could not attain 280 L/h for this MFC and was instead operated at 210 L/h for the maximum flow.

Table 3. Operation parameters for each run.

Reactor/Flow	Volume (L)	Flow rate (L/h)	Liquid velocity (m/s)	HRT (s)
1L-MFC_280	1	280	2,78E-02	12,9
1L-MFC_100	1	100	9,92E-03	36,0
1L-MFC_50	1	50	4,96E-03	72,0
1L-MFC_5	1	5	4,96E-04	720,2
0,5L-MFC_280	0,5	280	5,56E-02	6,4
0,5L-MFC_100	0,5	100	1,98E-02	18,0
0,5L-MFC_50	0,5	50	9,91E-03	36,0
0,5L-MFC_5	0,5	5	9,91E-04	360,1
0,01L-MFC_210	0,01	210	2,92E-01	0,2
0,01L-MFC_100	0,01	100	1,39E-01	0,4
0,01L-MFC_50	0,01	50	6,94E-02	0,7
0,01L-MFC_5	0,01	5	6,94E-03	7,2

1.3. Voltage monitoring

The MFC voltage was monitored every ten minutes using a Hewlett Packard 3456A Digital Voltmeter combined with an Agilent 34970A Data Acquisition/Switch Unit. If voltage dropped significantly before voltage stabilized, additional substrate was added into MFC medium to maintain a concentration of 500 mg COD/L. After four days post-voltage-stabilization, when the biofilm was considered to have matured, between 10 and 15 days for all MFCs, substrate was added to MFC medium to maintain the concentration at 500 mg COD/L. This was done in order to keep the system saturated in substrate, and thus, free from substrate limitation.

2. Residence time distribution

Residence time distribution (RTD) of the three MFCs at the different flow rates, for hydrodynamics influence study, was assessed to characterize the mixing and flow inside the MFC reactors and to compare it to ideal flow models (Figure 18) [130]. A known amount of a tracer was introduced at the system inlet. Its concentration was measured at the outlet and this distribution described the time fluid was spending inside the reactor. Stagnant fluid zones or short circuits could be detected. RTD was done here by introducing 0.5 mL of a 684 mM of ferrocyanide $[Fe(CN)_6]^{4-}$ (Sigma-Aldrich, Lyon, France) with a syringe into the reactor inlet tube. A screen-printed electrode, combining a gold electrode, a carbon counter electrode and

a silver reference electrode (PalmSens, Houten, The Netherlands) was inserted in the outlet tube. This combination electrode was connected to an Origastat OGS100 potentiostat (Origalys, Rilleux-la-pape, France) that continuously applied a potential of 1 V for the oxidation of ferrocyanide to ferricyanide $[Fe(CN)_6]^{3-}$ at the electrode. Current generated by this reaction was monitored by the potentiostat. As the current is proportional to the amount of ferrocyanide, it was used as a concentration measure of the tracer in the MFC effluent at the outlet, and noted C(t). E(t) is the exit age distribution for fluid flowing out of the reactor. It represents C(t) whose area under the curve would be unity and is calculated as [131]:

$$E(t) = \frac{C(t)}{\int_0^\infty C(t)dt}$$

Mean residence time $\bar{t}$ and variance σ^2 of E(t) were then calculated from this concentration distribution with the following formulas [130]:

$$\bar{t} = \frac{\int_0^\infty tC(t)dt}{\int_0^\infty C(t)dt}$$

$$\sigma^2 = \frac{\int_0^\infty t^2C(t)dt}{\int_0^\infty C(t)dt} - \bar{t}^{\,2}$$

The empirical Péclet number (Pe) was extracted from ferrocyanide concentration distribution for each MFC using the relation [131]:

$$\frac{\sigma^2}{\bar{t}^2} = \frac{2}{Pe} - \frac{2}{Pe^2} \times (1 - e^{-Pe})$$

The retention time distribution E(θ) was then plotted. E(θ) is E(t) expressed in function of a dimensionless time $\theta = {}^{t}/_{\bar{t}}$. It is calculated with the expression [130]:

$$E(\theta) = \frac{C(t)}{\int_0^\infty C(t)dt} \times \bar{t}$$

The corresponding variance ${\sigma_\theta}^2$ was calculated. It was used to calculate the dimensionless group $\frac{D_{ax}}{uL}$, where D_{ax} is the axial diffusion coefficient, u the fluid velocity and L the length of the reactor [130]:

$$\frac{{\sigma_\theta}^2}{2} = \frac{D_{ax}}{uL}$$

If $\frac{D_{ax}}{uL}$ is below 0.01, the reactor shows negligible dispersion and can be considered to be close to a plug flow reactor.

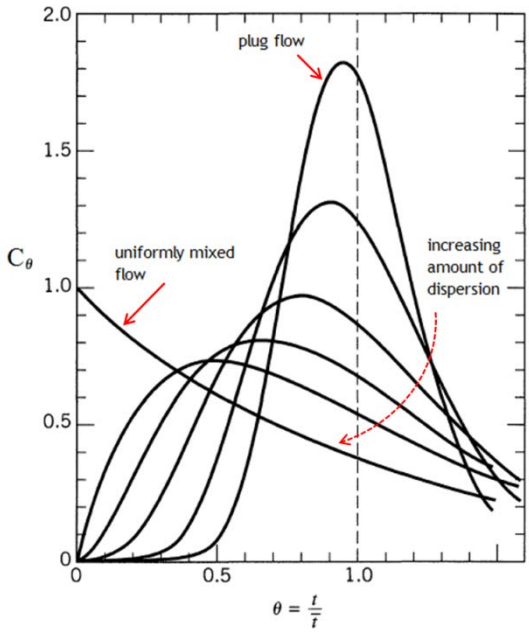

Figure 18. Hypothetical tracer response curves varying from plug flow to uniformly mixed flow reactors as adapted from Levenspiel [130]; θ is a dimensionless time unit $\theta = {}^{t}/_{\bar{t}}$ and C_θ is the tracer concentration in function of θ.

3. Electrochemical measures

3.1. Polarization curves

Polarization curves were recorded using a potentiostat (Origaflex OGF01A, Origalys Electrochem, France) with the anode as the working electrode and the cathode as both reference and auxiliary electrodes. Anode potential was scanned from the open circuit voltage (near 500 mV) to 0 V at a scanning rate of 1 mV/s [25] and current was recorded. A power curve was plotted from the polarization curve. It was used to extract the maximal power value which was considered as the electrical performance characteristic of each system.

In the case of 1L-MFCs used for current collectors study, potential drop on the anode was calculated with Comsol (Comsol France, Grenoble, France) from connection points where the local potential was assumed to be the equilibrium electrode potential measured against Ag/AgCl reference electrode. Titanium properties were taken from the Comsol material library. Electrical conductivity of the carbon cloth was set to 0.84 mS/m. This value is the mean conductivity of anodes (carbon cloth and biofilm) measured in six similar MFCs previously operated, after several days of operation.

3.2. Electrochemical impedance spectroscopy

EIS spectra for the anodes were recorded at the end of MFC operation before the polarization curve using a potentiostat (Origaflex OGF01A, Origalys Electrochem, France) at open circuit potential, in a frequency range of 1 kHz to 50 mHz, with an AC signal of 20 mV amplitude (peak-to-peak) and 20 frequencies per decade (*i.e.* per order of magnitude on a logarithmic scale). Measures used anode as the working electrode, cathode as counter electrode and an Ag/AgCl electrode inserted in the center of the chamber, equidistant between anode and cathode, as the reference electrode. Data were analyzed using Zview software (Scribner). Figure 19 shows the electrical equivalent circuit used to fit anode impedance data. The literature provides many equivalent circuits for MFC anodes [78,132–137]. After having tried different circuits such as the Randles model [132,136] or more complex circuits [78,137], it appeared that the diffusion phenomenon are not predominant at the anode when studied at open circuit potential. The circuit equivalent does not therefore include this element (Warburg impedance). R_{CT} is the charge transfer resistance and CPE_{DL} models the effective capacitance associated to the double layer. R_{Bio} is the biofilm resistance and CPE_{Bio} models the effective capacitance associated to the electrochemically active biofilm. The constant phase element (CPE) was used instead of a pure capacitor to account for electrochemical and microbiological inhomogeneity of the anode surface [82]. Charge transfer resistance expresses how easily the electron transfer occurs and is an important parameter to assess the efficiency of the electron transfer process. R_{ohm} is the ohmic resistance. Equivalent circuit was completed by an inductance in parallel to a resistor to account for the inductive behavior at high frequencies [138–140]. This deformation of the spectra is explained by instrumental artifacts and inductance of the electrode and connecting wires.

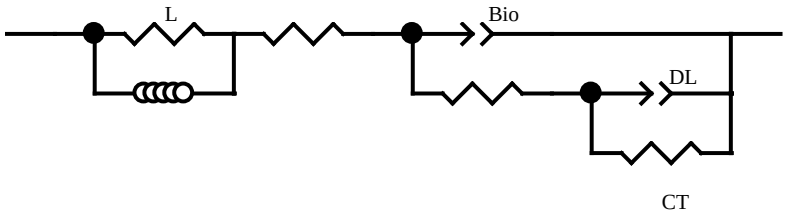

Figure 19. Electrical equivalent circuit used to fit anode impedance spectra. L: inductance; R_L: resistance from inductive behavior; R_{ohm}: electrolyte resistance; R_{CT}: charge transfer resistance; R_{Bio}: biofilm resistance; CPE_{DL} & CPE_{Bio}: constant phase elements respectively from double layer and biofilm.

Effective capacitance of processes were calculated from CPE parameters [141]:

$$C = R^{(\frac{1}{\alpha}-1)} * Q_{CPE}^{\frac{1}{\alpha}}$$

Where Q_{CPE} and α are CPE parameters, and R is the resistance of the process in parallel to the CPE (R_{CT} or R_{Bio}), all calculated by the fitting software ZView.

Electroactive surface areas of the anode were estimated for each MFC, assuming that the double layer capacity is usually around 20 µF.cm^{-2} in aqueous media [142–144].

4. Microbiological assays

For the work on current collectors, the anodes were sampled when voltage was stabilized by cutting off pieces (4 cm²) at different distances from the current collectors. In the case of the study about hydrodynamics effects, 2-cm² anode pieces were sampled at different locations on the anode (9 replicates for 1L-MFC and 0.5L-MFC, 2 replicates for 0.01L-MFC). All anodes samples were then gently rinsed with a sterile phosphate buffered saline solution (PBS).

The anode pieces were used for total DNA extraction using a DNA Soil Nucleospin kit (Macherey-Nagel). The sample lysis step was performed with a FastPrep bead beater system (MP Biomedicals) at a speed of 6 m/s for 20 s to detach bacteria from the anode. DNA was stored at -20 °C prior to following analyses.

4.1. qPCR assay

qPCR assays were conducted on a Rotor-Gene 6000 (Corbett Life Science). Each 20-µl reaction contained the following: 10 µl of SensiFAST SYBR No-ROX mix (Bioline), 0.8 µl of each primer (10 µM; Invitrogen) (Table 4), 6.4 µl H_2O, and 2 µl template DNA. PCR reactions were subjected to the following cycling parameters: 95 °C for 2 min, then 30 cycles of 95 °C 15 s, 20 s at the annealing temperature, and 72 °C for 25 s. Each assay included triplicate reactions per DNA sample with three standards (containing 7 different concentrations ranging from 10^3 to 10^9 copies/µL). Quantitation was calculated using Rotor-Gene 6000 Series Software.

4.2. 16S rRNA gene (*rrs*) sequencing

The variable V3 and V4 regions of the 16S rRNA gene was sequenced with the Illumina MiSeq system. Library was prepared following manufacturer's instructions [145]. A first PCR amplified the variable region with the forward and reverse primers (Table 4). Each 25 µL reaction contained 22.5 µL Platinum PCR SuperMix (Thermo Fisher scientific), 1 µL of 10 µM forward and reverse primers mix (Thermo Fisher scientific) and 1.5 µL DNA. PCR reactions were subjected to the following cycling parameters: 95 °C for 3 min, then 25 cycles of 95 °C for 30 s, 55 °C for 30 s, and 72 °C for 30 s and a last step at 72 °C for 5 min. Taxonomic assignation was done by the on-system MiSeq Reporter software based on the Greengenes database (http://greengenes.lbl.gov/Download/).

Table 4. Primer sequences for qPCR assay of "all bacteria" and for *Geobacter* sp. and for sequencing of the variable V3 and V4 regions of the 16S rRNA gene.

Assay	Names and sequences (5'-3')	Product size (bp)	Annealing temperature (°C)	Reference
"all bacteria"	**Eub338F** ; ACT CCT ACG GGA GGC AGC AG **Eub518R** ; ATT ACC GCG GCT GCT GG	200	53	Fierer *et al.* [146]
Geobacter sp.	**Geo561F** ; GCG TGT AGG CGG TTT CTT AA **Geo825R** ; TAC CCG CRA CAC CTA GTT CT	265	59	Stults *et al.* [147]
Primers for 16S V3 and V4 regions	**Fwd** ; TCG TCG GCA GCG TCA GAT GTG TAT AAG AGA CAG CCT ACG GGN GGC WGC AG **Rev** ; GTC TCG TGG GCT CGG AGA TGT GTA TAA GAG ACA GGA CTA CHV GGG TAT CTA ATC C	460	55	Illumina's instructions [145]

For the assessment of the effect of hydrodynamics, Shannon index was calculated to express the bacterial genus diversity in each sample, with the following equation:

$$Shannon\ index = \sum_{i=1}^{n} p_i \times \ln(p_i)$$

Where p_i is the relative abundance of the i^{th} genus detected in the sample [148].

5. MFCs characteristic numbers

Several operational parameters were calculated to describe each MFC. That electrolyte used here as MFC medium was considered to have the same physical properties as water. Values established for water were thus used in the following calculations (density, dynamic viscosity, kinematic viscosity, diffusion coefficient of substrate). Operational parameters and numbers are given below.

Reynolds (Re) number was used to describe the system [122]:

$$Re = \frac{u \times L_c}{\nu}$$

with u the bulk fluid velocity, ν kinematic viscosity of water and L_c the characteristic length, translated here as the diagonal length of the cross-section area available for flow [149]. Re allowed to define flow conditions as laminar if Re < 4000 and turbulent when Re > 4000.

Hydrodynamic boundary layer thickness was calculated as described by Daugherty *et al.* [150]:

under laminar flow conditions :

$$\delta_H = \frac{4.91 \times L_c}{Re^{0.5}}$$

under turbulent flow conditions :

$$\delta_H = \frac{0.377 \times L_c}{Re^{0.2}}$$

Bishop *et al*. [149] established a relationship between hydrodynamic and concentration boundary layer thicknesses over the biofilm that can be used to determine the concentration boundary layer thickness (δ_C) from the previously described number (δ_H) and the Schmidt number :

$$\frac{\delta_C}{\delta_H} = {S_c}^{1/3}$$

With S_c the Schmidt number defined as the ratio between kinematic viscosity of water, ν, and the diffusion coefficient of substrate in water, D [122]. Glucose was assumed to be representative of complex substrate used to feed MFC :

$$Sc = \frac{\nu}{D} = 2.01 \times 10^3$$

The Péclet number represents the ratio of characteristic times of mass transport due to convection to mass transport due to diffusion [78]:

$$Pe = \frac{L_c \times u}{D}$$

H is a modified Péclet number that expresses the ratio of mass transport due to convection in the flow direction along the length of the reactor (l) to mass transport due to diffusion perpendicular to the flow along the inter-electrodes distance (w).

$$H = \frac{l/u}{w^2/D} = \frac{l \times D}{w^2 \times u}$$

The characteristic time of substrate diffusion in the concentration boundary layer (τ_{CBL}) was introduced:

$$\tau_d = \frac{\delta_C^2}{D}$$

With flow, a shear stress occurs at the anode surface and was assessed with the skin friction coefficient C_f [151]:

under laminar flow conditions :

$$C_f = \frac{1.328}{\sqrt{Re}}$$

under turbulent flow conditions :

$$C_f = \frac{0.455}{(log_{10}(Re))^{2.58}}$$

This coefficient was linked to shear stress T [152]:

$$C_f = \frac{T}{0.5\rho {U_0}^2}$$

The Sherwood number represents the ratio of the convective mass transport to the diffusive mass transport [153]:

$$\mathrm{Sh} = 3.66 \times \left(1 + 0.095 \times \frac{L_c \times Pe}{l}\right)^{0.45}$$

6. Statistical modeling

6.1.1. Multivariable linear regression for maximum power modeling and *Geobacter* number modeling

A cross-validated LASSO (Least Absolute Shrinkage and Selection Operator) model was used to perform linear regression with variables selection. It minimizes residual sum of squares weighted by a shrinkage penalty to avoid complexity [154]. The “glmnet” R package was used and regressions were performed with R software [155].

6.1.2. Maximum power modeling with dimensionless groups

Variables were chosen to account for the different phenomena in the MFCs and subsequently dimensionless numbers were formed using the Vaschy-Buckingham theorem. This theorem states that it is possible to reduce a number of dimensional variables into a smaller number of dimensionless variables. n dimensional variables described with k dimensions can be expressed by a minimum number of i=n-k dimensionless variables. To form the dimensionless variables, k variables whose product was not dimensionless were selected. The dimensionless variables were formed with a power product of these k variables plus one other. Each was assigned with a convenient exponent that made the total product dimensionless. Linear regression using these dimensionless groups was then performed with XLSTAT.

Table 5. Parameters used in this study: * parameters used for the multiple linear regression with LASSO variable selection to model maximum power, ** parameters used to build dimensionless numbers, * parameters used for the multiple linear regression to model *Geobacter* number.**

V *,***	Volume (L)
Q *,***	Flow rate (L/h)
A *,***	Cross section area (m^2)
L_c *,**,***	Characteristic length
u *,**,***	Fluid velocity (m/s)
HRT *,***	Hydraulic retention time (s)
Re *,***	Reynolds number
Sh *,***	Sherwood number
k *,***	Mass transfer coefficient (m/s)
δ_H *,***	Hydrodynamic boundary layer thickness (m)
δ_C *,***	Concentration boundary layer thickness (m)
Pe *	Péclet number
H *,***	Ratio of axial convection to transverse diffusion
Pe_{RTD} *,***	Péclet number from RTD
τ_{CBL} *,***	Characteristic time of substrate diffusion in CBL (s)
C_f *,***	Skin friction coefficient
T *,**,***	Shear stress ($kg/s^2.m$)
E_{max} ***	Maximal voltage (V)
P_{max} ***	Maximal power (W)
R_{int} ***	Internal resistance (Ω)
B ***	Total bacteria number
G	Geobacter number from qPCR
g ***	Geobacter relative abundance (%)
h **	Inter-electrodes distance (m)
ρ **	Water density (kg/m3)
μ **	Water dynamic viscosity (kg/m.s)
S_c	Schmidt number
ν	Water kinematic viscosity (m^2/s)
D **	Glucose diffusion coefficient in water (m^2/s)

Chapter III - Anode Current Collectors Affect Microbial Fuel Cell Performance and Microbial Community

1. Introduction

As described previously, scale-up modifies specific parameters thought to be key aspects of MFC functioning at large scales. Anodic biofilms microbial community structure would be affected by scaling up MFCs and in turn their electron transfer efficiency might be reduced. This chapter investigated one of these parameters, the current collectors. The hypothesis was that with increasing anode size, more electroactive bacteria can develop but too few or badly arranged external electrical connections of the anode would limit electron flow and power, no matter the size of the MFC. Current collectors could shape and restrict spatial development of microbes, because of potential drop on the anode and ohmic resistance for electrons flowing from bacteria to the external connection.

This hypothesis was tested in a 1 L MFC, with up to 4 different external connection patterns on carbon cloth anodes. Power output was followed in relation to surface area and distance between current collectors. Electrochemical impedance spectroscopy (EIS) measurements were conducted to assess MFC internal resistance. qPCR tests were performed at increasing distance from collectors to quantify total bacteria number and more specifically *Geobacter*, a predominant electroactive genus in most of anodic biofilms fed and inoculated from complex environmental media (*e.g.*, wastewater)[156]. The 16S rRNA gene sequencing was used to describe the microbial community in each sample.

2. Results

2.1. Electrical performance

Collector configuration with four evenly spaced collectors (MFC-C, in Figure 17) had the maximal power output at 5.3 mW (Figure 20). Decreasing the number of collectors to two clearly resulted in a decrease of the maximal power generated: 2.9 mW in MFC-A and 2.4 mW in MFC-B. The maximal power decreased with the increase in distance between collector (15.5 cm in MFC-A and 33 cm in MFC-B). Finally, the MFC-D configuration with only one connection point of 1 cm² on one edge showed a very low power output of 1.7 µW.

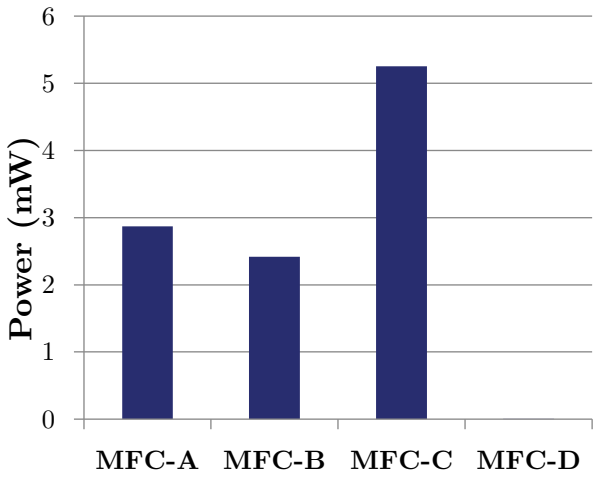

Figure 20. Maximal power output for each current collector configuration.

2.2. Electrochemical Impedance Spectroscopy

EIS spectra of the anode were recorded for each collector configuration at the end of each MFC operation. The Nyquist plots obtained from them were fitted (Figure 21) with the same electrical equivalent circuit (Figure 19). A good match between the experimental points and the fitting curve was observed. The parameters obtained are shown in Table 6. Impedance data from system D could not be fitted with this circuit and as MFC-D performance was very low, it was considered not to be limited by the same mechanisms as the other MFCs and therefore was not included in the comparison of charge transfer processes.

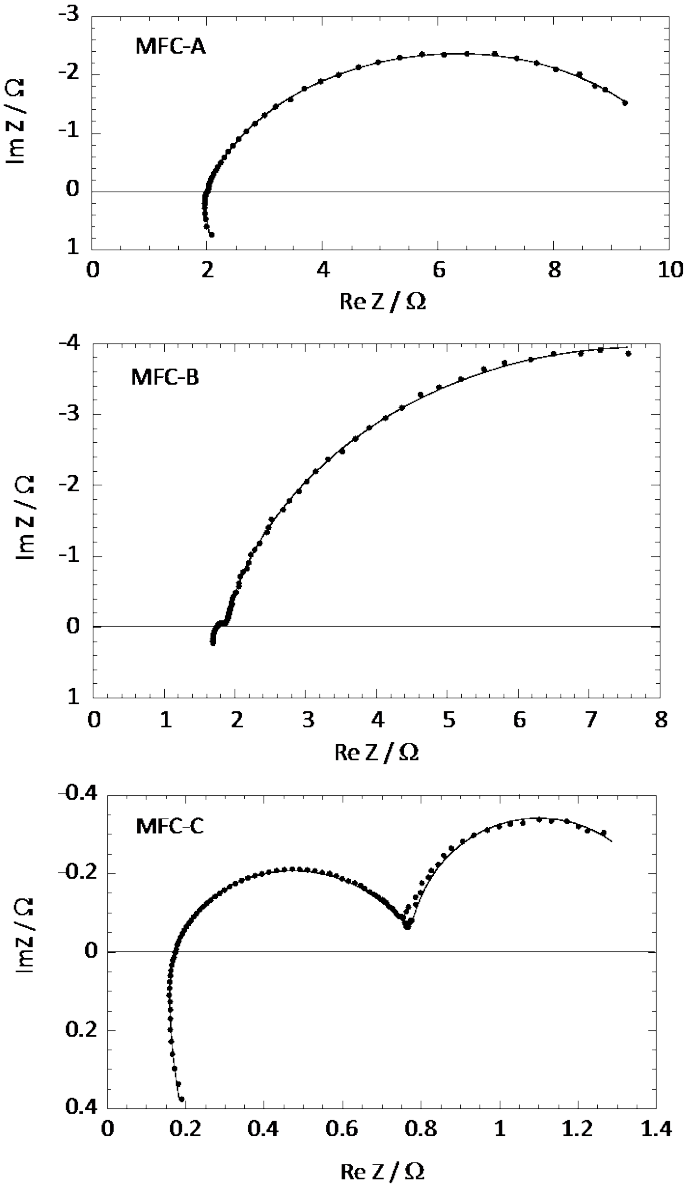

Figure 21. Nyquist plots for MFC-A, MFC-B and MFC-C. Experimental (dots) and fitted data (lines) are presented.

Table 6. Ohmic resistance R_{ohm}, biofilm resistance R_{Bio} and capacitance C_{Bio}, charge transfer resistance R_{CT}, double layer capacitance C_{DL}, total internal resistance R_{int} measured by EIS and electroactive surface area for MFC-A, MFC-B and MFC-C.

	MFC-A	MFC-B	MFC-C
R_{ohm} (Ω)	1.96 ± 0.06	1.62 ± 0.05	0.140 ± 0.005
R_{Bio} (Ω)	5.4 ± 0.2	0.33 ± 0.01	0.66 ± 0.02
C_{Bio} (F)	$(1.42 \pm 0.05) \times 10^{-3}$	$(4.6 \pm 0.2) \times 10^{-4}$	$(7.9 \pm 0.3) \times 10^{-6}$
R_{CT} (Ω)	3.3 ± 0.1	14.3 ± 0.5	0.62 ± 0.01
C_{DL} (F)	$(8.8 \pm 0.3) \times 10^{-3}$	0.071 ± 0.003	1.37 ± 0.4
$R_{int}= R_{ohm} + R_{Bio}+ R_{CT}$ (Ω)	10.7 ± 0.4	16.3 ± 0.6	1.42 ± 0.04
Electroactive surface area (m²)	4.4×10^{-2}	0.355	6.8

The lowest charge transfer resistance at interface anode/solution was observed in MFC-C (0.62 Ω) while MFCs-A and B had resistances of 3.3 and 14.3 Ω, respectively (Table 6). In parallel, the double layer capacitances showed similar difference: 8.8 mF for MFC-A, 71 mF for MFC-B and 1.37 F for MFC-C. The capacitances obtained were very high for MFC-C but are consistent with the large surface of the anode/solution interface. The electroactive surface area was estimated for MFC-C anode to be 6.8 m^2. Considering that the geometric surface of the anode was only 490 cm^2, the surface of the interface increased by 140X due to the high porosity of the plain carbon cloth. For the MFCs-A and B, the electroactive surface areas were estimated to be 440 (0.9X) and 3550 cm^2 (7X), respectively.

In the case of the second determined parameter, R_{Bio}, MFC-A showed a higher resistance for the biofilm of 5.4 Ω than MFC-B and C respectively of 0.33 and 0.66 Ω. Biofilm capacitances decreased: 1.42, 0.46 and 0.0079 mF for respectively MFC-A, B and C.

2.3. qPCR assay

qPCR results did not reveal significant differences in total bacteria number of the anodic biofilm at increasing distance from the collectors or between systems (Figure 22A). *Geobacter* numbers in MFC-A, B and C were not significantly different between samples at increasing distance from the collectors. MFC-D showed an increase of *Geobacter* number with distance from 3.84×10^5 gene copies/anode cm^2 at 0 cm to 6.06×10^6 at 25 cm. But overall *Geobacter* number was higher in B system (1.1×10^7 gene copies number) than in the three others (4.5×10^6, 3.9×10^6 and 3.9×10^6 for respectively MFC-A, C and D). *Geobacter*

abundances as ratios of *Geobacter* to total bacteria showed the same trend with distance than for *Geobacter* gene copies number as total bacteria number are not very different with distance. All *Geobacter* abundances were lower than 1 %.

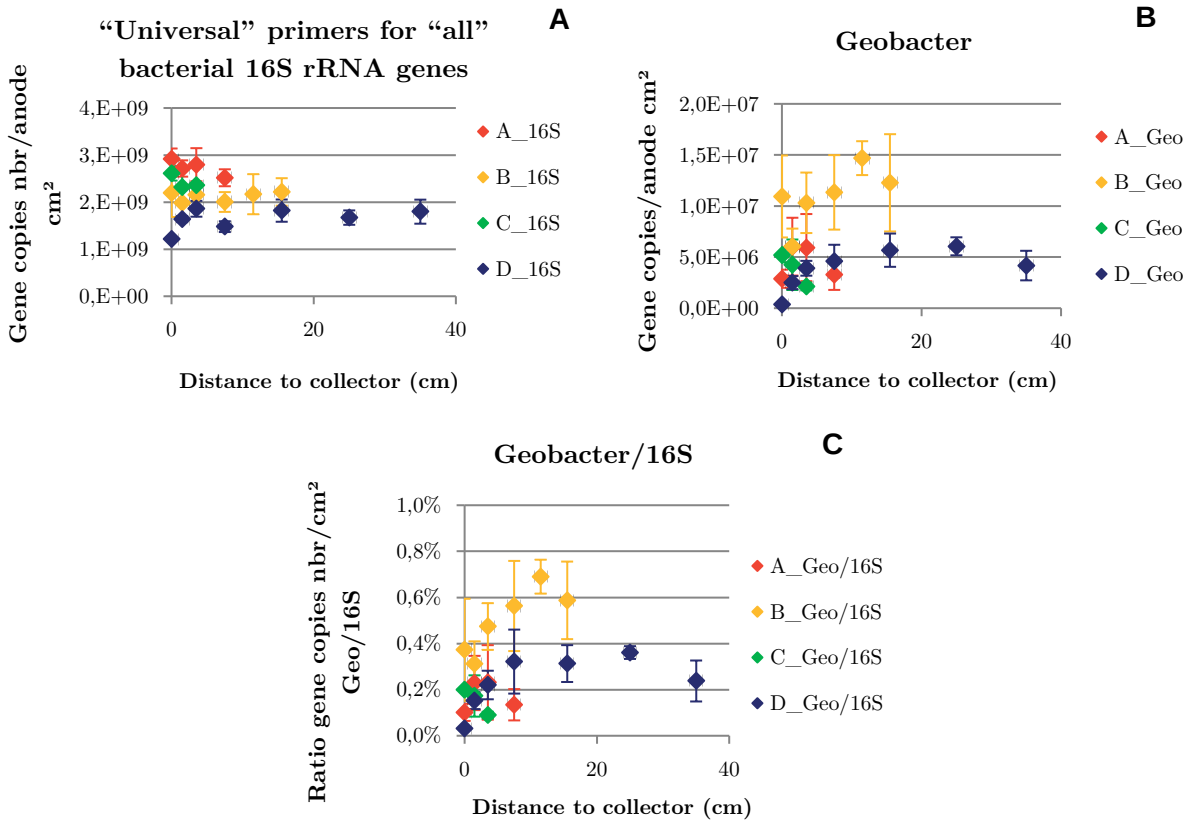

Figure 22. All bacteria (A) and *Geobacter* (B) quantification by qPCR as gene copies number per anode cm², (C) relative abundance of *Geobacter* as determined by qPCR ratios of *Geobacter* to total bacteria.

2.4. 16S rRNA gene (*rrs*) sequencing

Sequencing of a part of the 16S rRNA gene from the same anodic biofilm samples extracted DNA showed a higher *Geobacter* relative abundance than with qPCR: between 0.4 % (MFC-D, 0 cm distance from the collector) and 13.3 % (MFC-B, 11.5 cm from the collector) (Figure 23). The lower ratio with qPCR may be due to the specific primers that do not comprehensively target all *Geobacter* species. Moreover, the number of SSU rRNA gene copies is different between bacteria. *Geobacter* is thought to have one [157] whereas some members of microbial communities can have several [158]. Nevertheless, the trend for *Geobacter* relative abundances was coherent with qPCR results with the highest abundance in MFC-B, which was between 9.1 and 13.3 %.

MFC-A, B and C did not show significant difference in relative abundance of dominant genus with increasing distance from collectors. Only MFC-D (with only one collector) showed clear trends, both increasing and decreasing relative abundances, even at short distances (Figure 23). *Geobacter* is one of the genus with an increasing abundance with distance from 0.4 % at the collector to 4.2 % at 15 cm in MFC-D. The dominant genus were different between MFCs. Only *Geobacter*, *Desulfuromonas* and *Comamonas* to a lesser extent occurred as part of the most abundant bacteria in all four MFCs.

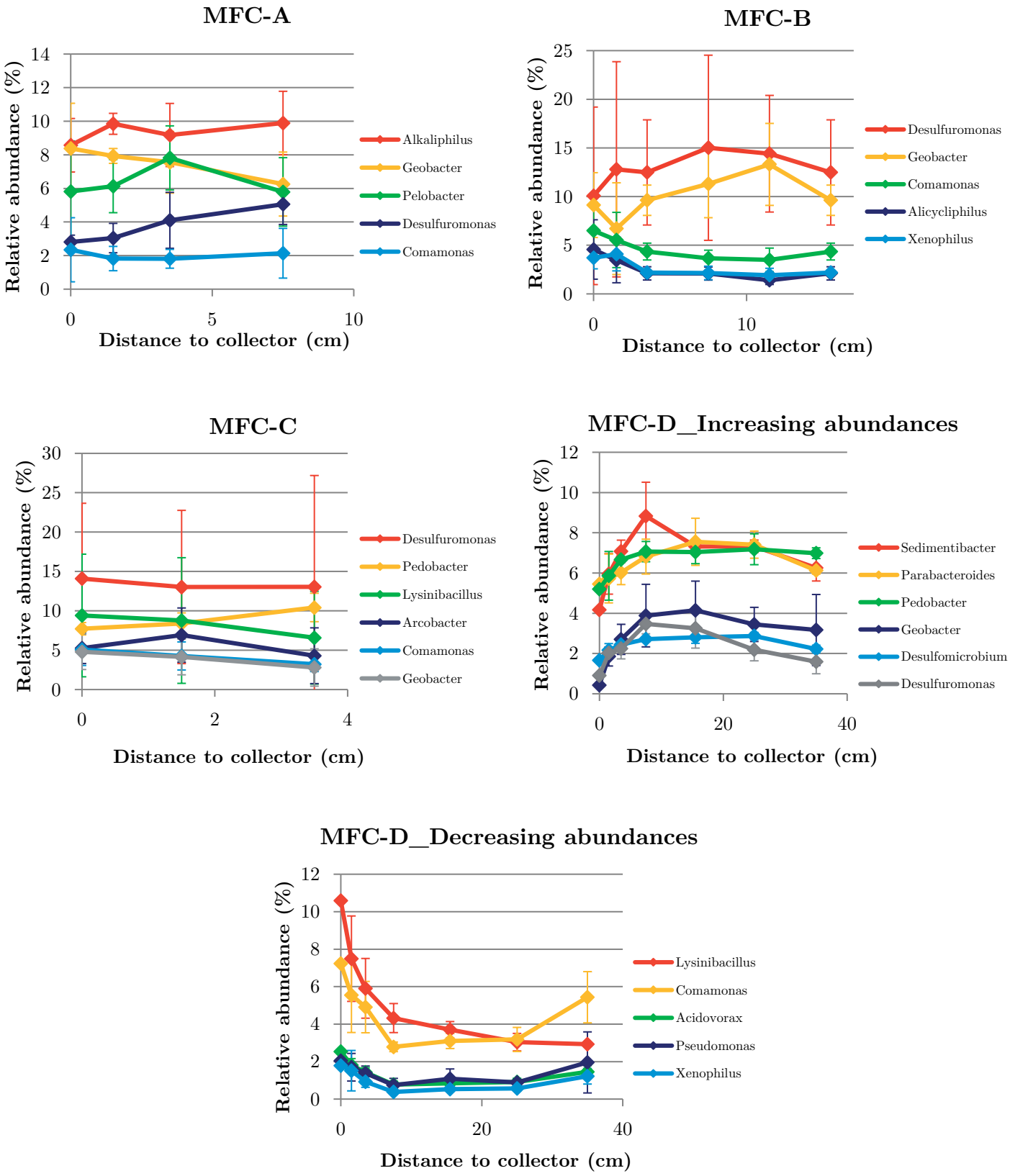

Figure 23. Relative abundance of genus of interest (highest abundances) in MFC-A, MFC-B, MFC-C and MFC-D for increasing and decreasing abundance.

3. Discussion

3.1. Collectors improve electron recovery

When comparing the different configurations, MFC-A, MFC-B, MFC-C and MFC-D, increasing the contact area and decreasing the maximal distance of the current collectors enhanced power output (Figure 20). The contact area between anode cloth and metal collectors increased from 1 cm^2 in MFC-D to 28 cm^2 in MFC-B and 70 cm^2 in MFC-C and maximal power increased from 1.7×10^{-4} mW to 2.4 mW and 5.3 mW, respectively. Moreover, when maximal distance to collector is reduced (from 16.5 cm in MFC-B to 7.75 cm in MFC-A) while maintaining the same contact area, the maximal power slightly increased from 2.4 to 2.9 mW. The MFC with a single collector (MFC-D) had an internal resistance of 160.7 Ω whereas MFC-A and MFC-B had 10.7 and 16.3 Ω internal resistances, respectively (Table 6). This higher internal resistance was coherent with its low maximal power. The MFC-D collector set-up had only one collection point of 1 cm^2 on the side of the electrode, which created a maximal distance to collector of 34.7 cm at the opposite end of the anode. This generated a constriction resistance at the leading out point and a higher current density around the collector due to the narrow passage for current [57]. The very low number of *Geobacter* at this collection point and its increase with distance might be explained by this concentration of current streamline. *Geobacter* might be sensitive to the higher current density in this area. Some other dominant bacteria (*Desulfomicrobium, Desulfuromonas, Parabacteroides, Pedobacter* and *Sedimentibacter*) also showed this potential sensitivity to the higher current density. Both *Parabacteroides* and *Sedimentibacter* can ferment and provide acetate for electroactive bacteria [159,160]. Fermentative microorganisms are usually found in mixed-species anodic biofilm of MFCs fed with complex substrates as they provide simple organic molecules to electroactive bacteria [29,161]. As there is no other fermenters among the dominant genus near this single connection point, they might be sensitive to current density as well. As a result, it may also be that *Geobacter* without this syntrophic relationship could not grow optimally due to the lack of fermentative end products needed as substrate. *Desulfuromonas*, which has been observed to be enriched in anodic biofilm elsewhere and possesses genes coding for cytochromes [162,163], might be an electroactive bacteria that is sensitive to current density, also. On the other hand, other electroactive bacteria, such as *Lysinibacillus* [164], *Comamonas* or *Pseudomonas* [165], showed a decreasing abundance with distance to the collector and that might imply that the high current density was positive for their growth. Out of the eleven most abundant genus on MFC-D anode, five

are electroactive bacteria and represent 21.1 % of the total community. Only one collection point does not appear sufficient to recover the maximum quantity of electrons from the entire anode independent of the amount of *Geobacter* or other electroactive bacteria present. This limitation is probably due to an ohmic resistance that is too large because of the distance to the collector. Therefore, a large part of the anode seems to be less useful for energy production and must deal with the probable congestion of electrons close to the collector.

Capacitor characteristics of the anode could be important for explaining the influence of current collectors on power production. Anode material/electrolyte interfaces act like a capacitor, *i.e*. electrical charges can be stored electrostatically on the electrode and can be released when the electrode potential is suitable. Capacitances of the double layer, *i.e*. at the anode material/electrolyte interface, showed different values between collector configurations. MFC-C (1.37 F) had the highest value followed by MFC-A and MFC-B with 8.8 mF and 71 mF, respectively. So, MFC-C had an electroactive surface area 19 times higher than that of MFC-B and 155 times higher than that of MFC-A (6.8 m² compared to 3550 cm² in MFC-B and 440 cm² in MFC-A), which is consistent with the very low charge transfer resistance found for MFC-C. Increasing the number of collectors increased the recovery of electrochemical signal from a larger part of anode surface. On the other hand, a reduced collection configuration made the anode surface appear smaller as the electric current conducted by only a part of the anode surface near the collector was recovered. This is also consistent with the observed charge transfer as R_{CT} was very low (0.62 Ω) for MFC-C compared to those for MFC-B (14.3 Ω) and MFC-A (3.3 Ω).

The double layer capacitance of the anode implies that a capacitive current was generated when the potential of the carbon cloth and the potential of the electrolyte and/or biofilm were different. This current also appeared during polarization curve measures, when the potential of the anode was scanned. This can be calculated from:

$$I_{DL} = C_{DL} \times \frac{dE}{dt}$$

where $\frac{dE}{dt}$ is the scanning rate, which was 1 mV/s in this case.

A capacitive current of 1.37 mA was generated in MFC-C during polarization measurements. This is significant at this low scanning rate, so a larger capacitive current would be generated during charge/discharge of such MFC, as the potential variation would be much faster. This effect has been observed previously during cycles of charge and discharge by opening and closing a MFC circuit that produced a burst of power at each circuit closing [82]. Duty cycles were not optimized, so the total energy recovered over a long period was lower with open/closed cycles than with continuously closed circuit [82]. However, in another case, duty

cycles were set to produce a higher total power harvest than with continuously closed circuit [166]. Current collectors, by increasing the capacitance of an MFC, are able to increase the overall power during charge/discharge cycles.

3.2. Collectors shape microbial communities

The external resistance used in this work was set low to avoid external resistance limiting electron flow. So limiting parameters in our work here should be kinetics, mass transfer and the presence of electroactive bacteria [33,167], which influence biofilm formation, development and function. From Figures 20 & 22, *Geobacter* number was not correlated with power output. The reported relationship between *Geobacter* abundance and electricity production in mixed-species biofilm is not straightforward. Miyahara *et al.* suggested that *Geobacter* was responsible for electricity production since they showed a correlation between maximal power of MFCs operated with different NaCl concentrations and *Geobacteraceae* protein content estimated by multiplying the total protein content by the abundance ratio of *Geobacteraceae* determined by qPCR [168]. A previous study conducted in our laboratory showed that voltage was associated with *Geobacter* growth [169]. On the other hand, Nevin *et al.* observed a cumulative charge curve shape similar to that of *Geobacter* growth in only one of their MFCs [70].

Table 7. Top 10 most abundant genus in each MFC, based on average of relative abundance in all samples.

A		B		C	
Genus	**Relative abundance average (%)**	**Genus**	**Relative abundance average (%)**	**Genus**	**Relative abundance average (%)**
*Alkaliphilus**	9.37	*Desulfuromonas*	13.20	*Desulfuromonas*	13.46
Geobacter	7.53	*Geobacter*	10.13	*Lysinibacillus*	8.59
*Pelobacter** **	6.39	*Comamonas*	4.57	*Pedobacter*	8.53
Pedobacter	5.46	*Sedimentibacter*	4.03	*Arcobacter*	5.74
*Parabacteroides**	5.02	*Alkaliphilus**	3.21	*Comamonas*	4.38
*Sedimentibacter**	4.90	*Pedobacter*	2.98	*Geobacter*	4.14
*Propionigenium**	4.04	*Xenophilus*	2.68	*Sedimentibacter**	3.42
Desulfuromonas	3.75	*Alicycliphilus*	2.58	*Alkaliphilus**	3.26
Arcobacter	2.66	*Parabacteroides**	2.40	*Parabacteroides**	3.14
*Clostridium** **	2.37	*Clostridium** **	2.37	*Olivibacter*	2.54

Fermenter producing acetate *
Fermenter producing H_2 **
Electroactive
Pedobacter and *Olivibacter* are aerobic bacteria [170,171], whereas anodic biofilm is supposed to be anaerobic and they have been identified as contaminants in typical DNA extraction kits and thus can be found erroneously in sequencing data. Despite their high abundance, they will not be taken into account in the following. References: [71,159,160,162,164,165,172–178]

The 16S rRNA gene sequencing showed that other electroactive bacteria, such as *Desulfuromonas, Arcobacter, Comamonas* and *Lysinibacillus*, were present and in high abundances on the anodes of MFCs-A, B and C (Table 7). Interestingly, despite the use of the same inoculum and substrate, the abundant genus were different between the three MFCs. For example, the three most abundant genus in MFC-B were electroactive with a cumulative relative abundance of 27.9 % while in MFC-A, which had a similar maximal power, cumulated electroactive genus had an abundance of 16.31 %. This supported the concept that the large distance between the collectors in MFC-B restrained the individual electroactivity of bacteria. In addition, among the ten most abundant genus in MFC-A, six were fermentative bacteria, which could provide acetate or H_2 to *Geobacter* [179]. In MFC-C, which had the highest maximal power and the most collectors, *Geobacter* was not the most abundant (4.14 %) and several other electroactive genus were present in high abundance. This indicates once more that *Geobacter* may not be the only key electroactive genus in mixed-species biofilms and some others might be able to contribute significantly to electron transfer to the anode when conditions are favorable, *i.e*. a high electrical contact area to reduce resistance for charge transfer.

It has been shown before that MFC-A had a lower electroactive surface area and a higher R_{Bio} than MFC-B whereas maximal power and R_{CT} are better in MFC-A than in MFC-B (Table 6). Interestingly, the more non electroactive genus are present, the higher the R_{Bio} is (Table 8). MFC-A showed a high R_{Bio} of 5.4 Ω and it corresponded to a high abundance of non electroactive genus (35.18 %), whereas in MFC-B this abundance decreased to 17.88 % for a R_{Bio} of 0.33 Ω. Several studies showed that electroactive genus such as *Geobacter* or *Shewanella* are able to produce nanowires, which are conductive proteins that improve biofilm conductivity, in pure or mixed-species biofilms [95,103,180]. Unfortunately whether the other electroactive genus are also involved in biofilm conductivity is not known yet, but the presence of electroactive genus seemed to be linked to a reduced biofilm resistance. The lower conductivity of MFC-A biofilm could then explain why the measured electroactive surface area is small. The current collectors set up allowed to recover electrons from a large area, but the poor nanowires network made it still difficult.

Table 8. Maximal power, R_{Bio}, electroactive surface area estimated from EIS measures and cumulative average relative abundances of non electroactive genus, among the 10 most abundant genus, from 16S sequencing data.

	MFC-A	MFC-B	MFC-C
Maximal power (mW)	2.9	2.4	5.2
R_{Bio} (Ω)	5.4 ± 0.2	0.33 ± 0.01	0.66 ± 0.02
Electroactive surface area (m^2)	4.4×10^{-2}	0.355	6.8
Cumulative average relative abundances of non electroactive genus	35.18	17.88	20.89

3.3. Local potential influences Geobacter development

The MFC-B had a larger number of *Geobacter* on its anode than in any other MFC whereas it did not shave the highest power production and did not have an optimal collectors set-up. To better understand what influenced *Geobacter* development on the anode, its abundance was compared to the local potential on the anode (Figure 24). The maximal potential drop of -0.102 V occurred for MFC-B from -0.318 V at the connection points to -0.42 V vs SHE at the middle of the anode, *i.e*. the point furthest from the collector. MFCs-A and C showed a lower potential drop of -0.038 V for MFC-A and -0.01 V for MFC-C due to lower distances between collectors. A large part of the anode in MFC-B was at a low potential. That

suggested that *Geobacter* together with *Desulfuromonas* (Table 7) could use the anode as an electron acceptor even at this potential and outcompeted other electroactive bacteria that could not use an electron acceptor in this low potential range. Acetate oxidation occurs at -0.28 V vs SHE [181], which is far above local potential on the MFC-B anode. However, hydrogen oxidation occurs at -0.41 V vs SHE , which was the minimum on MFC-B anode. Bacteria capable of using hydrogen as electron donor can develop at such low potential. That is the case of *Geobacter* and some *Desulfuromonas* species [179,182], and that could explain their high abundance in this MFC.

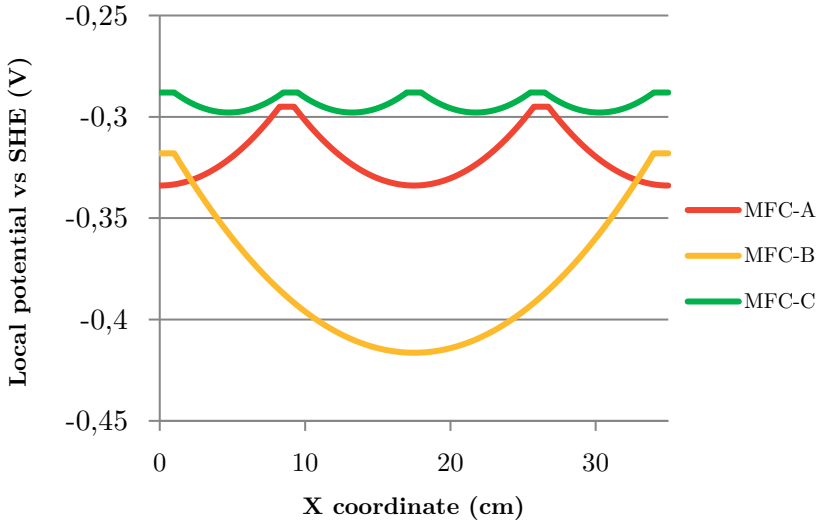

Figure 24. Local potential on anode surface, along the length of the reactor.

Commault *et al.* suggested that the anode potential can select for different strains of *Geobacter* that can also adjust their respiration chain to a potential drop [183]. Sequencing data revealed between 8 and 9 different *Geobacter* strains in our biofilm samples. Dominant strains among them were *G. sulfurreducens* and *G. pickeringii*. Figure 25 shows their relative abundance versus total abundance of *Geobacter* genus. *G. sulfurreducens* was most abundant in the MFC-B, implying that this particular strain was able to grow at a low potential. In MFC-A, *G. pickeringii* accounted for 65 % of *Geobacter* sequences. Both strains are closely related and belong to the *G. metallireducens* clade [184]. Ishii *et al.* described the *G. metallireducens* clade along with *Desulfuromonas* as being associated with low anode potential and the low current production of MFC-A was coherent with their observation [161]. In their study, the *Geobacter* species composition varied from the *G. metallireducens* clade in the early stages (first month) to *Geobacter* subsurface clade 2 in the later stages (third month). The microbial community described here would probably change with time, but our

study showed that the current collectors set-up had an effect on *Geobacter* species composition from the early stage of MFC operation.

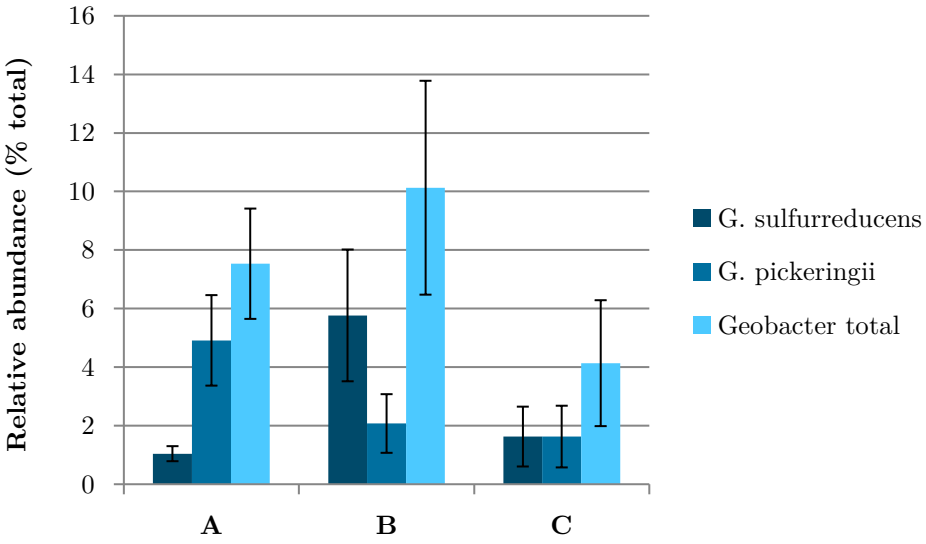

Figure 25. Relative abundance of two main *Geobacter* strains and total abundance of *Geobacter*.

4. Conclusion

The impact of current collector design on overall power production through anodic potential drop and its influence on bacterial development should be taken into account in MFC scale-up. Increasing current collector number improved maximal power. Only one connection point was not enough to recover electrons from a large surface and decreased *Geobacter* and *Desulfuromonas* abundance near that one connection point. *Geobacter* was not correlated to power but its abundance seemed to be associated with fermentative microorganisms presence and low anode local potential. Biofilm resistance decreased with electroactive bacteria abundance. Low anode potential favored the development of *Geobacter* species from *G. metallireducens* clade. The double layer capacitance of the anode increased with current collectors and it generated a not negligible capacitive current which is able to raise overall power during charge and discharge. Thus, current collectors would be an even more important design feature for power increase in MFC operated with charge/discharge cycles. Significant additional work is needed to improve knowledge of the mechanisms involved in conductivity and electron transfer in biofilm, and to include economic consideration and find a balance between power output improvement and cost (due to current collector material or used quantity).

Chapter IV - Hydrodynamic Influence on Microbial Fuel Cell Performance and Statistical Modeling: Application to Scale-up

1. Introduction

Extensive hydrodynamic characterization of microbial fuel cell (MFCs) is rare. Yet, as previously described, this aspect is a major consideration of such bioreactor functioning and electrical performance of MFCs is dependent on their hydrodynamics, especially at a larger than laboratory scale. This work tested the hypothesis that flow regime, with all the associated parameters, can explain in large part MFC performance. Three MFCs of different volumes were operated under continuous-flow conditions at different flow rates. Hydrodynamic characterization of the systems, using dimensionless numbers, electrochemical parameters and quantitative descriptions of biofilms were the basis of correlations between these parameters and MFC electrical performance. Data-driven statistical models were developed to highlight typical parameters that drive power output.

2. Results

2.1. Residence time distribution

Residence time distribution tests were performed on the three MFCs for each flow rate to assess the mixing inside. The non-symmetrical shape of all curves showed presence of dispersion inside the reactor in a similar magnitude (Figure 26). The three reactors at each flow rates corresponded to a dispersed plug flow model [130]. The dimensionless group $\frac{D_{ax}}{uL}$ was above the threshold of 0.01 for all of them, indicating a non-negligible extent of dispersion in the reactors [130]. Nevertheless, a regular velocity profile is assumed inside the reactors for the following, as a first simple approach of these systems. Residence time distribution curve for

the 1L-MFC at the lowest flow rate (5 L/h) could not be done because the tracer could not be concentrated enough, and due to the low flow, no signal could be detected at the reactor's exit.

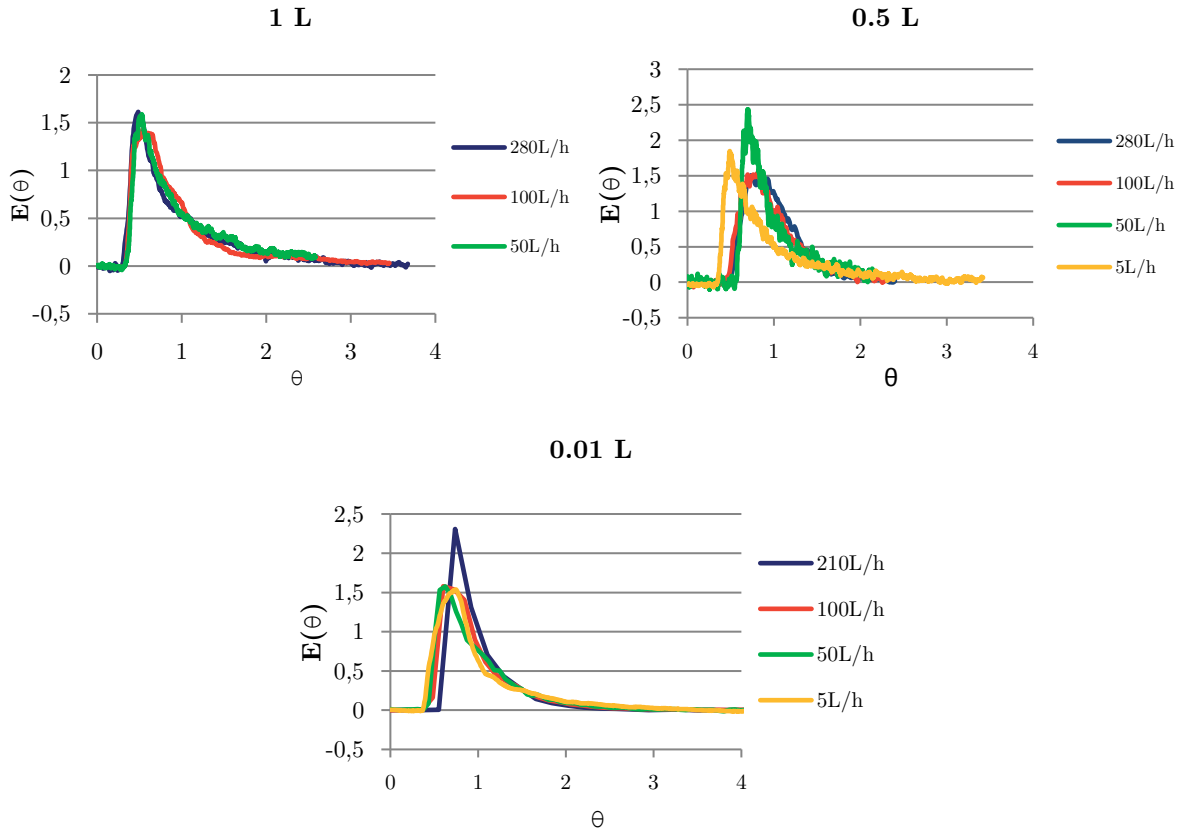

Figure 26. Residence time distribution at each flow rate for 1L-MFC, 0.5L-MFC and 0.01L-MFC.

2.2. Electrical performance

Maximum voltage globally increased with flow rate. In 0.5L- and 1L-MFC, it varied respectively from 0.276 V at 5 L/h to 0.405 V at 280 L/h, and from 0.214 V to 0.296 V (Figure 27A). 0.5L-MFC showed the highest maximum voltage at 280 L/h. The smallest MFC showed much lower maximum voltage. Its highest value was 0.062 V at the highest flow rate (210 L/h). It then decreased to 0.006 V at 100 L/h but increased to 0.02 V at 5 L/h. The maximum power was obtained in the 0.5L-MFC at the highest flow rate (280 L/h) with 9.63 mW (*i.e.* 6.88 W/anode m²) (Figure 27B). At the two highest flow rates, *i.e.* 280 and 100 L/h, the 0.5L-MFC showed a higher maximal power output than the 1L-MFC respectively 9.63 and 3.65 mW for 0.5L-MFC and 6.42 and 2.4 mW for 1L-MFC. The 0.01L-MFC shown the lowest power output in all flow conditions, from 2 µW at 100 L/h to 127 µW at 210 L/h. This was expected due to the low reactor volume and anode surface (5 cm²) but the maximal power density was also lower than 1- and 0.5L-MFCs in all conditions (from 0.01 W/m² at

100 L/h to 0.64 W/m² at 210 L/h). Power tended to decrease with slower flow rates from 280 to 50 L/h for all MFC volumes. This decrease was more important in 0.5L-MFC (9.63 to 0.62 mW) than in 1L-MFC (6.42 to 2.22 mW). But from 50 L/h to 5 L/h, the power increased, unlike maximum voltage, from 2.22 to 3.07 mW in 1L-MFC, 0.62 to 5.38 mW in 0.5L-MFC and 6 to 34 µW in 0.01L-MFC. Again, the increase was more important for 0.5L-MFC.

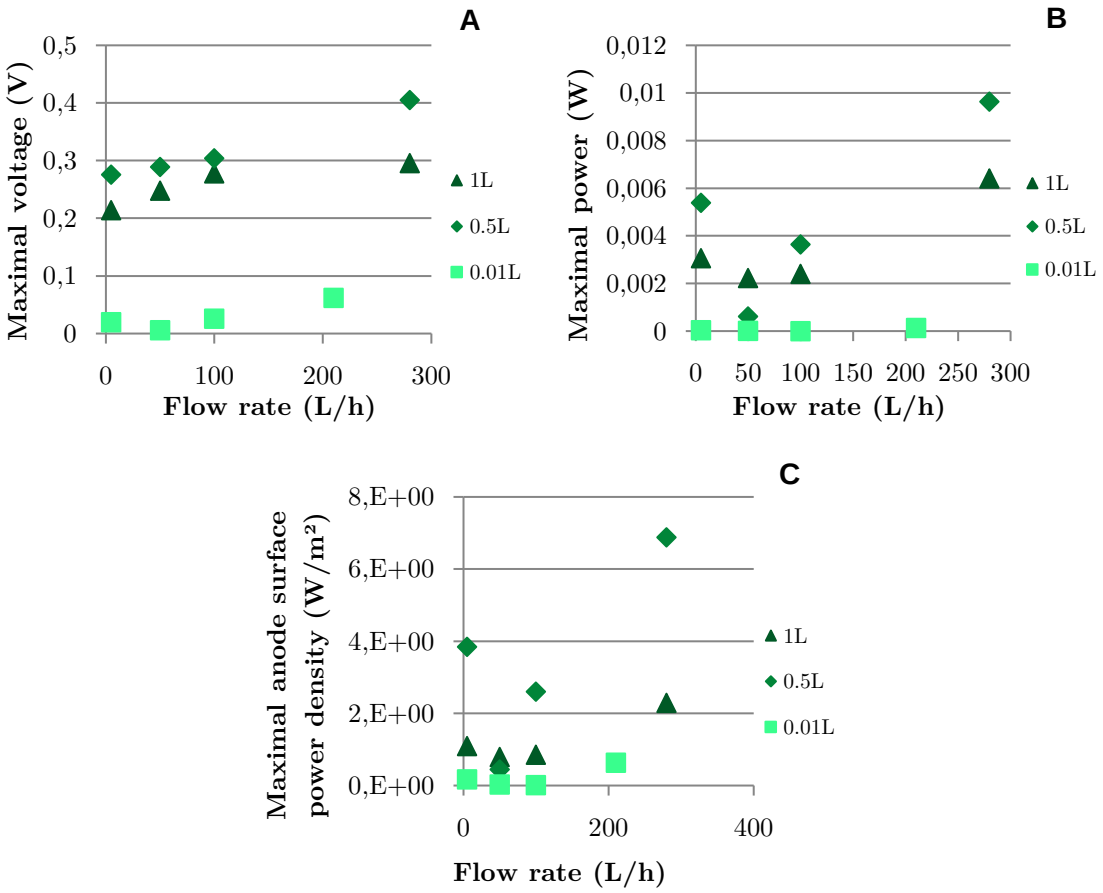

Figure 27. Maximum voltage (A), maximal power (B) and maximal surface power density (C) for each flow condition.

2.3. qPCR assay

For both total bacteria number and *Geobacter* number, no clear trend related to MFC volume or flow rate can be inferred (Figure **28**). While in 0.5L-MFC and in 1L-MFC total bacteria and *Geobacter* numbers are not significantly different with increasing flow rates, much larger differences appeared in 0.01L-MFC. It can be noted that *Geobacter* number in most of the cases is higher than total bacteria number. This apparently illogical result can be explained by a different sensitivity for both primers pairs but it showed that the relative abundance of *Geobacter* among the total microbial population is very high.

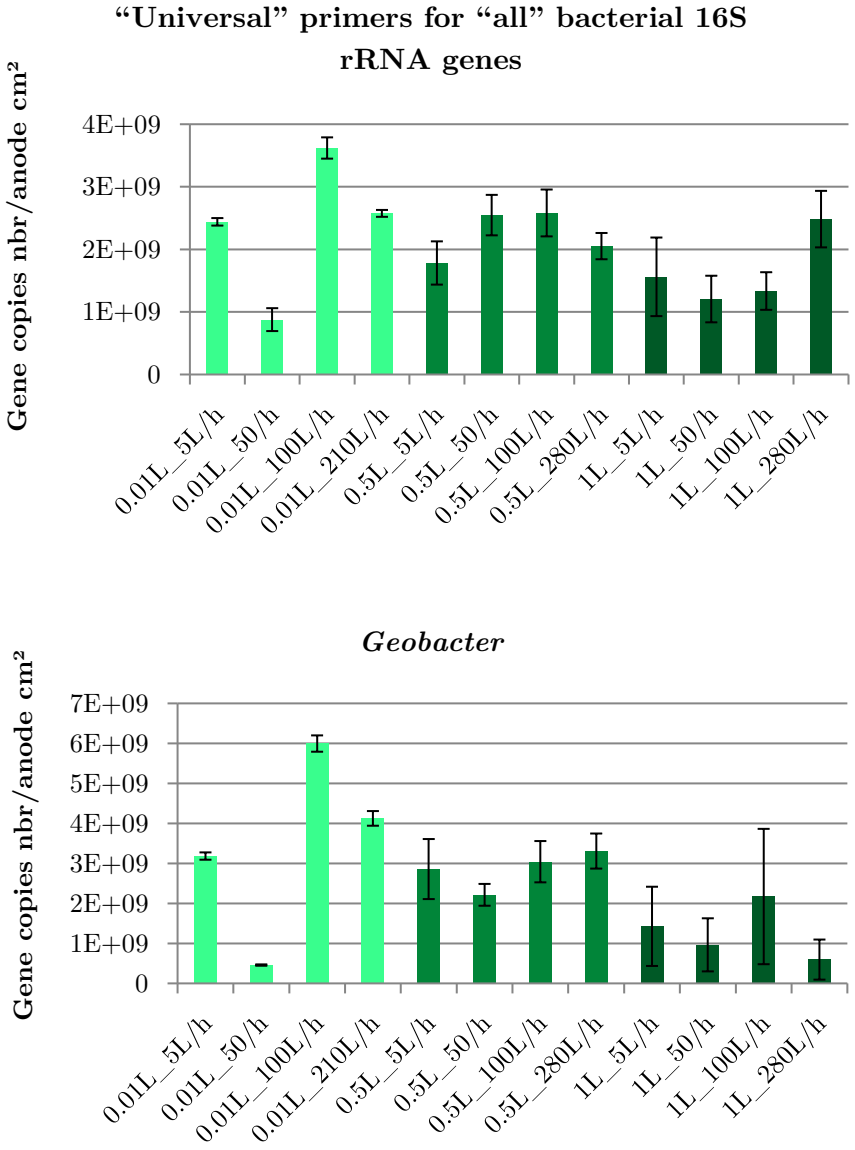

Figure 28. All bacteria and *Geobacter* quantification by qPCR as gene copies number per anode cm², for 0.01L-MFC (light green), 0.5L-MFC (green) and 1L-MFC (dark green) at different flow rates.

2.4. 16S rRNA gene (*rrs*) sequencing

The 16S rRNA gene sequencing confirmed the high relative abundance of *Geobacter* in the anodic biofilm. The highest relative abundance (69.3 %) was in the 0.5L-MFC at 5 L/h flow rate and the lowest (25.9 %) was in the 0.01L-MFC at 50 L/h flow rate (Figure 29). The diversity of the community is shown with the Shannon index and was not high due to the *Geobacter* relative abundance. The lowest Shannon index (2) was found with the highest *Geobacter* relative abundance and inversely the highest Shannon index (4) was found with the biofilm having the lowest *Geobacter* relative abundance (Figure 29). *Geobacter* relative abundance showed the same trend with flow rate as maximal power (Figure 27B). *Geobacter* relative abundance decreased with decreasing flow rate in all MFCs: from 54.7 % in 0.01L-MFC at 210 L/h to 25.9 % at 50 L/h, from 68.5 % in 0.5L-MFC at 280 L/h to 50.9 % at 50 L/h, and from 42.1 % in 1L-MFC at 280 L/h to 27.4 % at 50 L/h. At 5 L/h in the three MFCs, *Geobacter* relative abundance increased back to a value similar to its abundance at 280 L/h.

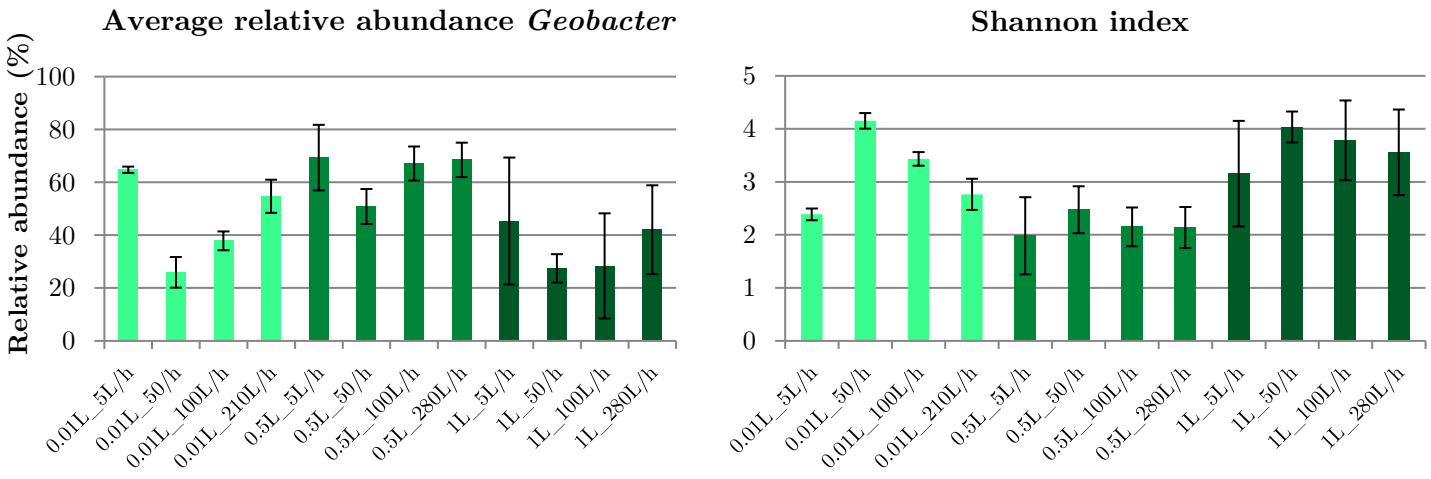

Figure 29. Relative abundance of genus *Geobacter* and Shannon diversity index for 0.01L-MFC (light green), 0.5L-MFC (green) and 1L-MFC (dark green) at different flow rates.

3. Discussion

3.1. Power prediction model

3.1.1. Multivariable linear regression

Maximal power showed no simple individual relationship to any of the common variables as described above. It was not proportional to volume, flow rate, total bacteria, nor *Geobacter* numbers (Figures 27 & 22). A negative linear correlation between maximum power density and the logarithm of the anode surface area has been described previously [107], but here the volume of the MFCs was proportional to the anode surface area and no correlation maximum power density was observed (Figure 30). Flow rate has also been described previously to be linearly correlated with power density [185]. As described above, no obvious linear relationship existed here between these two parameters for any of the volumes and flow rates tested (Figure 27C).

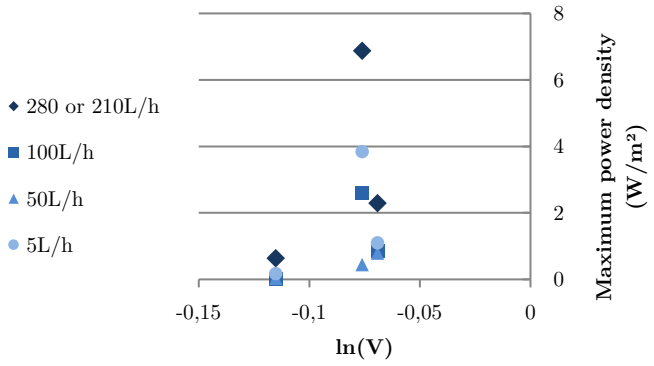

Figure 30. Maximum surface power density vs logarithm of the volume.

None of the parameters listed here could explain (or predict) the power output individually, however, a combination of several parameters might account for the power output. Statistical models were chosen to avoid complicating engineering model construction, which needs equations to describe each of the processes that should be part of the model [186]. These statistical models used experimental data to find relationships between input and output values and select relevant parameters to explain output values. Input values are simple parameters such as reactor dimensions, flow rate, mass transfer coefficient. For easy interpretability and simple model structure, linear regression was used here as a first approach for this strategy to model MFC behavior. For practical reasons, only initial parameters were used to model the maximum power as they were the only values that could

be chosen for the *a priori* construction of MFCs. Sixteen parameters were integrated into the first steps of the multiple linear regression (cross-validated LASSO model) (Table 5 & S1) to predict maximum power and select variables.

As shown before, the lowest flow rate (5 L/h) for all MFC volumes did not fit the trend of the higher flow rates for maximal power, voltage, *Geobacter* abundance or total bacteria number. This was confirmed by statistical modeling: the goodness of the linear regression always dropped significantly when observations of 5 L/h were integrated in the model (data not shown). Therefore, those observations were not used for following modeling. This very low flow rate, leading to high retention times for the largest MFCs, probably greatly limited substrate supply to some areas of the biofilm. This uneven distribution would lead to a more heterogeneous biofilm, as indicated by the large error bars for the qPCR and 16S rRNA gene sequencing results from the 1 L-MFC and 0.5 L-MFCs operated at 5 L/h. This modeling approach might not be adapted to flow conditions that lead to non-homogeneous substrate distribution.

The linear regression, without observations made at 5 L/h, reasonably fit the data (R^2= 0.9574) with five selected variables. From normalized coefficients, flow rate (0.81) and shear stress (-0.51) were the two parameters that most influenced the output power (Table 9). Hydrodynamic forces were thus probably the most critical process in our MFCs for estimating power output. Flow rate and shear stress had opposite effects. The flow rate was positively correlated to maximum power while shear stress was negatively correlated. Several studies about flow rate have reached different conclusions. Depending on the system, increasing flow rate improved power production [185,187], decreased it [188] or had an effect dependent on other parameters such as external resistance [74]. On the other hand, an increase of shear stress had been shown to increase the current and power and improve bacterial adhesion and biofilm stability [116,119], unlike what we observed here. Increasing flow rate improves mass transport to biofilm and this is positive for power production, but increases shear forces applied on the biofilm and that could have a negative effect if that leads to biofilm disruption [117]. The model generated here integrated these two aspects. The positive coefficient of the flow rate could account for substrate transport to the biofilm and the negative coefficient of the shear stress for the physical forces applied on the anode. This model with variable selection showed a good fit to the data but several limitations appeared in addition to reduced flow rate range as explain above. Prediction performance is strongly dependent on the number of observations and on the validation on a test dataset [189]. This could not be done here. Due to strong disturbance of the biofilm by polarization curve measurements, only one maximum power was measured at the end of each MFC operation. Continuous-power measurements and modeling would better fit the behavior of MFC as a dynamic system, because the model determined here might not fit the power output at an earlier time.

Table 9. Maximum power model parameters from multivariable linear regression.

Selected variable	Coefficients	Normalized coefficients
Flow rate (Q)	2.83E-05	0.81
Mass transfer coefficient (k)	-1.20E+01	-0.06
Péclet number from RTD (Pe_{RTD})	1.24E-04	0.21
Characteristic time of substrate diffusion in CBL	4.66E-12	0.10
Shear stress (T)	-8.55E-03	-0.51

3.1.2. Linear regression with dimensionless variables

The Vaschy-Buckingham theorem was used to create dimensionless variables. This theorem is widely use in engineering for scale-up and scale-down to reduce degrees of freedom of a problem and thus provide simple laws, in particular in new process studies when equations are not well defined and articulated [190]. This strategy was applied here. The variables were chosen to represent each of the phenomena involved in MFC (Table 5 & S2): characteristic length, water density, water dynamic viscosity, fluid velocity, shear stress and inter-electrodes distance. Four dimensionless numbers were generated:

$$\Pi_1 = Re = \frac{u \times L_c \times \rho}{\mu}$$

$$\Pi_2 = Pe = \frac{u \times L_c}{D}$$

$$\Pi_3 = \frac{T}{u \times \rho}$$

$$\Pi_4 = \frac{h}{L_c}$$

The linear regression with these four numbers to model maximum power had a linear regression coefficient (R^2) of 0.811. This coefficient was lower than for the previous model, probably because of the lower number of variables used. Péclet number (Π_2) was useless in this model as its coefficient was zero. In the previous model, the experimental Péclet number appeared in the model expression. Theoretical and empirical Péclet numbers are very different (Figure 31). Theoretical Péclet numbers were all between 10^5 and 10^8, while the same number extracted from RTD varied between 3 and 20. This number represents the ratio of the convection transport rate to that for diffusion and dispersion, combined.

Dispersion occurred to a large extent in the reactors, probably because of the lack of precision in the MFC construction, which prevented the flow to be regular.

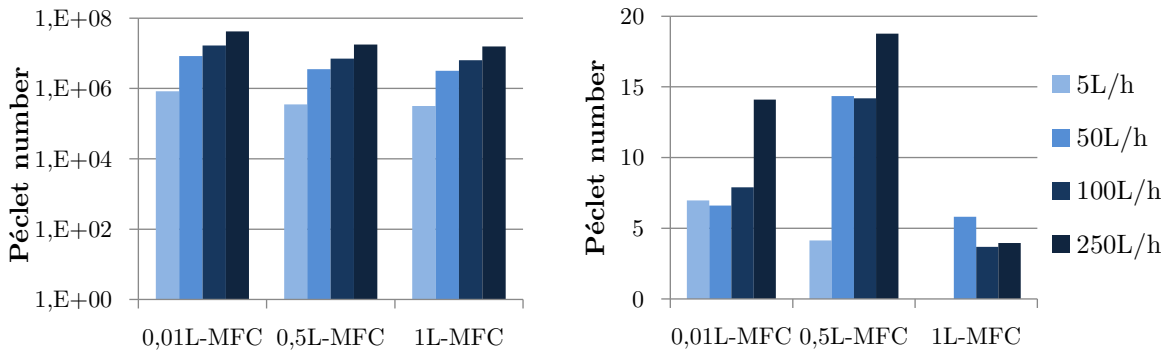

Figure 31. Calculated Péclet number from theoretical expression (A) and Péclet number extracted from RTD experiment (B).

The Sherwood number was then added to the model. This number is a dimensionless number whose expression has been empirically modified [153] and used in previous MFC studies [191] and was thus not retrievable from Vaschy-Buckingham theorem. With this fifth number, linear regression coefficient R^2 increased to 0.892. None of the coefficients is much more important than the others, as shown by the normalized coefficients (Table 10). Shear stress, expressed in Π_3, was negatively correlated with maximum power. Fluid speed was mainly described by the Reynolds number and was positively correlated to maximum power. Both of these observations confirmed the previous model and therefore, showed coherence between both models. For this model, variables were chosen based on the process they represented, or the process they were related to, whereas in the previous model, the statistical tool chose them. The coherence between these two models suggested that the two approaches were either able to predict maximum power and are subjected to the same biases inherent in the dataset.

Table 10. Maximum power model parameters from linear regression based on dimensionless numbers.

Variables	Coefficients	Normalized coefficients
Π1 = Re	3.72×10^{-6}	2.19
Π3	$-1.08\times10^{+1}$	-2.21
Π4	1.10×10^{-2}	1.15
Sh	-6.67×10^{-6}	-1.04

3.2. Modeling of *Geobacter* numbers

Configuration and operational parameters act on electricity output by shaping the electroactive biofilm microbial community. This effect was not integrated in the previous models because no measurements were used as variables. *Geobacter* was the most abundant genus in the biofilm of all MFCs (Figure 29), hence, a model including measured physical and chemical parameters (Table 5 & S3) was designed to predict its number obtained from qPCR. Unfortunately, the model based on cross-validated LASSO variable selection could not select variables and perform linear regression. First, it meant that maximum power was not simply correlated to *Geobacter* numbers, confirming that the *Geobacter* abundance was not a good representative of electricity production potential. This was also suggested in the previous chapter for current collector set-up and anode surface potential. Other statistical tools might be used to fit *Geobacter* numbers, but linear regression was not the good choice here. Thus, the influence of configuration and operational parameters was not straightforward. The modeling of a particular actor of power production seemed to be harder to interpret than the modeling of the global output of the system.

4. Conclusion

Hydrodynamics is an important process in continuously-fed MFCs. Statistical models using configuration and operational parameters were developed and successfully simulated maximum power output results. The LASSO model selected five variables of interest while another model was based on dimensionless numbers built with the Vaschy-Buckingham theorem. Both models showed reasonable linear regression coefficients and a consistent evaluation of the influence of fluid flow rate and shear stress. The *Geobacter* population was not a good explicative variable for maximum power despite its very high abundance on the anode. This might imply that power and biofilm electroactivity ability were not directly linked to *Geobacter* numbers. Data-based modeling could be a promising approach to better identify important parameters, predict electricity output and help design efficient scaled-up MFCs.

General Discussion and Perspectives

After a decade of MFC research, the global feeling is that scaled-up MFC for electricity production by MFC will not be viable one day, so research is going into alternative (production of biomolecules, biosensors, etc.), but some aspects, such current collectors and flow regime, were not taken into account (or not published). They are important parts of MFC, especially in a scaling up perspective and for industrial application. For instance a lot of chemical fuel cells studies are about current collectors [57–60], and a large part about electrochemical reactors development and design is dedicated to the study of flow influence on performance, with process engineering tools [61–64]. MFC are not so different: it's an electrochemical reactor with biological catalyst. These kinds of tools should be used and could really improve their development or, if not, explicit the limits.

This work also tried to combine microbiology and engineering. Fundamental research about electroactive bacteria and biofilm development is often completely separated from scaling up studies. Both aspects are important and full studies should focused on, but studies linking both aspects would for instance help to understand how an operation parameter modifies the anodic community and how this modification is related to MFC performance, or is the biofilm homogeneous over a large anode in a scaled-up MFC and what can improve that. MFC is powered by bacteria and even in large-scale MFCs, inoculated with a mixed community sludge sample and fed with complex substrate changing with time, such as wastewater, microbial ecology questions are still relevant and should be tackled. Today, molecular biology tools, microscopy or chemical analysis are commonly used methods and can be quite easily incorporated in MFC study. In addition, process engineering tools and statistic modeling could improve and formalize the current development of MFC scale-up, which remains mainly empirical. Process engineering provides methods and tools to design, optimize and operate reactors, which is exactly what is chased by scale-up MFC studies. Data-driven statistics modeling could provide empirical models to predict MFC performance which would help to design the system and set operational parameters. Computational models for biofilm structure or MFC performance are currently mostly based on physical and chemical equations that describe the system. Such models account more and more for the complexity of bacteria development and interactions and of mass transport. But a MFC based on complex inoculum and substrate cannot yet be fully described by such equations. Thus, it is still very difficult to build a computational model that efficiently predicts MFC behavior. On the other hand, statistical models only use input and output data to build a mathematical relation between them, regardless of the physical meaning of parameters

used. MFC is still seen as a “black box” in this case, and this cannot be final goal, but both approaches can be useful. Despite obvious limits for use in a single MFC study (*e.g.* limited measured parameters and replicates number), statistical models can in particular be useful to summarize and learn from the gigantic set of data generated for MFC study and identify interesting parameters with system theory (system identification) or machine learning (neural network method).

We highlighted here two aspects to improve electricity production in MFC: better connect the anode to the external circuit and choose flow rate based upon reactor design to control hydrodynamics inside the MFC. More than just noticing differences between conditions, we tried to generalize results by coupling it with microbial ecology analysis to understand and explain MFC performance. That way, this work showed that anodic current collectors are not just pieces of metal connecting the anode to the external circuit but they are influencing the biofilm structure by shaping current flow lines and electric field. It also appeared that power and anode biofilm response to flow condition is not linear with flow rate increase: a breaking point seemed to exist between too low flow rates (here 5 L/h) and higher flow rates, suggesting different behaviors of MFCs regarding flow conditions. Besides, interesting results about *Geobacter* appeared. It particularly showed that *Geobacter* number does not linearly correlate with power, in both studies, in batch or in flow (Figure 32) and that its modeling based on configuration and operational parameters used here is difficult. Ratio of *Geobacter* density to maximum power density varied from 1.1×10^{7} to 1.5×10^{12}, and it did not seem to be linked to flow rate or volume. On the other hand *Geobacter* density was greatly improve in presence of continuous flow (Figure 33), from around 10^{6} gene copies number/anode cm^2 in batch MFCs to around 10^{9} in continuous MFCs, showing that *Geobacter*’s growth is influenced by MFC operational conditions. It suggested that configuration and operation parameters of MFC have not a straightforward effect on mixed-species biofilm and on *Geobacter* in particular. Mixed effects on bacterial selection, *Geobacter* electroactivity or microbial interactions are difficult to sort out, probably because of the complexity of such inoculum and mostly because sludge inoculum are not reproducible even from the same source. *Geobacter* is still an important member in these anodic biofilms, but its presence and electroactivity depending on conditions are not so clear. More information is needed about the features of each clade, the way they are selected in such environment and their relationships and exchanges with the other members of the biofilm.

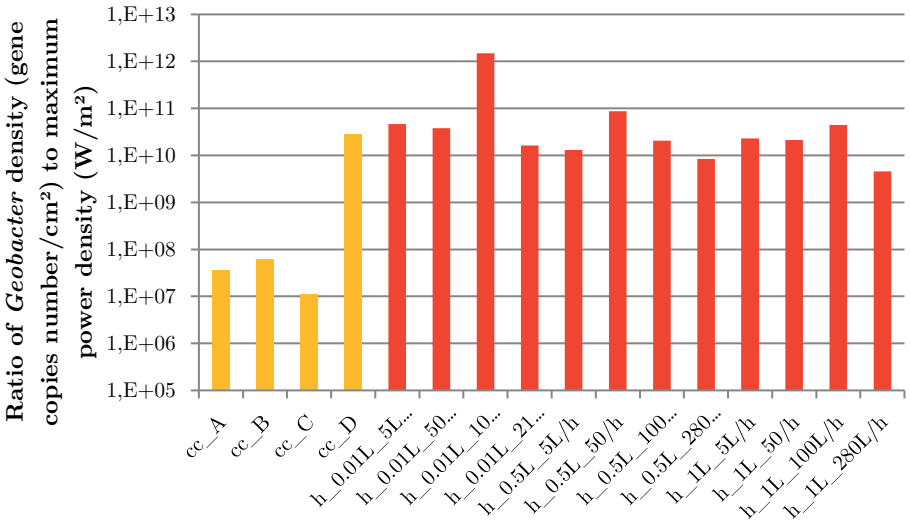

Figure 32. Ratio of *Geobacter* density to maximum power density in MFCs used for the study of current collectors ("cc", yellow) in batch, and hydrodynamics effects ("h", red), in continuous flow.

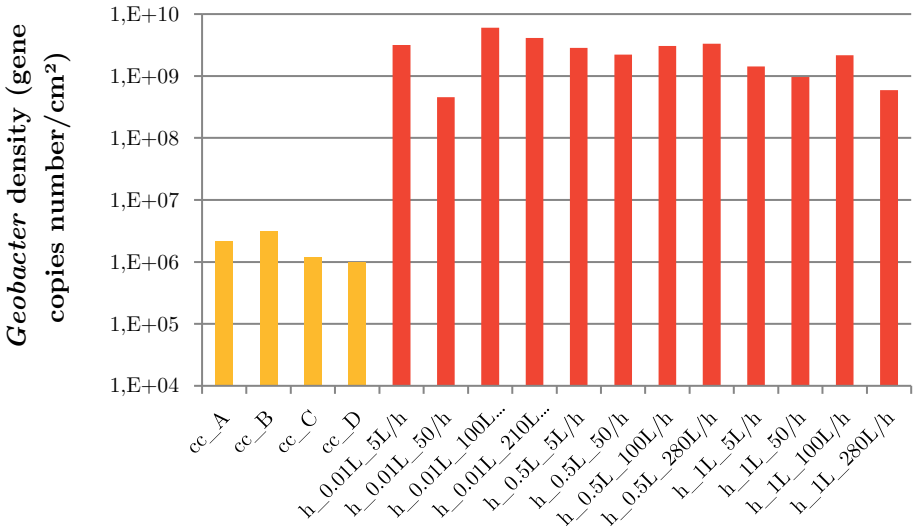

Figure 33. *Geobacter* density in MFCs used for the study of current collectors ("cc", yellow) in batch, and hydrodynamics effects ("h", red), in continuous flow.

Maximal power has been modeled based on MFC parameters. As stated in the chapter four, these results should be interpreted very cautiously because of the too few observations. They are used here as a proof-of-concept of the interest of using such data-driven statistic tools in scaling up MFC. A simulation based on the LASSO model predicted the importance of MFC width, length and flow rate (Figure 34). Length (from inlet to outlet) and width (width of the cross-sectional area; inter-electrodes distance is unchanged) were varied from 1 cm to 3 m. Length did not show significance in maximal power produced but increasing width from 1 to 15 cm increased maximal power from 8.7 to 9.06 mW (Figure 34A). This increase is almost negligible compared to the effect of flow rate (Figure 34B). Flow rate was varied from 50 L/h to 500 L/h and the maximal power increased steadily from 3 to 15 mW. From this

quick simulation it appeared that flow rate is the parameter with the largest effect on maximal power among the three tested here. Increased length and width improved power, but to a much lesser extent than flow rate. The simulation could be use a starting point for optimization: from a MFC 35 cm long and 15 cm wide, increase flow rate to improve power and check the model validity with other observations. For the moment, it is suggested that a large MFC with the current configuration would not be optimized. This sort of models can thus be useful to determine up to which MFC enlargement one should go. Then the MFC scaling up strategy could be to multiply this maximum-sized MFC and develop low voltages converters to harvest energy and optimize operation in charge/discharge duty cycles. Such smaller units would also limit the technical issues inherent to the construction of large air-cathode MFC (large surface area air-cathode manufacture, impermeability of the reactor, etc.).

A

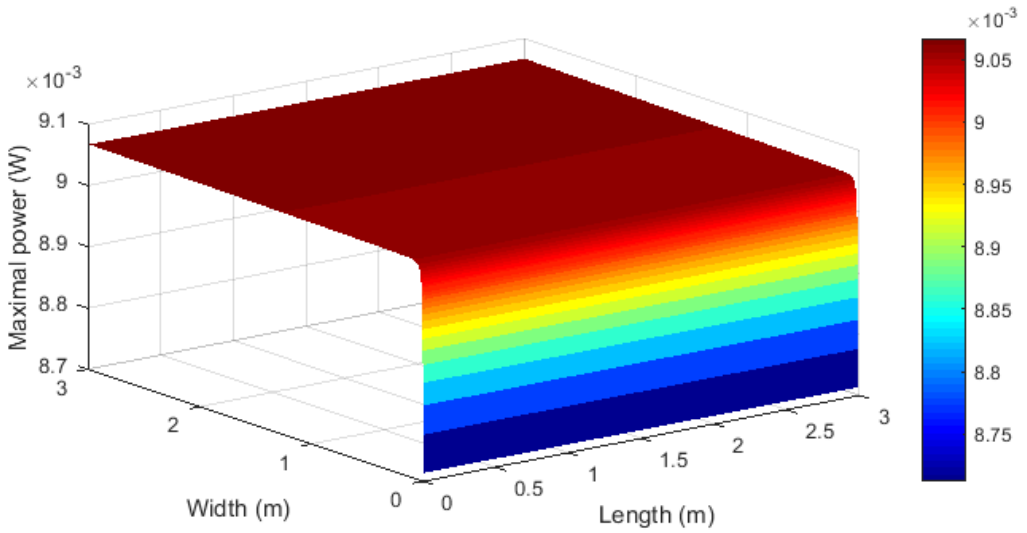

B

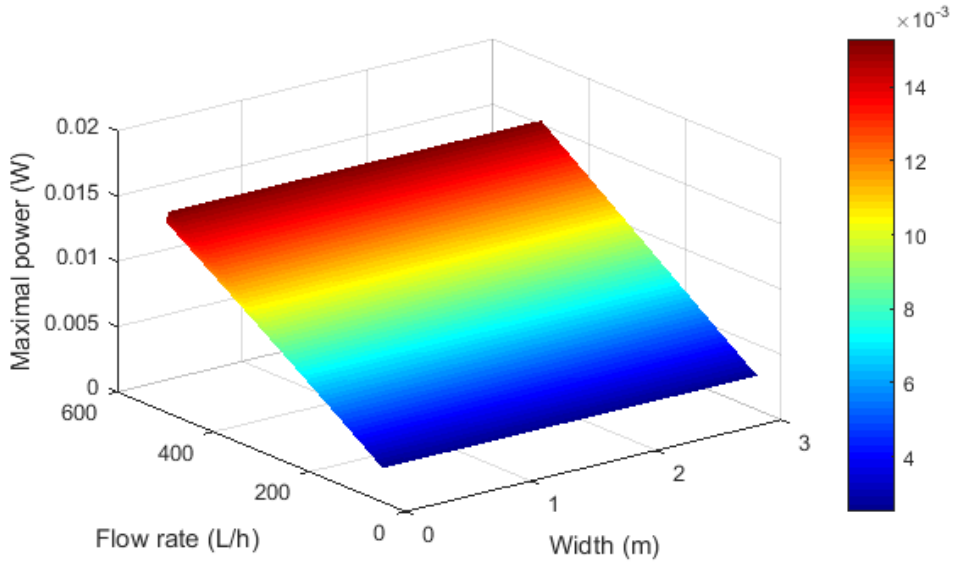

Figure 34. Simulation of maximal power generated by changing the length, the width and the flow rate applied to the flat-plate air-cathode MFC used in this work, at a constant flow rate of 280 L/h (A) or at a constant length of 0.35 m (B).

References

1. Ministère de l'Environnement, de l'Energie et de la Mer. Available at: http://www.developpement-durable.gouv.fr/. (Accessed: 17th January 2017)
2. Les énergies renouvelables, IFP. Available at: http://www.ifpenergiesnouvelles.fr/Espace-Decouverte/Les-cles-pour-comprendre/Les-sources-d-energie/Les-energies-renouvelables. (Accessed: 19th January 2017)
3. *Réunion d'Échanges – Station d'épuration Aqualyon La Feyssine – Grand Lyon*. (Groupe de Recherche Rhône-Alpes sur les Infrastructures et l'Eau, 2012).
4. Vers l'autonomie énergétique des stations d'épuration. *Actu-Environnement* Available at: http://www.actu-environnement.com/ae/news/station-epuration-energie-methanisation-boues-procedes-11734.php4. (Accessed: 19th January 2017)
5. Point sur les stations d'épuration - Ministère du Développement durable. Available at: http://www.developpement-durable.gouv.fr/Point-sur-les-stations-d-epuration.html. (Accessed: 22nd June 2015)
6. Les stations d'épuration à boues activées - Irstea. *www.irstea.fr* Available at: http://www.irstea.fr/lespace-jeunesse/approfondir/lepuration-des-eaux-usees-les-avancees/les-stations-depuration-boues. (Accessed: 22nd June 2015)
7. Observatoire de l'eau. *Suivi des systèmes d'assainissement collectif en Seine-et-Marne, 2011*. (Conseil Général de Seine-et-Marne, 2011).
8. Lardet, S. La gestion de l'énergie dans les stations d'épuration, optimisation de l'aération. (2013).
9. Heduit, A. & Tabuchi, J.-P. Vers une plus grande autonomie énergetique des stations d'épuration? *Sciences, Eaux et Territoires* (2012).
10. Shizas, I. & Bagley, D. M. Experimental determination of energy content of unknown organics in municipal wastewater streams. *J. Energy Eng.* **130,** 45–53 (2004).
11. Lefebvre, O., Uzabiaga, A., Chang, I. S., Kim, B.-H. & Ng, H. Y. Microbial fuel cells for energy self-sufficient domestic wastewater treatment—a review and discussion from energetic consideration. *Appl. Microbiol. Biotechnol.* **89,** 259–270 (2011).

12. Tchobanoglous, G., Burton, F. & Stensel, D. *Wastewater engineering treatment and reuse*. (Metcalf & Eddy).
13. Potter, M. C. Electrical effects accompanying the decomposition of organic compounds. *Proc. R. Soc. Lond. Ser. B Contain. Pap. Biol. Character* 260–276 (1911).
14. He, Z., Zhang, F. & Ge, Z. *Using microbial fuel cells to treat raw sludge and primary effluent for bioelectricity generation: final report*. (2013).
15. Valorisation énergétique - Les valorisations énergétiques des biogaz et gaz d... – ADEME. Available at: http://www.ademe.fr/expertises/dechets/passer-a-laction/valorisation-energetique/valorisations-energetiques-biogaz-gaz-synthese. (Accessed: 8th February 2017)
16. Lee, H.-S., Parameswaran, P., Kato-Marcus, A., Torres, C. I. & Rittmann, B. E. Evaluation of energy-conversion efficiencies in microbial fuel cells (MFCs) utilizing fermentable and non-fermentable substrates. *Water Res.* **42,** 1501–1510 (2008).
17. Logan, B. E. *Microbial fuel cells*. (Wiley-Interscience, 2008).
18. Notion d'équivalent-habitant (EH) | Société Publique de la Gestion de l'Eau. Available at: http://www.spge.be/fr/notion-d-equivalent-habitant-eh.html?IDC=1094&IDD=1368. (Accessed: 8th February 2017)
19. Assainissement : le traitement collectif des eaux usées : Observation et statistiques. Available at: http://www.statistiques.developpement-durable.gouv.fr/lessentiel/ar/306/1168/assainissement-traitement-collectif-eaux-usees.html. (Accessed: 7th February 2017)
20. Bilan électrique de la France : que retenir de 2015 ? *Connaissance des Énergies* (2016). Available at: http://www.connaissancedesenergies.org/bilan-electrique-de-la-france-que-retenir-de-2015-160203. (Accessed: 8th February 2017)
21. Etat des lieux de la méthanisation des boues de stations d'épuration des eaux | MAGAZINE ET PORTAIL FRANCOPHONE DES BIOÉNERGIES. Available at: https://www.bioenergie-promotion.fr/35192/etat-des-lieux-de-la-methanisation-des-boues-de-stations-depuration-des-eaux/. (Accessed: 8th February 2017)

22. Logan, B. E. Extracting hydrogen and electricity from renewable resources. *Environ. Sci. Technol.* (2004).

23. Liu, H., Cheng, S. & Logan, B. E. Production of electricity from acetate or butyrate using a single-chamber microbial fuel cell. *Environ. Sci. Technol.* **39,** 658–662 (2005).

24. Janicek, A., Fan, Y. & Liu, H. Design of microbial fuel cells for practical application: a review and analysis of scale-up studies. *Biofuels* **5,** 79–92 (2014).

25. Logan, B. E. *et al.* Microbial fuel cells: methodology and technology. *Environ. Sci. Technol.* **40,** 5181–5192 (2006).

26. Kumar, G. G., Sarathi, V. G. S. & Nahm, K. S. Recent advances and challenges in the anode architecture and their modifications for the applications of microbial fuel cells. *Biosens. Bioelectron.* **43,** 461–475 (2013).

27. Rismani-Yazdi, H., Carver, S. M., Christy, A. D. & Tuovinen, O. H. Cathodic limitations in microbial fuel cells: An overview. *J. Power Sources* **180,** 683–694 (2008).

28. Wei, J., Liang, P. & Huang, X. Recent progress in electrodes for microbial fuel cells. *Bioresour. Technol.* **102,** 9335–9344 (2011).

29. Kiely, P. D., Regan, J. M. & Logan, B. E. The electric picnic: synergistic requirements for exoelectrogenic microbial communities. *Curr. Opin. Biotechnol.* **22,** 378–385 (2011).

30. Pant, D., Van Bogaert, G., Diels, L. & Vanbroekhoven, K. A review of the substrates used in microbial fuel cells (MFCs) for sustainable energy production. *Bioresour. Technol.* **101,** 1533–1543 (2010).

31. Zhu, F., Wang, W., Zhang, X. & Tao, G. Electricity generation in a membrane-less microbial fuel cell with down-flow feeding onto the cathode. *Bioresour. Technol.* **102,** 7324–7328 (2011).

32. Scott, K., Murano, C. & Rimbu, G. A tubular microbial fuel cell. *J. Appl. Electrochem.* **37,** 1063–1068 (2007).

33. Jung, S. & Regan, J. M. Influence of external resistance on electrogenesis, methanogenesis, and anode prokaryotic communities in microbial fuel cells. *Appl. Environ. Microbiol.* **77,** 564–571 (2011).

34. Lyon, D. Y., Buret, F., Vogel, T. M. & Monier, J.-M. Is resistance futile? Changing external resistance does not improve microbial fuel cell performance. *Bioelectrochemistry* **78,** 2–7 (2010).
35. Boesen, T. & Nielsen, L. P. Molecular dissection of bacterial nanowires. *mBio* **4,** e00270-13-e00270-13 (2013).
36. Gorby, Y. A. *et al.* Electrically conductive bacterial nanowires produced by Shewanella oneidensis strain MR-1 and other microorganisms. *Proc. Natl. Acad. Sci.* **103,** 11358–11363 (2006).
37. Zhi, W., Ge, Z., He, Z. & Zhang, H. Methods for understanding microbial community structures and functions in microbial fuel cells: A review. *Bioresour. Technol.* **171,** 461–468 (2014).
38. Zhao, F., Slade, R. C. & Varcoe, J. R. Techniques for the study and development of microbial fuel cells: an electrochemical perspective. *Chem. Soc. Rev.* **38,** 1926–1939 (2009).
39. Patil, S. A., Hägerhäll, C. & Gorton, L. Electron transfer mechanisms between microorganisms and electrodes in bioelectrochemical systems. *Bioanal. Rev.* **4,** 159–192 (2012).
40. Logan, B. E. Essential data and techniques for conducting microbial fuel cell and other types of bioelectrochemical system experiments. *ChemSusChem* **5,** 988–994 (2012).
41. Ewing, T. *et al.* Scale-up of sediment microbial fuel cells. *J. Power Sources* **272,** 311–319 (2014).
42. Plant-e. Available at: http://www.plant-e.com/en/. (Accessed: 5th March 2017)
43. Yang, H., Zhou, M., Liu, M., Yang, W. & Gu, T. Microbial fuel cells for biosensor applications. *Biotechnol. Lett.* **37,** 2357–2364 (2015).
44. Lalaurette, E. Hydrogen production from cellulose fermentation end products using microbial electrolysis cells. (The Pennsylvania State University, 2008).
45. Nevin, K. P. *et al.* Electrosynthesis of organic compounds from carbon dioxide is catalyzed by a diversity of acetogenic microorganisms. *Appl. Environ. Microbiol.* **77,** 2882–2886 (2011).

46. Cambrian Innovation. *Cambrian Innovation* Available at: http://cambrianinnovation.com/. (Accessed: 5th March 2017)

47. Cao, X. *et al.* A new method for water desalination using microbial desalination cells. *Environ. Sci. Technol.* **43,** 7148–7152 (2009).

48. Dennis, P. G., Harnisch, F., Yeoh, Y. K., Tyson, G. W. & Rabaey, K. Dynamics of cathode-associated microbial communities and metabolite profiles in a glycerol-fed bioelectrochemical system. *Appl. Environ. Microbiol.* **79,** 4008–4014 (2013).

49. Jiang, D. & Li, B. Granular activated carbon single-chamber microbial fuel cells (GAC-SCMFCs): A design suitable for large-scale wastewater treatment processes. *Biochem. Eng. J.* **47,** 31–37 (2009).

50. Zhang, F., Ge, Z., Grimaud, J., Hurst, J. & He, Z. In situ investigation of tubular microbial fuel cells deployed in an aeration tank at a municipal wastewater treatment plant. *Bioresour. Technol.* **136,** 316–321 (2013).

51. Zhang, F., Ge, Z., Grimaud, J., Hurst, J. & He, Z. Improving electricity production in tubular microbial fuel cells through optimizing the anolyte flow with spiral spacers. *Bioresour. Technol.* **134,** 251–256 (2013).

52. Zhang, F., Ge, Z., Grimaud, J., Hurst, J. & He, Z. Long-term performance of liter-scale microbial fuel cells treating primary effluent installed in a municipal wastewater treatment facility. *Environ. Sci. Technol.* **47,** 4941–4948 (2013).

53. Hiegemann, H. *et al.* An integrated 45L pilot microbial fuel cell system at a full-scale wastewater treatment plant. *Bioresour. Technol.* (2016). doi:http://dx.doi.org/10.1016/j.biortech.2016.06.052

54. Ge, Z. & He, Z. Long-term performance of a 200-liter modularized microbial fuel cell system treating municipal wastewater: treatment, energy, and cost. *Env. Sci Water Res Technol* (2016). doi:10.1039/C6EW00020G

55. Feng, Y. *et al.* A horizontal plug flow and stackable pilot microbial fuel cell for municipal wastewater treatment. *Bioresour. Technol.* **156,** 132–138 (2014).

56. Aelterman, P., Freguia, S., Keller, J., Verstraete, W. & Rabaey, K. The anode potential regulates bacterial activity in microbial fuel cells. *Appl. Microbiol. Biotechnol.* **78,** 409–418 (2008).

57. Taheri, P., Mansouri, A., Schweitzer, B., Yazdanpour, M. & Bahrami, M. Electrical constriction resistance in current collectors of large-scale lithium-ion batteries. *J. Electrochem. Soc.* **160,** A1731–A1740 (2013).

58. Jiang, S. Effect of contact between electrode and current collector on the performance of solid oxide fuel cells. *Solid State Ion.* **160,** 15–26 (2003).

59. Yang, W. M., Chou, S. K. & Shu, C. Effect of current-collector structure on performance of passive micro direct methanol fuel cell. *J. Power Sources* **164,** 549–554 (2007).

60. Lee, C.-W. *et al.* Study on the effect of current collector structures on the performance of MCFCs using three-dimensional fluid dynamics analysis. *J. Ind. Eng. Chem.* **51,** 153–161 (2017).

61. Vázquez, L., Alvarez-Gallegos, A., Sierra, F. Z., de León, C. P. & Walsh, F. C. CFD evaluation of internal manifold effects on mass transport distribution in a laboratory filter-press flow cell. *J. Appl. Electrochem.* **43,** 453–465 (2013).

62. Frías-Ferrer, á., González-García, J., Sáez, V., de León, C. P. & Walsh, F. C. The effects of manifold flow on mass transport in electrochemical filter-press reactors. *AIChE J.* **54,** 811–823 (2008).

63. Liu, Y. & Tay, J.-H. The essential role of hydrodynamic shear force in the formation of biofilm and granular sludge. *Water Res.* **36,** 1653–1665 (2002).

64. Celmer, D., Oleszkiewicz, J. A. & Cicek, N. Impact of shear force on the biofilm structure and performance of a membrane biofilm reactor for tertiary hydrogen-driven denitrification of municipal wastewater. *Water Res.* **42,** 3057–3065 (2008).

65. Degrenne, N. *et al.* Comparison of 3 self-starting step-up DC: DC converter topologies for harvesting energy from low-voltage and low-power microbial fuel cells. in *Power Electronics and Applications (EPE 2011), Proceedings of the 2011-14th European Conference on* 1–10 (IEEE, 2011).

66. Wu, P. K., Biffinger, J. C., Fitzgerald, L. A. & Ringeisen, B. R. A low power DC/DC booster circuit designed for microbial fuel cells. *Process Biochem.* **47,** 1620–1626 (2012).

67. Brown, R. K., Harnisch, F., Dockhorn, T. & Schröder, U. Examining sludge production in bioelectrochemical systems treating domestic wastewater. *Bioresour. Technol.* **198,** 913–917 (2015).

68. Zhang, C., Liang, P., Jiang, Y. & Huang, X. Enhanced power generation of microbial fuel cell using manganese dioxide-coated anode in flow-through mode. *J. Power Sources* **273,** 580–583 (2015).

69. Liu, W., Cheng, S. & Guo, J. Anode modification with formic acid: A simple and effective method to improve the power generation of microbial fuel cells. *Appl. Surf. Sci.* **320,** 281–286 (2014).

70. White, H. K., Reimers, C. E., Cordes, E. E., Dilly, G. F. & Girguis, P. R. Quantitative population dynamics of microbial communities in plankton-fed microbial fuel cells. *ISME J.* **3,** 635–646 (2009).

71. Nevin, K. P. *et al.* Anode biofilm transcriptomics reveals outer surface components essential for high density current production in geobacter sulfurreducens fuel cells. *PLoS ONE* **4,** e5628 (2009).

72. Dolch, K. *et al.* Characterization of microbial current production as a function of microbe–electrode-interaction. *Bioresour. Technol.* **157,** 284–292 (2014).

73. Kimura, Z. & Okabe, S. Acetate oxidation by syntrophic association between Geobacter sulfurreducens and a hydrogen-utilizing exoelectrogen. *ISME J.* **7,** 1472–1482 (2013).

74. Aelterman, P., Versichele, M., Marzorati, M., Boon, N. & Verstraete, W. Loading rate and external resistance control the electricity generation of microbial fuel cells with different three-dimensional anodes. *Bioresour. Technol.* **99,** 8895–8902 (2008).

75. Richter, H. *et al.* Cyclic voltammetry of biofilms of wild type and mutant Geobacter sulfurreducens on fuel cell anodes indicates possible roles of OmcB, OmcZ, type IV pili, and protons in extracellular electron transfer. *Energy Environ. Sci.* **2,** 506 (2009).

76. Shen, L. *et al.* Anodic concentration loss and impedance characteristics in rotating disk electrode microbial fuel cells. *Bioprocess Biosyst. Eng.* **39,** 1627–1634 (2016).

77. Sekar, N. & Ramasamy, R. P. Electrochemical impedance spectroscopy for microbial fuel cell characterization. *J. Microb. Biochem. Technol.* **6,** (2013).

78. Dominguez-Benetton, X., Sevda, S., Vanbroekhoven, K. & Pant, D. The accurate use of impedance analysis for the study of microbial electrochemical systems. *Chem. Soc. Rev.* **41,** 7228 (2012).

79. Uría, N., Muñoz Berbel, X., Sánchez, O., Muñoz, F. X. & Mas, J. Transient storage of electrical charge in biofilms of Shewanella oneidensis MR-1 growing in a microbial fuel cell. *Environ. Sci. Technol.* **45,** 10250–10256 (2011).

80. Schrott, G. D., Bonanni, P. S., Robuschi, L., Esteve-Nuñez, A. & Busalmen, J. P. Electrochemical insight into the mechanism of electron transport in biofilms of Geobacter sulfurreducens. *Electrochimica Acta* **56,** 10791–10795 (2011).

81. Lu, Z. *et al.* Biological capacitance studies of anodes in microbial fuel cells using electrochemical impedance spectroscopy. *Bioprocess Biosyst. Eng.* **38,** 1325–1333 (2015).

82. Fradler, K. R. *et al.* The effect of internal capacitance on power quality and energy efficiency in a tubular microbial fuel cell. *Process Biochem.* **49,** 973–980 (2014).

83. Jiang, D. *et al.* A pilot-scale study on utilizing multi-anode/cathode microbial fuel cells (MAC MFCs) to enhance the power production in wastewater treatment. *Int. J. Hydrog. Energy* **36,** 876–884 (2011).

84. Liu, H., Cheng, S. & Logan, B. E. Power generation in fed-batch microbial fuel cells as a function of ionic strength, temperature, and reactor configuration. *Environ. Sci. Technol.* **39,** 5488–5493 (2005).

85. Ge, Z., Wu, L., Zhang, F. & He, Z. Energy extraction from a large-scale microbial fuel cell system treating municipal wastewater. *J. Power Sources* **297,** 260–264 (2015).

86. Dong, Y. *et al.* A 90-liter stackable baffled microbial fuel cell for brewery wastewater treatment based on energy self-sufficient mode. *Bioresour. Technol.* **195,** 66–72 (2015).

87. Kiseleva, L. *et al.* Taxonomic and functional metagenomic analysis of anodic communities in two pilot-scale microbial fuel cells treating different industrial wastewaters. *J. Integr. Bioinforma.* **12,** 273 (2015).

88. Kim, M., Cha, J., Yu, J. & Kim, C. Stackable and submergible microbial fuel cell modules for wastewater treatment. *Bioprocess Biosyst. Eng.* (2016). doi:10.1007/s00449-016-1597-6

89. Ghadge, A. N. & Ghangrekar, M. M. Performance of low cost scalable air–cathode microbial fuel cell made from clayware separator using multiple electrodes. *Bioresour. Technol.* **182,** 373–377 (2015).

90. Wu, S. *et al.* A novel pilot-scale stacked microbial fuel cell for efficient electricity generation and wastewater treatment. *Water Res.* (2016). doi:10.1016/j.watres.2016.04.043

91. Huggins, T., Fallgren, P. H., Jin, S. & Ren, Z. J. Energy and performance comparison of microbial fuel cell and conventional aeration treating of wastewater. *J. Microb. Biochem. Technol.* (2013). doi:10.4172/1948-5948.S6-002

92. Ter Heijne, A. *et al.* Performance of a scaled-up microbial fuel cell with iron reduction as the cathode reaction. *J. Power Sources* **196,** 7572–7577 (2011).

93. Dekker, A., Heijne, A. T., Saakes, M., Hamelers, H. V. & Buisman, C. J. Analysis and improvement of a scaled-up and stacked microbial fuel cell. *Environ. Sci. Technol.* **43,** 9038–9042 (2009).

94. Zhuang, L., Yuan, Y., Wang, Y. & Zhou, S. Long-term evaluation of a 10-liter serpentine-type microbial fuel cell stack treating brewery wastewater. *Bioresour. Technol.* **123,** 406–412 (2012).

95. Li, C., Lesnik, K. L., Fan, Y. & Liu, H. Redox conductivity of current-producing mixed species biofilms. *PLOS ONE* **11,** e0155247 (2016).

96. Malvankar, N. S. & Lovley, D. R. Microbial nanowires for bioenergy applications. *Curr. Opin. Biotechnol.* **27,** 88–95 (2014).

97. Clauwaert, P. *et al.* Open air biocathode enables effective electricity generation with microbial fuel cells. *Environ. Sci. Technol.* **41,** 7564–7569 (2007).

98. NSF Certified Activated Carbon & Charcoal | GC 8x30 | General Carbon. *General Carbon Corporation*

99. Logan, B., Cheng, S., Watson, V. & Estadt, G. Graphite fiber brush anodes for increased power production in air-cathode microbial fuel cells. *Environ. Sci. Technol.* **41,** 3341–3346 (2007).

100. Feng, Y., Lee, H., Wang, X., Liu, Y. & He, W. Continuous electricity generation by a graphite granule baffled air–cathode microbial fuel cell. *Bioresour. Technol.* **101,** 632–638 (2010).

101. Oh, S.-E. & Logan, B. E. Voltage reversal during microbial fuel cell stack operation. *J. Power Sources* **167,** 11–17 (2007).

102. Cheng, S. & Logan, B. E. Increasing power generation for scaling up single-chamber air cathode microbial fuel cells. *Bioresour. Technol.* **102,** 4468–4473 (2011).

103. Reguera, G. *et al.* Biofilm and nanowire production leads to increased current in Geobacter sulfurreducens fuel cells. *Appl. Environ. Microbiol.* **72,** 7345–7348 (2006).

104. Newton, G. J., Mori, S., Nakamura, R., Hashimoto, K. & Watanabe, K. Analyses of current-generating mechanisms of Shewanella loihica PV-4 and Shewanella oneidensis MR-1 in microbial fuel cells. *Appl. Environ. Microbiol.* **75,** 7674–7681 (2009).

105. Yi, H. *et al.* Selection of a variant of Geobacter sulfurreducens with enhanced capacity for current production in microbial fuel cells. *Biosens. Bioelectron.* **24,** 3498–3503 (2009).

106. Dominguez-Benetton, X., Navarro-Avila, S. G. & Carrera-Figueiras, C. Electrochemical evaluation of Ti/TiO2-polyaniline anodes for microbial fuel cells using hypersaline microbial consortia for synthetic-wastewater treatment. *J. New Mater. Electrochem. Syst.* **13,** (2010).

107. Dewan, A., Beyenal, H. & Lewandowski, Z. Scaling up microbial fuel cells. *Environ. Sci. Technol.* **42,** 7643–7648 (2008).

108. Damiano, L., Jambeck, J. R. & Ringelberg, D. B. Municipal solid waste landfill leachate treatment and electricity production using microbial fuel cells. *Appl. Biochem. Biotechnol.* **173,** 472–485 (2014).

109. Koroglu, E. O., Cetinkaya, A. Y., Ozkaya, B. & Demir, A. Simultaneous production of bioelectricity and treatment of membrane concentrate in multitube microbial fuel cell. *J. Biosci. Bioeng.* (2016). doi:10.1016/j.jbiosc.2016.04.002

110. Liu, H., Ramnarayanan, R. & Logan, B. E. Production of electricity during wastewater treatment using a single chamber microbial fuel cell. *Environ. Sci. Technol.* **38,** 2281–2285 (2004).

111. Logan, B. E. Scaling up microbial fuel cells and other bioelectrochemical systems. *Appl. Microbiol. Biotechnol.* **85,** 1665–1671 (2010).

112. Sonawane, J. M., Gupta, A. & Ghosh, P. C. Multi-electrode microbial fuel cell (MEMFC): A close analysis towards large scale system architecture. *Int. J. Hydrog. Energy* **38,** 5106–5114 (2013).

113. Liu, H., Cheng, S., Huang, L. & Logan, B. E. Scale-up of membrane-free single-chamber microbial fuel cells. *J. Power Sources* **179,** 274–279 (2008).

114. Cheng, S., Ye, Y., Ding, W. & Pan, B. Enhancing power generation of scale-up microbial fuel cells by optimizing the leading-out terminal of anode. *J. Power Sources* **248,** 931–938 (2014).

115. Moon, H., Chang, I. S., Jang, J. K. & Kim, B. H. Residence time distribution in microbial fuel cell and its influence on COD removal with electricity generation. *Biochem. Eng. J.* **27,** 59–65 (2005).

116. Pham, H. T. *et al.* High shear enrichment improves the performance of the anodophilic microbial consortium in a microbial fuel cell. *Microb. Biotechnol.* **1,** 487–496 (2008).

117. Stewart, P. S. Mini-review: Convection around biofilms. *Biofouling* **28,** 187–198 (2012).

118. Zhang, W. *et al.* A novel planar flow cell for studies of biofilm heterogeneity and flow-biofilm interactions. *Biotechnol. Bioeng.* **108,** 2571–2582 (2011).

119. Chen, M. J., Zhang, Z. & Bott, T. R. Direct measurement of the adhesive strength of biofilms in pipes by micromanipulation. *Biotechnol. Tech.* **12,** 875–880 (1998).

120. Kwok, W. K. *et al.* Influence of biomass production and detachment forces on biofilm structures in a biofilm airlift suspension reactor. *Biotechnol. Bioeng.* **58,** 400–407 (1998).

121. Liu, Y. & Tay, J.-H. Metabolic response of biofilm to shear stress in fixed-film culture. *J. Appl. Microbiol.* 337–342 (2001).

122. Picioreanu, C., Vanloosdrecht, M. & Heijnen, J. Discrete-differential modelling of biofilm structure. *Water Sci. Technol.* **39,** 115–122 (1999).

123. Rivera, F. F., de León, C. P., Nava, J. L. & Walsh, F. C. The filter-press FM01-LC laboratory flow reactor and its applications. *Electrochimica Acta* **163,** 338–354 (2015).

124. Logan, B. E. *et al.* Assessment of microbial fuel cell configurations and power densities. *Environ. Sci. Technol. Lett.* **2,** 206–214 (2015).

125. Oh, S.-E. & Logan, B. E. Proton exchange membrane and electrode surface areas as factors that affect power generation in microbial fuel cells. *Appl. Microbiol. Biotechnol.* **70,** 162–169 (2006).

126. Zuo, Y., Cheng, S., Call, D. & Logan, B. E. Tubular membrane cathodes for scalable power generation in microbial fuel cells. *Environ. Sci. Technol.* **41,** 3347–3353 (2007).

127. Cheng, S., Liu, H. & Logan, B. E. Increased performance of single-chamber microbial fuel cells using an improved cathode structure. *Electrochem. Commun.* **8,** 489–494 (2006).

128. Rivero, E. P., Cruz-Díaz, M. R., Almazán-Ruiz, F. J. & González, I. Modeling the effect of non-ideal flow pattern on tertiary current distribution in a filter-press-type electrochemical reactor for copper recovery. *Chem. Eng. Res. Des.* **100,** 422–433 (2015).

129. *OECD guideline for the testing of chemicals*. (H.M.S.O, 1983).

130. Levenspiel, O. *Chemical reaction engineering*. (Wiley, 1999).

131. Kashid, M. N., Renken, A. & Kiwi-Minsker, L. *Microstructured devices for chemical processing*. (John Wiley & Sons Ltd, 2015).

132. Ramasamy, R. P., Ren, Z., Mench, M. M. & Regan, J. M. Impact of initial biofilm growth on the anode impedance of microbial fuel cells. *Biotechnol. Bioeng.* **101,** 101–108 (2008).

133. Ramasamy, R. P., Gadhamshetty, V., Nadeau, L. J. & Johnson, G. R. Impedance spectroscopy as a tool for non-intrusive detection of extracellular mediators in microbial fuel cells. *Biotechnol. Bioeng.* **104,** 882–891 (2009).

134. Liang, D.-W. *et al.* Enhancement of hydrogen production in a single chamber microbial electrolysis cell through anode arrangement optimization. *Bioresour. Technol.* **102,** 10881–10885 (2011).

135. Lepage, G., Albernaz, F. O., Perrier, G. & Merlin, G. Characterization of a microbial fuel cell with reticulated carbon foam electrodes. *Bioresour. Technol.* **124,** 199–207 (2012).

136. Ter Heijne, A. *et al.* Analysis of bio-anode performance through electrochemical impedance spectroscopy. *Bioelectrochemistry* **106,** 64–72 (2015).

137. Agostino, V. *et al.* Electrochemical analysis of microbial fuel cells based on enriched biofilm communities from freshwater sediment. *Electrochimica Acta* **237,** 133–143 (2017).

138. Andreasen, S. J., Vang, J. R. & Kær, S. K. High temperature PEM fuel cell performance characterisation with CO and CO2 using electrochemical impedance spectroscopy. *Int. J. Hydrog. Energy* **36,** 9815–9830 (2011).

139. Lasia, A. Electrochemical impedance spectroscopy and its applications. in *Modern aspects of electrochemistry* 143–248 (Springer, 2002).

140. Göhr, H., Mirnik, M. & Schiller, C. A. Distortions of high frequency electrode impedance: Their causes and how to avoid them. *J. Electroanal. Chem. Interfacial Electrochem.* **180,** 273–285 (1984).

141. Hsu, C. H. & Mansfeld, F. Concerning the conversion of the constant phase element parameter Y0 into a capacitance. *Corrosion* **57,** 747–748 (2001).

142. Devanathan, M. A. V. & Ramakrishnaiah, K. Differential capacitance of some solid metal/aqueous-electrolyte interfaces. *Electrochimica Acta* **18,** 259–264 (1973).

143. Bernabeu, P. & Caprani, A. Influence of surface charge on adsorption of fibrinogen and/or albumin on a rotating disc electrode of platinum and carbon. *Biomaterials* **11,** 258–264 (1990).

144. Fievet, P., Mullet, M., Reggiani, J. C. & Pagetti, J. Influence of surface charge on adsorption of a hydrophobic peptide onto a carbon surface by capacitance measurements. *Colloids Surf. Physicochem. Eng. Asp.* **144,** 35–42 (1998).

145. 16S Metagenomic Sequencing Library Preparation.

146. Fierer, N., Jackson, J. A., Vilgalys, R. & Jackson, R. B. Assessment of soil microbial community structure by use of taxon-specific quantitative PCR assays. *Appl. Environ. Microbiol.* **71,** 4117–4120 (2005).

147. Stults, J. R., Snoeyenbos-West, O., Methe, B., Lovley, D. R. & Chandler, D. P. Application of the 5' fluorogenic exonuclease assay (TaqMan) for quantitative ribosomal DNA and rRNA analysis in sediments. *Appl. Environ. Microbiol.* **67,** 2781–2789 (2001).

148. Cover, T. M. & Thomas, J. A. *Elements of information theory*. (Wiley-Interscience, 2006).

149. Bishop, P. L., Gibbs, J. T. & Cunningham, B. E. Relationship between concentration and hydrodynamic boundary layers over biofilms. *Environ. Technol.* **18,** 375–385 (1997).

150. Daugherty, R. L., Franzini, J. B. & Finnemore, E. J. *Fluid mechanics with engineering applications*. (McGraw-Hill, 1985).

151. Streeter, V. & Wylie, B. E. *Fluid mechanics*. (McGraw-Hill, 1975).

152. White, F. M. *Fluid mechanics*. (McGraw-Hill, 2009).

153. Hayes, R. E. & Kolaczkowski, S. T. Mass and heat transfer effects in catalytic monolith reactors. *Chem. Eng. Sci.* **49,** 3587–3599 (1994).

154. Tibshirani, R. Regression shrinkage and selection via the lasso. *J. R. Stat. Soc.* **58,** 267–288 (1996).

155. Friedman, J., Hastie, T., Simon, N. & Tibshirani, R. *Package 'glmnet'*. (2017).

156. Lee, J., Phung, N. T., Chang, I. S., Kim, B. H. & Sung, H. C. Use of acetate for enrichment of electrochemically active microorganisms and their 16S rDNA analyses. *FEMS Microbiol. Lett.* **223,** 185–191 (2003).

157. Holmes, D. E. *et al.* Microbial communities associated with electrodes harvesting electricity from a variety of aquatic sediments. *Microb. Ecol.* **48,** 178–190 (2004).

158. Fogel, G. B., Collins, C. R., Li, J. & Brunk, C. F. Prokaryotic genome size and SSU rDNA copy number: estimation of microbial relative abundance from a mixed population. *Microb. Ecol.* **38,** 93–113 (1999).

159. Sakamoto, M. Reclassification of Bacteroides distasonis, Bacteroides goldsteinii and Bacteroides merdae as Parabacteroides distasonis gen. nov., comb. nov., Parabacteroides goldsteinii comb. nov. and Parabacteroides merdae comb. nov. *Int. J. Syst. Evol. Microbiol.* **56,** 1599–1605 (2006).

160. Breitenstein, A. Reclassification of Clostridium hydroxybenzoicum as Sedimentibacter hydroxybenzoicus gen. nov., comb. nov., and description of Sedimentibacter saalensis sp. nov. *Int. J. Syst. Evol. Microbiol.* **52,** 801–807 (2002).

161. Ishii, S. *et al.* Microbial population and functional dynamics associated with surface potential and carbon metabolism. *ISME J.* **8,** 963–978 (2014).

162. Bond, D. R. Electrode-reducing microorganisms that harvest energy from marine sediments. *Science* **295,** 483–485 (2002).

163. Alves, A. S., Paquete, C. M., Fonseca, B. M. & Louro, R. O. Exploration of the 'cytochromome' of Desulfuromonas acetoxidans, a marine bacterium capable of powering microbial fuel cells. *Metallomics* **3,** 349 (2011).

164. Nandy, A., Kumar, V. & Kundu, P. P. Utilization of proteinaceous materials for power generation in a mediatorless microbial fuel cell by a new electrogenic bacteria Lysinibacillus sphaericus VA5. *Enzyme Microb. Technol.* **53,** 339–344 (2013).

165. Juang, D.-F., Yang, P.-C., Chou, H.-Y. & Chiu, L.-J. Effects of microbial species, organic loading and substrate degradation rate on the power generation capability of microbial fuel cells. *Biotechnol. Lett.* **33,** 2147–2160 (2011).

166. Walter, X. A., Greenman, J. & Ieropoulos, I. A. Intermittent load implementation in microbial fuel cells improves power performance. *Bioresour. Technol.* **172,** 365–372 (2014).

167. González del Campo, A., Cañizares, P., Lobato, J., Rodrigo, M. & Fernandez Morales, F. J. Effects of external resistance on microbial fuel cell's performance. in *Environment,*

Energy and Climate Change II (eds. Lefebvre, G., Jiménez, E. & Cabañas, B.) **34,** 175–197 (Springer International Publishing, 2014).

168. Miyahara, M., Kouzuma, A. & Watanabe, K. Effects of NaCl concentration on anode microbes in microbial fuel cells. *AMB Express* **5,** (2015).
169. Paitier, A. *et al.* Microbial fuel cell anodic microbial population dynamics during MFC start-up. *Biosens. Bioelectron.* **92,** 357–363 (2017).
170. Steyn, P. L. *et al.* Classification of heparinolytic bacteria into a new genus, Pedobacter, comprising four species: Pedobacter heparinus comb. nov., Pedobacter piscium comb. nov., Pedobacter africanus sp. nov. and Pedobacter saltans sp. nov. proposal of the family Sphingobacteriaceae fam. nov. *Int. J. Syst. Evol. Microbiol.* **48,** 165–177 (1998).
171. Ntougias, S., Fasseas, C. & Zervakis, G. I. Olivibacter sitiensis gen. nov., sp. nov., isolated from alkaline olive-oil mill wastes in the region of sitia, crete. *Int. J. Syst. Evol. Microbiol.* **57,** 398–404 (2007).
172. Richter, H., Lanthier, M., Nevin, K. P. & Lovley, D. R. Lack of electricity production by Pelobacter carbinolicus indicates that the capacity for Fe(III) oxide reduction does not necessarily confer electron transfer ability to fuel cell anodes. *Appl. Environ. Microbiol.* **73,** 5347–5353 (2007).
173. Schink, B. & Pfennig, N. Propionigenium modestum gen. nov. sp. nov. a new strictly anaerobic, nonsporing bacterium growing on succinate. *Arch. Microbiol.* **133,** 209–216 (1982).
174. Fedorovich, V. *et al.* Novel electrochemically active bacterium phylogenetically related to arcobacter butzleri, isolated from a microbial fuel cell. *Appl. Environ. Microbiol.* **75,** 7326–7334 (2009).
175. Hasan, S. M. & Hall, J. B. The physiological function of nitrate reduction in Clostridium perfringens. *J. Gen. Microbiol.* **87,** 120–128 (1975).
176. Zhang, H., Bruns, M. A. & Logan, B. E. Biological hydrogen production by Clostridium acetobutylicum in an unsaturated flow reactor. *Water Res.* **40,** 728–734 (2006).

177. Zhilina, T. N., Zavarzina, D. G., Kolganova, T. V., Lysenko, A. M. & Tourova, T. P. Alkaliphilus peptidofermentans sp. nov., a new alkaliphilic bacterial soda lake isolate capable of peptide fermentation and Fe(III) reduction. *Microbiology* **78,** 445–454 (2009).

178. Koch, C. & Harnisch, F. Is there a specific ecological niche for electroactive microorganisms? *ChemElectroChem* **3,** 1282–1295 (2016).

179. Sun, D., Call, D. F., Kiely, P. D., Wang, A. & Logan, B. E. Syntrophic interactions improve power production in formic acid fed MFCs operated with set anode potentials or fixed resistances. *Biotechnol. Bioeng.* **109,** 405–414 (2012).

180. Malvankar, N. S. & Lovley, D. R. Microbial nanowires: a new paradigm for biological electron transfer and bioelectronics. *ChemSusChem* **5,** 1039–1046 (2012).

181. Rabaey, K. & Rozendal, R. A. Microbial electrosynthesis — revisiting the electrical route for microbial production. *Nat. Rev. Microbiol.* **8,** 706–716 (2010).

182. Vandieken, V. Desulfuromonas svalbardensis sp. nov. and Desulfuromusa ferrireducens sp. nov., psychrophilic, Fe(III)-reducing bacteria isolated from Arctic sediments, Svalbard. *Int. J. Syst. Evol. Microbiol.* **56,** 1133–1139 (2006).

183. Commault, A. S., Lear, G., Packer, M. A. & Weld, R. J. Influence of anode potentials on selection of Geobacter strains in microbial electrolysis cells. *Bioresour. Technol.* **139,** 226–234 (2013).

184. Lovley, D. R. *et al.* Geobacter: the microbe electric's physiology, ecology, and practical applications. in *Advances in Microbial Physiology* **59,** 1–100 (Elsevier, 2011).

185. Juang, D. F., Yang, P. C. & Kuo, T. H. Effects of flow rate and chemical oxygen demand removal characteristics on power generation performance of microbial fuel cells. *Int. J. Environ. Sci. Technol.* **9,** 267–280 (2012).

186. Luo, S., Sun, H., Ping, Q., Jin, R. & He, Z. A review of modeling bioelectrochemical systems: engineering and statistical aspects. *Energies* **9,** 111 (2016).

187. Aaron, D., Tsouris, C., Hamilton, C. Y. & Borole, A. P. Assessment of the effects of flow rate and ionic strength on the performance of an air-cathode microbial fuel cell using electrochemical impedance spectroscopy. *Energies* **3,** 592–606 (2010).

188. Ieropoulos, I., Winfield, J. & Greenman, J. Effects of flow-rate, inoculum and time on the internal resistance of microbial fuel cells. *Bioresour. Technol.* **101,** 3520–3525 (2010).

189. He, Y.-J. & Ma, Z.-F. A data-driven gaussian process regression model for two-chamber microbial fuel cells. *Fuel Cells* **16,** 365–376 (2016).

190. Sonin, A. A. A generalization of the Π-theorem and dimensional analysis. *Proc. Natl. Acad. Sci. U. S. A.* **101,** 8525–8526 (2004).

191. Ter Heijne, A., Hamelers, H. V. M., Saakes, M. & Buisman, C. J. N. Performance of non-porous graphite and titanium-based anodes in microbial fuel cells. *Electrochimica Acta* **53,** 5697–5703 (2008).

Annexes

Table S1. Parameters used in the multiple linear regression with LASSO variables selection to model maximum power.

Reactor/Flow	Maximum power (W)	Volume (L)	Flow rate (L/h)	Cross section area (m²)	Characteristic length	Fluid velocity (m/s)	Hydraulic retention time (s)	Reynolds number	Sherwood number
	P_{max}	V	Q	A	L_c	u	HRT	Re	Sh
1L-MFC_280	**6.42E-03**	1.00E-03	2.80E+02	2.80E-03	1.41E-01	2.78E-02	1.29E+01	3.92E+03	1.53E+03
1L-MFC_100	**2.40E-03**	1.00E-03	1.00E+02	2.80E-03	1.41E-01	9.92E-03	3.60E+01	1.40E+03	9.63E+02
1L-MFC_50	**2.22E-03**	1.00E-03	5.00E+01	2.80E-03	1.41E-01	4.96E-03	7.20E+01	7.00E+02	7.05E+02
0,5L-MFC_280	**9.63E-03**	5.00E-04	2.80E+02	1.40E-03	7.28E-02	5.56E-02	6.43E+00	4.04E+03	1.20E+03
0,5L-MFC_100	**3.65E-03**	5.00E-04	1.00E+02	1.40E-03	7.28E-02	1.98E-02	1.80E+01	1.44E+03	7.53E+02
0,5L-MFC_50	**6.22E-04**	5.00E-04	5.00E+01	1.40E-03	7.28E-02	9.91E-03	3.60E+01	7.20E+02	5.51E+02
0,01L-MFC_210	**1.27E-04**	1.00E-05	2.10E+02	2.00E-04	2.24E-02	2.92E-01	1.72E-01	6.51E+03	2.19E+03
0,01L-MFC_100	**2.00E-06**	1.00E-05	1.00E+02	2.00E-04	2.24E-02	1.39E-01	3.60E-01	3.10E+03	1.57E+03
0,01L-MFC_50	**6.00E-06**	1.00E-05	5.00E+01	2.00E-04	2.24E-02	6.94E-02	7.20E-01	1.55E+03	1.15E+03

Reactor/Flow	Mass transfer coefficient (m/s)	Hydrodynamic boundary layer thickness (m)	Concentration boundary layer thickness (m)	Péclet number	Péclet number from RTD	Characteristic time of substrate diffusion in CBL (s)	Skin friction coefficient	Shear stress (kg/s².m)
	k	δ_H	δ_C	Pe	Pe_{RTD}	τ_{CBL}	C_f	T
1L-MFC_280	5.41E-06	1.02E-02	1.28E-01	4.54E-08	3.95E+00	3.30E+07	1.68E-02	6.47E-03
1L-MFC_100	3.40E-06	1.86E-02	2.34E-01	1.27E-07	3.69E+00	1.10E+08	3.55E-02	1.75E-03
1L-MFC_50	2.49E-06	2.63E-02	3.31E-01	2.55E-07	5.81E+00	2.19E+08	5.02E-02	6.17E-04
0,5L-MFC_280	8.22E-06	5.22E-03	6.58E-02	2.27E-08	1.88E+01	8.65E+06	1.66E-02	2.57E-02
0,5L-MFC_100	5.17E-06	9.42E-03	1.19E-01	6.36E-08	1.42E+01	2.82E+07	3.50E-02	6.88E-03
0,5L-MFC_50	3.79E-06	1.33E-02	1.68E-01	1.27E-07	1.44E+01	5.64E+07	4.95E-02	2.43E-03
0,01L-MFC_210	4.90E-05	1.46E-03	1.84E-02	6.06E-10	1.41E+01	6.74E+05	1.44E-02	6.12E-01
0,01L-MFC_100	3.51E-05	1.69E-03	2.13E-02	1.27E-09	7.90E+00	9.07E+05	1.81E-02	1.74E-01
0,01L-MFC_50	2.57E-05	2.79E-03	3.52E-02	2.55E-09	6.61E+00	2.47E+06	3.37E-02	8.13E-02

Table S2. Dimensionless numbers used in the multiple linear regression to model maximum power.

Reactor/Flow	Maximum power (W)	Π_1	Π_2	Π_3	Π_4	Sh
1L-MFC_280	**6.42E-03**	3.93E+03	7.86E+06	2.33E-04	1.41E-01	1.53E+03
1L-MFC_100	**2.40E-03**	1.40E+03	2.81E+06	1.76E-04	1.41E-01	9.63E+02
1L-MFC_50	**2.22E-03**	7.01E+02	1.40E+06	1.24E-04	1.41E-01	7.05E+02
0,5L-MFC_280	**9.63E-03**	4.05E+03	8.10E+06	4.62E-04	2.75E-01	1.20E+03
0,5L-MFC_100	**3.65E-03**	1.44E+03	2.88E+06	3.48E-04	2.75E-01	7.53E+02
0,5L-MFC_50	**6.22E-04**	7.21E+02	1.44E+06	2.45E-04	2.75E-01	5.51E+02
0,01L-MFC_210	**1.27E-04**	6.53E+03	1.31E+07	2.09E-03	8.94E-01	2.19E+03
0,01L-MFC_100	**2.00E-06**	3.11E+03	6.22E+06	1.25E-03	8.94E-01	1.57E+03
0,01L-MFC_50	**6.00E-06**	1.55E+03	3.10E+06	1.17E-03	8.94E-01	1.15E+03

$$\Pi_1 = Re = \frac{u \times L_c \times \rho}{\mu}$$

$$\Pi_2 = Pe = \frac{u \times L_c}{D}$$

$$\Pi_3 = \frac{T}{u \times \rho}$$

$$\Pi_4 = \frac{h}{L_c}$$

$$\mathrm{Sh} = 3.66 \times \left(1 + 0.095 \times \frac{L_c \times Pe}{l}\right)^{0.45}$$

Table S3. Parameters used in the multiple linear regression with LASSO variables selection to model *Geobacter* numbers.

Reactor/Flow	*Geobacter* number from qPCR	Volume (L)	Flow rate (L/h)	Maximum voltage (V)	Maximum power (W)	Internal resistance (Ω)	Total bacteria number	*Geobacter* relative abundance (%)	Cross section area (m²)	Characteristic length	Fluid velocity (m/s)
	G	V	Q	Emax	P_{max}	R_{int}	B	g	A	L_c	u
1L-MFC_280	**9.64E+08**	1.00E-03	2.80E+02	2.96E-01	6.42E-03	1.13E+01	2.48E+09	4.21E+01	2.80E-03	1.41E-01	2.78E-02
1L-MFC_100	**3.04E+09**	1.00E-03	1.00E+02	2.78E-01	2.40E-03	4.78E+00	1.33E+09	2.84E+01	2.80E-03	1.41E-01	9.92E-03
1L-MFC_50	**4.13E+09**	1.00E-03	5.00E+01	2.48E-01	2.22E-03	5.33E+00	1.21E+09	2.74E+01	2.80E-03	1.41E-01	4.96E-03
0,5L-MFC_280	**2.17E+09**	5.00E-04	2.80E+02	4.05E-01	9.63E-03	6.30E+00	2.05E+09	6.85E+01	1.40E-03	7.28E-02	5.56E-02
0,5L-MFC_100	**3.31E+09**	5.00E-04	1.00E+02	3.04E-01	3.65E-03	7.44E+00	2.58E+09	6.71E+01	1.40E-03	7.28E-02	1.98E-02
0,5L-MFC_50	**2.86E+09**	5.00E-04	5.00E+01	2.89E-01	6.22E-04	3.39E+02	2.55E+09	5.09E+01	1.40E-03	7.28E-02	9.91E-03
0,01L-MFC_210	**5.95E+08**	1.00E-05	2.10E+02	6.20E-02	1.27E-04	1.67E+02	2.58E+09	5.47E+01	2.00E-04	2.24E-02	2.92E-01
0,01L-MFC_100	**1.43E+09**	1.00E-05	1.00E+02	2.60E-02	2.00E-06	7.92E+02	3.62E+09	3.79E+01	2.00E-04	2.24E-02	1.39E-01
0,01L-MFC_50	**2.21E+09**	1.00E-05	5.00E+01	6.00E-03	6.00E-06	1.65E+04	8.77E+08	2.59E+01	2.00E-04	2.24E-02	6.94E-02

Reactor/Flow	Hydraulic retention time (s)	Reynolds number	Sherwood number	Mass transfer coefficient (m/s)	Hydrodynamic boundary layer thickness (m)	Concentration boundary layer thickness (m)	Péclet number	Péclet number from RTD	Characteristic time of substrate diffusion in CBL (s)	Skin friction coefficient	Shear stress (kg/s².m)
	HRT	Re	Sh	k	δ_H	δ_C	Pe	Pe_{RTD}	τ_{CBL}	C_f	T
1L-MFC_280	1.29E+01	3.92E+03	1.53E+03	5.41E-06	1.02E-02	1.28E-01	4.54E-08	3.95E+00	3.30E+07	1.68E-02	6.47E-03
1L-MFC_100	3.60E+01	1.40E+03	9.63E+02	3.40E-06	1.86E-02	2.34E-01	1.27E-07	3.69E+00	1.10E+08	3.55E-02	1.75E-03
1L-MFC_50	7.20E+01	7.00E+02	7.05E+02	2.49E-06	2.63E-02	3.31E-01	2.55E-07	5.81E+00	2.19E+08	5.02E-02	6.17E-04
0,5L-MFC_280	6.43E+00	4.04E+03	1.20E+03	8.22E-06	5.22E-03	6.58E-02	2.27E-08	1.88E+01	8.65E+06	1.66E-02	2.57E-02
0,5L-MFC_100	1.80E+01	1.44E+03	7.53E+02	5.17E-06	9.42E-03	1.19E-01	6.36E-08	1.42E+01	2.82E+07	3.50E-02	6.88E-03
0,5L-MFC_50	3.60E+01	7.20E+02	5.51E+02	3.79E-06	1.33E-02	1.68E-01	1.27E-07	1.44E+01	5.64E+07	4.95E-02	2.43E-03
0,01L-MFC_210	1.72E-01	6.51E+03	2.19E+03	4.90E-05	1.46E-03	1.84E-02	6.06E-10	1.41E+01	6.74E+05	1.44E-02	6.12E-01
0,01L-MFC_100	3.60E-01	3.10E+03	1.57E+03	3.51E-05	1.69E-03	2.13E-02	1.27E-09	7.90E+00	9.07E+05	1.81E-02	1.74E-01
0,01L-MFC_50	7.20E-01	1.55E+03	1.15E+03	2.57E-05	2.79E-03	3.52E-02	2.55E-09	6.61E+00	2.47E+06	3.37E-02	8.13E-02

FOLIO ADMINISTRATIF

THESE DE L'UNIVERSITE DE LYON OPEREE AU SEIN DE L'INSA LYON

NOM : PAITIER DATE de SOUTENANCE : 17 novembre 2017

Prénoms : Agathe

TITRE : Etude de la mise à l'échelle des piles à combustible microbiennes: collecteurs de courant et hydrodynamique

NATURE : Doctorat Numéro d'ordre : 2017LYSEI107

Ecole doctorale : EEA Spécialité : Ingénierie pour le vivant

RESUME :

Les problématiques environnementales et économiques encouragent le développement d'énergies renouvelables est nécessaire et de nouvelles technologies alternatives comptent tirer profit de sources d'énergie négligées. Le potentiel énergétique des eaux usées peut être exploité par de nouvelles technologies telles que les piles à combustible microbiennes (PACM). Ces piles, pouvant produire de l'électricité à partir d'eaux usées, montrent un rendement énergétique intéressant à petite échelle. Toutefois, leur efficacité diminue de manière drastique lorsque leur taille augmente, ce qui empêche leur application industrielle. Ces travaux de thèse visent à identifier certains verrous de ce changement d'échelle et à proposer de nouvelles directions pour leur optimisation. Une première partie de l'étude s'est intéressée à l'influence des collecteurs de courant anodiques sur les performances électriques et sur le développement du biofilm électroactif. Nous avons émis l'hypothèse qu'à grande échelle, les collecteurs de courant peuvent être un élément limitant à la production d'électricité. Pour vérifier cette hypothèse, quatre PACM avec une anode de 490cm² connectée de différentes manières ont été étudiées. L'augmentation du nombre de collecteurs a permis une hausse de la puissance produite par les PACM. Le gradient de potentiel formé par la disposition des collecteurs a influencé la structure microbiologique du biofilm. La suite du travail s'est attachée à considérer les PACM comme des bioréacteurs et à prendre en compte différents aspects physiques, notamment l'aspect hydrodynamique, afin de modéliser leur fonctionnement. Pour cela, trois PACM de volumes différents ont été mises en œuvre et testées à différents débits. Les données de configuration, d'opération et de performances de ces piles ont permis de construire deux modèles statistiques de régression linéaire multiple prédisant la valeur de puissance maximale et ont montré que la puissance maximale produite était principalement corrélée à la vitesse de l'électrolyte et à la contrainte de cisaillement qu'il applique à l'anode.

MOTS-CLÉS : Pile à combustible microbienne ; Mise à l'échelle ; Collecteurs de courant ; Hydrodynamique

Laboratoire (s) de recherche : Laboatoire Ampère

Directeur de thèse: Hervé Morel

Président de jury : Pascal Simonet

Composition du jury : Théodore Bouchez Wafa Achouak
Giuliano Premier Timothy Vogel